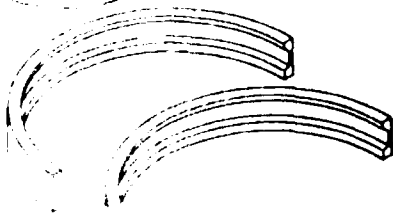# Structural Performance of Cylindrical Pressure Housings of Different Ceramic Compositions Under External Pressure Loading

Part IV, Silicon Carbide Particulate Reinforced Alumina Ceramic

94-35278

R. R. Kurkchubasche
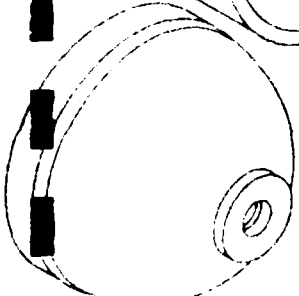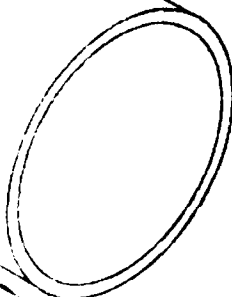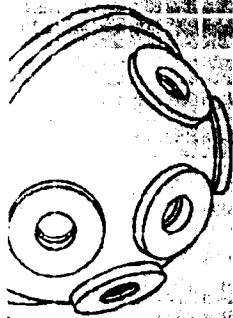R. P. Johnson
J. D. Stachiw
NRaD

T.A. Johnson
Lanxide Corporation

Structural Performance of Cylindrical Pressure Housings of Different Ceramic Compositions Under External Pressure Loading

Part IV, Silicon Carbide Particulate Reinforced Alumina Ceramic

R. R. Kurkchubasche
R. P. Johnson
J. D. Stachiw
NRaD

T. A. Johnson
Lanxide Corporation

**NAVAL COMMAND, CONTROL AND
OCEAN SURVEILLANCE CENTER
RDT&E DIVISION
San Diego, California 92152–5001**

K. E. EVANS, CAPT, USN
Commanding Officer

R. T. SHEARER
Executive Director

ADMINISTRATIVE INFORMATION

ACKNOWLEDGMENT

SUMMARY

Twelve 12-inch-outside-diameter (OD) by 18-inch-long silicon-carbide particulate reinforced alumina-ceramic cylinders ($SiC/Al_2O_3/Al$) were fabricated, nondestructively inspected, and assembled by Lanxide Corporation. They were subsequently instrumented and pressure tested at Southwest Research Institute (SRI) under the supervision of the Naval Command, Control and Ocean Surveillance Center (NCCOSC) RDT&E Division (NRaD) under the program for the Application of Ceramic to Large Housings for Underwater Vehicles. Lanxide's material, designated 90-X-089, was chosen for its high specific compressive strength, specific elastic modulus, and fracture toughness. Furthermore, this composition is manufactured by a proprietary directed metal oxidation (DIMOX™) process which makes possible the fabrication of cylinders to near net shape with little or no diamond grinding. This adds the potential of great cost and time savings, and the ability of eventually fabricating very large ceramic components without the limitations of typical ceramic fabrication equipment. Of the twelve ceramic cylinders fabricated by Lanxide, ten had a 12-inch OD, 18-inch length, and 0.412-inch wall thickness. The two remaining cylinders were left in "as-cast" condition with only 1.5-inches at each end being ground to final dimension. Each cylinder was radiographically inspected and fitted with epoxy-bonded titanium end rings. After being instrumented with strain gages, the cylinders were pressure tested cyclically and to destruction.

Lanxide Corporation has demonstrated that it can successfully and repeatably cast 12-inch-OD by 18-inch-long cylinders from its 90-X-089 SiC/Al_2O_3/Al composition. All twelve cylinders passed proof testing to at least 10,000 psi. Cylinder failures were due either to cyclic fatigue or intentional pressurization to critical collapse pressure. Actual failure pressure closely matched predictions made by hand and computer calculations. Cyclic testing was inconclusive in regard to formulating a correlation between the number of cycles to failure and stress levels. However, a maximum design stress level of 182,038 psi is recommended for a cyclic fatigue life of 1,000 cycles to design depth.

Lanxide 90-X-089 performs better than WESGO's AL-600 96-percent alumina-ceramic composition, the base of comparison. Lanxide 90-X-089 is lighter, has improved cyclic fatigue life, and can be designed to higher stress levels. However, the resulting improvement in weight-to-displacement (W/D) ratio, a 10-percent reduction, does not justify the 10-fold increase in cost over AL-600 96-percent alumina ceramic.

Lanxide has demonstrated that "as-cast" cylinders can be fabricated with dimensions close enough to fully machined cylinders without presenting any significant weight penalty. Pressure testing has demonstrated that "as-cast" cylinders are structurally sound. However, the 10-percent cost reduction gained by buying "as-cast" cylinders instead of fully machined does not justify their use. These savings may be more important should the size of the cylinders be scaled up to a 20-inch OD or greater.

Lanxide 90-X-089 has been found to be an acceptable material candidate for fabricating external pressure housings used in ocean engineering applications. A maximum compressive membrane design stress of 182,039 psi is recommended if a cyclic fatigue life of 1,000 cycles is desired. Cylinders may be nondestructively inspected by radiography or pulse-echo ultrasonic inspection. Although the advantages of Lanxide's 90-X-089 do not justify the high cost in the 12-inch-OD by 18-inch-long cylinder size range, it is highly recommended that the DIMOX™ process be scaled up for fabrication of greater than 20-inch-OD cylinders and hemispheres. The benefits of the DIMOX™ process will be of greater advantage in larger components. The capability of fabricating cylinders to near-net dimensions will result in cost and time savings since less grinding will be required. Furthermore, there is a possibility that internal residual stresses present in sintered parts may not be present in parts made by the DIMOX™ process.

CONTENTS

FIGURES

TABLES

INTRODUCTION

Unmanned underwater vehicles (UUVs) require pressure-resistant housings for containment of their electronics and power supply. Currently, such housings are fabricated from metals such as aluminum, titanium, or steel. However, these materials result in very heavy pressure-resistant housings when vehicles are designed to operate at depths as great as 20,000 feet. Ceramic materials, because of their high specific compressive strength and high specific elastic modulus, are ideally suited for application to external pressure-resistant housings for underwater vehicles. A more detailed justification for using ceramic materials in external pressure-resistant housings may be found in the outline for the program under which this work was performed by Naval Command, Control and Ocean Surveillance Center (NCCOSC) RDT&E Division (NRaD) (reference 1). One of the objectives of this program was to evaluate various advanced ceramic compositions for use in pressure-resistant housings. Compositions evaluated include silicon nitride, zirconia-toughened alumina, and silicon carbide particulate-reinforced aluminum ($SiC/Al_3O_3/Al$). The common base of comparison for testing these materials was 96-percent alumina ceramic manufactured by WESGO, Inc. This report summarizes the fabrication, nondestructive inspection, and testing of twelve 12-inch-OD by 18-inch-long by 0.412-inch-thick $SiC/Al_2O_3/Al$ ceramic cylinders fabricated by Lanxide Corporation using their proprietary directed metal oxidation (DIMOX™) process.

BACKGROUND

NRaD has been procuring and testing cylindrical and hemispherical components made from ceramic over the last decade. Most of the work, however, has focused on 94- and 96-percent alumina-ceramic compositions fabricated by Coors Ceramics and WESGO. When the program for the application of ceramic to large housings for underwater vehicles began, the most extensive testing had been completed on 94-percent alumina-ceramic housings, only. Testing showed limited cyclic fatigue life under repeated pressurizations

(references 2 and 3). The eventual failure of components due to repeated pressurization was attributed to a radial tensile stress at the ceramic-to-titanium metal-bearing interface (see figure 25, reference 1). This stress leads to internal circumferential cracks which run through the wall, eventually breaking off in shards, causing leakage or catastrophic failure. It is believed that one way of increasing the cyclic fatigue life of ceramic components is to use compositions having higher fracture toughness than the 94-percent alumina ceramic. The program for the application of ceramics to large housings for underwater vehicles gave NRaD the opportunity to test some new ceramic compositions exhibiting greater fracture toughness. These include silicon nitride, zirconia-toughened alumina ceramic, and Lanxide's silicon-carbide (SiC) particulate reinforced alumina-ceramic composition, designated 90-X-089.

Lanxide has developed a family of composite materials based on SiC particulate preforms infiltrated with a matrix of pure aluminum oxide using the DIMOX™ process. The mechanical properties of these composites depend largely on the particular reinforcing phase, especially its particle size and packing density. Large particle sizes act to limit the strength of the composite, while smaller reinforcing particles result in the strongest composite materials.

Lanxide 90-X-089, the composite system most suitable for submersible applications, contains a reinforcing phase of 500 grit (16 μm size) SiC particles. This relatively high-strength variation of $SiC/Al_2O_3/Al$ composite material was selected for submersible housings because of its high compressive strength and fracture toughness as well as its potential for being fabricated in large sizes.

Property requirements for ceramic pressure housing components for deep submersion include high compressive modulus, high compressive strength, high fracture toughness, and low density. Many traditional ceramics exhibit these properties, and some are being evaluated for this application. The ceramic matrix composites made by the DIMOX™ process are highly tailorable composite materials that combine properties of their phases. In addition to the ceramic constituents, a small amount of metal alloy permeates the ceramic matrix giving

the materials a degree of toughness that is expected to be important under cyclic stress conditions.

SiC particulate-reinforced alumina-matrix composites made by the DIMOX™ process combine the high strength and low density of a highly loaded carbide-reinforcement phase with the high strength and hardness of an aluminum oxide matrix toughened by residual metal alloy in the form of micron-sized capillary channels. The process for making these composites lends itself nicely to fabricating large shapes because it is essentially a near-net-shape process. Total dimensional changes during processing are typically less than one to two percent.

The family of SiC/Al₂O₃/Al composites developed by Lanxide covers a wide range of properties and processing characteristics, but one composite system that exhibits the requisite strength and modulus, 90-X-089, was selected for submersible application because it is amenable to processing in large sizes.

Other composite systems offer higher strengths, but are not as suited for fabrication into large shapes for submersible housings. Table 1[1] summarizes the properties of several SiC/Al₂O₃/Al composite materials fabricated by the DIMOX™ process.

DIMOX™ FABRICATION PROCESS

The DIMOX™ process produces dense, tough ceramic composites. For the material selected for external pressure housings, it is a process in which SiC particles are locked together in a matrix of pure alumina containing microchannels of aluminum alloy.

To achieve this special microstructure, preforms of SiC particles are placed into contact with specially alloyed aluminum at 900 degrees C. The aluminum alloy simultaneously oxidizes around the SiC particles as it wicks into the preform. The SiC particles are locked into place without the traditional ceramic processing shrinkage associated with

---

[1] Figures and tables are placed at the end of the text.

sintering. As the alloy continues to wet through the preform and oxidizes, fresh aluminum metal is fed to the "growth front" through micron-sized channels. Oxygen diffuses through the "ungrown" preform from its "air side" to the growth front (figure 1).

Barrier coatings on the "air side" of the preform stop the directed metal oxidation process at the preform surface when infiltration is complete, yielding a smooth net-shape finish. Upon completion of growth, the alloy and composite are separated. The resultant ceramic composite net shape is strong (because of the SiC-reinforced matrix of pure alumina) and tough (because of the metal-filled microchannels).

OVERVIEW OF PROCESSING STEPS

The production of ceramic composite pressure vessels by the DIMOX™ process can be divided into three steps:

1. Preform Production
2. Composite Production (Growth or Matrix Infiltration)
3. Post Growth Processing

These steps are illustrated in figure 2. Preform production involves sediment casting the cylinder preform in a mold, freezing the cast preform and mold, and drying the frozen preform. An aqueous slurry of 500-grit (16 μm particle size) SiC, organic binder, and colloidal alumina is poured into a rubber mold which is vibrated. The vibrational energy accelerates the settling of the SiC particles into a densely packed sediment in the shape of the final part.

The excess liquid from the casting slurry ends up on top of the cast part, where it is decanted off. The mold containing the sediment SiC particles and binders then is frozen to attain sufficient strength of the preform to allow removal from the mold without damage or distortion.

The frozen preform is packed in coarse refractory grain for support and dried with air. The packing also slows and controls the rate of drying to prevent cracking of the preform.

Prior to composite formation (growth), the binder-strengthened and now-dry preform is sprayed with

2

two coatings. One coating enhances the initiation of the DIMOX™ process at the alloy-preform interface. The second coating stops the DIMOX™ process at the "airside" of the preform.

The preform is sealed onto the floor of a refractory shell with a refractory plaster. At growth temperatures, molten alloy is added to the annulus between the shell and the preform. Oxygen is fed to the center to assure consistent high-quality product throughout the composite. After draining the remaining alloy and cooling the composite, the residual alloy skin and barrier coatings are removed by grit blasting.

Applications for marine exposure call for materials that are resistant to seawater corrosion or materials that can be easily protected from the corrosive effects of saltwater. Lanxide 90-X-089 contains about 52 volume percent SiC particulate filler and 30 volume percent aluminum-oxide (Al_2O_3) matrix. Both of these ceramic materials are quite inert to the effects of saltwater corrosion or any common corrosive materials at temperatures below several hundred degrees. The remaining 18 volume percent of the material is in the form of aluminum alloy dispersed throughout the material in micron-sized capillary channels. Thus, this composite material can be considered to be 82-percent inert, with a small phase susceptible to corrosion. The corrosion rate of this material should be self limiting with respect to depth due to the shape and small size of the alloy channels.

Protecting the material totally from corrosion will require proven coating techniques developed for protecting aluminum alloys. Anodizing and painting with an epoxy paint (per WS22351 Rev. C-MK 48 Torpedo Protective Coating System) has proved effective for this material.

In a previous program performed by Lanxide and sponsored by NRaD[2], SiC particulate-reinforced alumina-ceramic matrix composites were evaluated as potential materials for deep-sea submersible hulls. In this 1990-1991 evaluation, 6-inch-OD scale-model cylinders of SiC/Al_2O_3/Al composite indicated a potential for use as a deep-

___

[2]NRaD was previously Naval Ocean Systems Center (NOSC).

sea pressure housing material. Results of the 6-inch-OD cylinder program may be found in reference 4. The 1990–1991 program was only a preliminary evaluation of SiC/Al_2O_3/Al composites. Further evaluation was required to determine if the DIMOX™ process produces material of the same quality when scaled up to medium and large cylinders. Scale-up from 6-inch ODs to 12-inch ODs proved to be difficult during the 1990–1991 program.

During 1992, manufacturing techniques were developed by Lanxide at contractor expense to produce 12-inch-OD cylinders. The first 12-inch-OD cylinder was delivered before award of the contract for twelve 12-inch-OD by 18-inch-long cylinders, as proof of the contractor's ability to fabricate these cylinders. This first cylinder, however, was not full length; it was 12 inches long instead of the preferred 18 inches. This cylinder was cyclically tested at 10,000-psi external pressure and failed on the 826th cycle. A full description of the testing and of the test results is in appendix A. The conclusions of this test were that the material properties of Lanxide's 90-X-089 in the 12-inch-OD cylinder are identical to the material properties of the same composite in 6-inch-OD cylinders. In addition, the fabrication process for producing large cylinders from Lanxide 90-X-089 appears to have satisfied all the criteria associated with the scaling up of laboratory processes.

A firm fixed-price contract was let to Lanxide in December, 1992 for the fabrication of twelve 12-inch-OD by 18-inch-long by 0.412-inch-thick cylinders using Lanxide's DIMOX™ process. Ten cylinders were fabricated to the specifications of drawing 55910-0126845 (figure 3), and two to those of drawing 55910-0125727 (figure 4). The differences between these two drawings lie in the amount of grinding required. Ten cylinders were ground on **all** surfaces to the dimensions and tolerances shown on the drawing. The two extra cylinders, designated "as-cast," were ground only at both ends to facilitate the fitting of titanium end rings. These cylinders were fabricated to "as-cast" dimensions to demonstrate the feasibility of doing this and to determine the effect on the structural

performance of cylinders when they are not ground to final dimensions.

OBJECTIVES

There were four objectives for fabricating and testing Lanxide's 12-inch-OD 90-X-089 cylinders:

1. Demonstrate the ability of Lanxide to scale up the proprietary DIMOX™ process to fabricate 12-inch-OD by 18-inch-long by 0.412-inch-thick wall ceramic composite cylinders of equal quality to the 6-inch-OD by 9-inch-long by 0.206-inch-thick cylinders previously supplied to NRaD. Determine the uniformity and repeatability of these composite cylinders in a quantity scale up to twelve cylinders.

2. Determine the structural performance of the cylinders under external hydrostatic pressure loading.

3. Compare the performance of the 90-X-089 cylinders against the baseline composition, Al-600 96-percent alumina ceramic manufactured by WESGO, Inc., Belmont, CA. The structural performance parameters investigated include cyclic fatigue life and failure pressure.

4. Determine the ability of the DIMOX™ process to produce cylinders close enough to net shape that only the ends of the cylinders require machining without loss of performance.

APPROACH

The test plan for the twelve cylinders included fabrication, characterization of material properties, nondestructive evaluation (NDE), and pressure testing.

FABRICATION

Preform Mold Fabrication

The preform mold was fabricated by an outside vendor. It had two aluminum base plates, two fiberglass/epoxy outside shells, two rubber inner elements, and a tapered fiberglass/epoxy center-core element. A schematic of the mold is shown in figure 5. Photos are shown in figure 6.

The rubber elements of the mold were cast against an aluminum cylinder model, machined to specification. During the program, it became necessary to cast a cylinder with a thicker wall to provide sufficient material for overcoming a slight out-of-round condition of the preforms cast in the original mold configuration. This condition originated from the poor dimensional stability of the tapered, two-piece, fiberglass/epoxy center-core element.

The mold was easily modified by recasting the center rubber element with the original model inside the mold. The cylinder model was modified by laminating a 0.050-inch-thick layer of sheet wax on its inside wall. A new inner rubber element was cast in the mold assembled with the modified model. This yielded a modified mold that cast a preform with a 0.050-inch-thicker wall on the inner diameter.

Cylinder Preform Casting

An SiC slurry was prepared from SiC powder mixed with binders and dispersion aids in a proprietary composition. This slurry was cast into the mold and allowed to settle under vibratory conditions. After a predetermined time, the mold assembly was placed into a freezer to avoid thawing, which could result in distortion or fracture. Figure 7 shows two demolded, frozen preforms inside a freezer.

Preform Drying

Special procedures were developed to dry the frozen preforms carefully, avoiding stresses that distort or fracture the preforms during the critical period between the frozen state and the dry state. Controlled moisture removal from all surfaces at a uniform rate is critical. Maintaining constant preform support to avoid stress concentrations was also important. A proprietary drying system was developed to perform this function.

Not one preform warped or cracked during drying in the entire program when using the system developed. This is notable because prior cylinder programs incurred heavy losses during drying.

Figure 8 shows a dried cylinder preform inside the dryer.

Preform Control

The dimensional control of dried cylinder preforms is a function of the quality of the mold and the drying process. It was not practical to dimension frozen preforms, which would be necessary to determine the dimensional effects of the drying process. The dimensional data on preforms includes mold and freezing effects as well as the effects of drying.

All cylinder preforms prepared for this project were out of round. The orientation of the elliptical cylinders matched the orientation of the cylinders when they were cast in the mold. Thus, the out of roundness is a mold problem and does not occur during drying or growth. When a new rubber mold element was made to increase the wall thickness by 0.050 inch on the inside surface, the orientation of the two-piece fiberglass center core of the mold was rotated about 90 degrees to the orientation it had in the original mold. The cylinders cast in the modified mold were out of round in the same orientation as the center core (i.e., the orientation of the elliptical axis had rotated 90 degrees in the same direction as the core).

Three cylinder preforms cast in the original mold configuration (thin walled) were dimensioned accurately prior to their growth. Thirteen diameters were measured every 15 degrees from the mold index mark for each of six sections along the cylinder length. Even though all these parts were out of round, they were compared to determine the cylinder-to-cylinder repeatability of diameters obtained from the same mold, along the same elliptical axis orientations. There were six maximum and six minimum diameters for the ID and the OD. The results are shown in table 2.

The diameter range along the maximum elliptical axis of the inside surface was 0.047 inch. The minimum axis range was 0.023 inch. Similar results were seen for the OD: maximum axis range was 0.010 and minimum axis range was 0.050 inch.

Even with the unstable mold, tolerances of ±0.025 inch were obtained. This is a tolerance of 0.2 percent over the cylinder diameter. With a more rigid mold design, it would not be unreasonable to expect tolerances of 0.1 percent.

Two cylinders cast from the modified mold (thicker wall) were also dimensioned, with results even tighter than the three cylinders discussed above. The total inside diameter (ID) range along the maximum axis was 0.012 inch and along the minimum axis, it was 0.016 inch. Note that these parts were still cast in the same mold (just one rubber mold element was replaced) and the parts were out of round equally to the cylinders cast in the original mold configuration.

Preform Preparation for Infiltration

Special refractory shells were cast and fired in preparation for the DIMOX™ processing of the preforms. These assemblies had three components. The design of these preforms is a key element of the DIMOX™ growth process for these cylinders.

Prior to the infiltration using the DIMOX™ process, two preparation steps must be made to the cylinder preforms. First, a proprietary coating is applied to the inside of the cylinder by spraying. This coating is a barrier to the infiltration process, preventing the oxide from building up beyond the surface of the preform when infiltration has been completed. While the bulk of the infiltration is controlled by time, some regions in the preform will complete infiltration before other regions. Without the barrier, regions of aluminum oxide scale will build up as the oxidation proceeds beyond the preform surface. This scale bonds with the composite wall and is difficult to remove without damaging the surface of the composite. Another proprietary coating is applied to the outside surface of the cylinder preform. This coating makes the initiation of the oxidation process uniform over the surface of the cylinder in contact with the molten alloy. Figure 9 shows two preforms with barrier and initiation coatings, ready for matrix infiltration. Figure 10 shows a growth shell with a preform inside it.

Preform Growth

Oxide matrix infiltration in the DIMOX™ process takes place at an elevated temperature of 1,650

degrees F (900 degrees C). Two refractory shell assemblies containing two preforms at a time are placed inside an electric furnace for the process (figure 11).

Each furnace is instrumented with eleven thermocouples, monitored by an L&N Micromax system to track the process temperatures of both preforms and throughout the furnace itself. This data was collected by computer, stored on magnetic disk, and used to produce graphs of the thermocouple traces. The technique was capable of detecting the initial melting of the growth alloy, the drop of the alloy into the shell, and even the initiation of the DIMOX™ process exotherm that occurs when aluminum alloy oxidizes.

Alloy Draining

A considerable quantity of aluminum alloy is required for the infiltration of a preform as large as these cylinders. Once the growth process has been completed, the infiltration part has to be removed from the molten alloy during cooling of the part. In this case, several hundred pounds of molten aluminum alloy is involved. A procedure has been developed to drain this alloy safely while the infiltrated part remains undisturbed while cooling in its refractory shell inside the furnace. Figures 12 and 13 show technicians draining the alloy from a shell inside the furnace. The alloy is drained into a graphite mold where it solidifies into ingots of a size convenient for reuse.

This procedure was reviewed to determine its safety. Based on the findings of the review, minor modifications were made and the procedure adopted for all composite cylinders made in this program. The procedure proved to be efficient and safe, simplifying reuse of the spent alloy for subsequent cylinder growth runs. A chemical analysis was performed on each batch of alloy drained from each shell, and adjustments were made for the next infiltration run by adding alloying elements to bring the chemistry back into specification. Since a significant quantity of the aluminum in the alloy is consumed by its oxidation during infiltration, most of the adjustment to the used alloy is to bring the aluminum content back to the original specification.

Grown Cylinder Control

Diameters of cylinders completing the growth cycle were dimensioned as described above to determine the dimensional control maintained through the process. Eleven grown cylinders were measured, with one measured only for ID control. Table 3 summarizes the data obtained for all cylinders.

It can be seen that even with the dimensionally unstable mold design and the resulting out-of-round cylinders, the basic shape of each cylinder was reproduced with a tolerance averaging ±0.018 inch for all inside and outside diameters. The standard deviations for these cylinder dimensions ranged from 0.008 to 0.014 inch. From this data, it appears that, given a dimensionally stable mold capable of casting very round preforms, the DIMOX™ infiltration process could make twelve-inch-diameter composite cylinders that have diameters reproducible within 0.010 to 0.015 inch.

These cylinders would not require machining except for trimming and squaring of the ends and removing high spots on the inside and outside surfaces to provide adequate clearance for the end fittings.

To define the dimensional changes incurred by the DIMOX™ growth process, it is necessary to evaluate the dimensions of the cylinders both before and after growth. Since the diameters of cylinders BL, BM, and BO (tables 2 and 3) were measured in approximately the same positions before and after their infiltration, the changes in each measurement can be calculated before and after the growth cycle. The results indicate that the dimensional changes that occurred during growth averaged −0.013 inch for the ID and −0.002 inch for the OD. The statistics are summarized in table 4, and the actual numbers for each cylinder are shown in tables 5, 6, and 7. The ID of these three cylinders shrank by 0.11 percent. The OD of two cylinders shrank by 0.02 percent.

Machining

NRaD supplied two drawings for the program. Drawing 55910–0126845 (figure 3) is for the ten housings totally machined on all surfaces ("fully machined"). Drawing 55910–0125727 (figure 4) is

for the two housings machined only on each end, leaving the center region of both the inside and outside surfaces in the "as-cast" or net-shape condition.

The grown cylinders had to be shot-blasted before machining. Figures 14 and 15 show a cylinder before and after shot-blasting, respectively.

All machining of the "fully machined" cylinders was done at Unas Grinding Corp, 28 Cherry St., P.O. Box 280535, East Hartford, CT. Machining of the "as-cast" cylinders also was performed at Unas Grinding except for one which was machined at Alanx Products, 101 Lake Drive, Newark, DE. Figure 16 shows a "fully-machined" cylinder. Figure 17 shows an "as-cast" cylinder.

Epoxy Coating

A 12-inch-diameter cylinder of Lanxide 90-X-089 reinforced ceramic was sent to Technicote, Inc., 396 Roosevelt Ave., Central Falls, RI 02863, for coating per WS22351, Rev C (MK 48 Torpedo Protective Coating System). This is an epoxy coating normally applied to aluminum torpedo tubes. The process involves applying a surface pre-treatment (chromate), followed by epoxy resin, and then heat curing. Technicote requested a practice run to establish proper heat cure cycles for the ceramic composite material.

A sample was sent to Technicote, coated, and returned. The cure was inadequate; areas of the epoxy could be easily flaked off the surface. Two more samples were sent to Technicote for more trials. These samples had greater integrity than the first coated sample; the bond with the substrate was very good. Technicote performed tests on the surface of one of the samples showing acceptable performance of the coating.

One of the coated samples was sent to Artech Corp., Newark, DE for salt fog/spray test (per ASTM B-117). The exposure time was 48 hours in a cabinet maintained at 95 degrees F, with a 5-percent sodium-chloride solution supplying a condensing fog. The results are reported in a letter from Artech (appendix B). The epoxy surface showed no sign of oxidation, corrosion, or any

other effect from the test. The unpainted back of the coupon had a small amount of white deposit which was easily rubbed off. Note that the entire coupon was anodized prior to coating, so the unpainted back demonstrated a level of protection from salt corrosion.

It was concluded that the epoxy coating applied by Technicote was adequately cured and would be acceptable for the two deliverable cylinders. Cylinder 3375-BO was shipped for coating and delivered as Cylinder LAN 007. This cylinder is shown in figure 18 and again in figure 38.

CHARACTERIZATION OF MATERIAL PROPERTIES

Preform Density

Each cylinder is cast about 30 inches long. After drying, each preform has a one-inch section removed from each end. The density of each cylinder preform end is determined (ASTM C914-79, Standard Test Method for Bulk Density of Solid Refractories by Wax Immersion) and recorded on data sheets. This data was used to judge the quality of each preform that was cast.

Each grown cylinder was cut to about an 18.5-inch length for machining. A two-inch-long section was removed directly adjacent to each end. Both of these rings were used for testing to characterize the properties of the material in that cylinder. The data was correlated with respect to the end of the cylinder, identified as "top" or "bottom." Figure 19 shows a schematic of the preform and the location of the co-processed rings that were removed from the preform.

The properties measured included density, compressive strength, flexural strength, and fracture toughness. The modulus of elasticity was determined from the flexural test as well as from strain-gage instrumented compression test samples. It has been the experience at Lanxide that the latter method of modulus determination is more accurate for these high-modulus materials.

Cylinder Density

Each cylinder was measured to determine its density after the ends were removed for the

co-processed testing. Density was determined using the ASTM B311-86 method.

Compression testing was performed in accordance with ASTM Standard Designation C773-88, Standard Test Method for Compression (Crushing) Strength of Fired Whiteware Materials. Specimens measured 6.25-mm diameter by 12.7-mm high (0.250 inch by 0.500 inch) right cylindrical specimens. Tungsten carbide platens were used for each of the test specimens.

Flexural strength testing was performed in accordance with MIL-STD-1942A, Flexural Strength of High Performance Ceramics at Ambient Temperature. Specimen size was 6 mm by 3 mm by 45 mm (2:1 cross-section width-to-thickness). Lower span was 40 mm, upper span was 20 mm (Lanxide drawing No. A-P-0024). Hardened steel fixturing was used. A drawing of the specimen is shown in appendix C.

Fracture toughness was determined in accordance with reference 5. Specimens measured 4.8 mm by 6 mm by 45 mm (Lanxide drawing No. A-P-0027). A drawing of the specimen is shown in appendix C. The same fixture was used for both flexural strength and fracture toughness determination.

Raw materials data are presented in appendix D, tables D-1 through D-24. Average properties for each cylinder are in table 8, sheets 1 and 2.

Quantitative Image Analysis

Samples from each test ring were mounted and polished for microstructural evaluation. The evaluation was made using a Cambridge Quantimet 520 Image Analysis System and an optical microscope. Multiple fields (minimum of 200, 0.01784 mm, 2 per field) of each sample were analyzed at 500× magnification for: SiC filler, metal phases, porosity, and alumina matrix. The fields were averaged and the results for each cylinder are summarized in appendix D and table 8, sheet 1.

NONDESTRUCTIVE EVALUATION (NDE)

Dye-Penetrant Inspection

All cylinders were evaluated to determine the presence of surface cracks using a dye pe ʳant test. Testing was performed by both Lanx   MQS Inspections, Inc., 310 Cornall Drive, v.   gton, DE.

None of the cylinders showed any flaws during dye-penetrant testing. This means that none of the cylinders had any surface cracks or flaws penetrating into the material.

Dimensional Inspection

Machined cylinders were measured for conformance to NRaD Drawing 55910–0126845 and Drawing 22910–0125727, depending on which cylinder was inspected. These inspections were taken and reported by the facility machining the cylinder.

Witness Cylinder

A witness specimen was prepared for calibration of the NDE inspection equipment. This specimen was a Lanxide 90-X-089 cylinder with a 12-inch-OD, 0.412-inch wall thickness, and incorporated internal defects typical of the composites produced by the DIMOX™ process. These defects were in the form of spherical inclusions approximating the following fraction-of-an-inch diameters: 0.032, 0.063, 0.125, 0.187, and 0.250.

Three types of defects typically occur in these composite materials. One type is an open void, another is a metal inclusion, and a third is an inclusion of pure oxide matrix containing no SiC particulate.

Duplicating these flaws is not simple due to the nature of the DIMOX™ process. Unlike traditional ceramics where open flaws can be produced by incorporating organic material that will burn out upon firing, the DIMOX™ process, by its nature, infiltrates the interstices of the preform (and any voids) with aluminum oxide matrix, thus filling voids with dense oxide.

To simulate an oxide inclusion, the cylinder was cast with spheres of an organic material to burn

8

out during the DIMOX™ process leaving a void to fill with oxide matrix. For this, graphite spheres were selected in the appropriate size range.

Simulating an open pore, or void, was more difficult. Graphite spheres of appropriate diameters were coated with SiC using chemical vapor infiltration (CVI) and cast inside the preform wall. This coating either protects the graphite from oxidation during the DIMOX™ process, or remains if the graphite oxidizes. Either way, a spherical inclusion of low material density would remain protected from infiltration of the oxide matrix, effectively simulating a void in the material.

Copper spheres of appropriate diameters were cast inside the preform to simulate the metal-filled inclusion. During infiltration, molten aluminum reaches the copper inclusions before the copper melts. The molten aluminum dissolves the copper, and fills the void with molten metal rather than oxide, resulting in metal-filled inclusions of the desired diameters.

These techniques of creating inclusions were found to be successful. A cylinder preform was cast with two regions of spheres; one at each end and 180 degrees across from each other. Five spheres of each material (Cu, graphite, SiC/graphite) were cast into the wall in alignment. This created three rows of spheres, each row representing one type of flaw.

After matrix infiltration, half of the cylinder was machined smooth on the inside and outside surfaces. This gave both machined and unmachined regions of simulated flaws. The unmachined region was required to determine if the flaws could be detected in the cylinders retaining their rougher "as-cast" surface.

Radiographic Inspection of Witness Cylinder

All features placed into the preforms were well delineated in the radiographs of the infiltrated composite cylinder. Even the smallest spherical feature (1/32 inch) showed up quite well. Resolution was such that the very thin SiC coating on the graphite spheres simulating low-density flaws was visible. The roughness of the surfaces in the "as-cast",

unmachined region was visible, but there was no difficulty seeing any of the features.

The witness cylinder showed that similar flaws in any of the production cylinders would be quite visible and easily detectable.

Ultrasonic Inspection Of Witness Cylinder

The witness cylinder was also inspected by the full-immersion pulse-echo technique at Sonic Testing and Engineering, Inc. (Southgate, CA). Sonic Testing and Engineering used a 3/8-inch diameter, 3-inch focal length,10-MHz transducer to perform the inspection. The pulse-echo C-scan turned out to be so "noisy" that it was deemed unusable for the detection of flaws. It appeared that there were more flaws in the ceramic than intentionally planted. This may well have been the case as a full inspection of one of the deliverable cylinders resulted in a "clean" and uniform C-scan. More information on the NDE of ceramic components may be found in reference 6.

NDE of Deliverable Cylinders

The initial NDE plan included radiography of each cylinder blank prior to machining as well as radiography of the machined cylinders. After six cylinder blanks were radiographed without detected flaws, radiography before machining was dropped to streamline the delivery of parts for machining.

The NDE requirement was to locate and map all flaws that measured 0.030 inch, or greater, and locate and map all regions that varied in material density by more than 5 percent. Radiography was selected for this composite because prior experience with ultrasonic NDE had not been as promising for these composites as was hoped.

All radiographs were taken with a Mil Standard, 0.50-inch aluminum penetrameter in each shot to qualify the radiograph. In all radiographs, the "2T" hole was easily resolved (0.02-inch diameter, 0.01-inch thick).

Each radiograph also included a small step wedge machined from the Lanxide 90-X-089 ceramic composite. The wedge was machined with seven steps ranging from 0.3506 inch to 0.4744 inch. It was 0.5 inch wide and 1.75 inches long. This is a

thickness standard varying from a nominal 0.4125 inch ±5 percent, ±10 percent, and ±15 percent increments. The step wedge image in each radiograph was used to calibrate the individual radiograph's gray levels with actual material densities. The step wedge is necessary to correlate film density with material density for accurate results when the radiograph is digitized.

Radiography was performed by MQS Inspections, Inc. The source-to-film distance was 48 inches, and the spot size of the beam was 1.5 mm. These parameters yield a geometric unsharpness factor of 0.0005 inch. Sixteen films were used to shoot the entire circumference of each of the eight segments, with two films overlapping to cover both ends of the cylinder.

Initially, plans included digitizing the radiographs, but the radiographs of the witness specimen showed that the smallest features (0.030 inch) were easily detected. While digitization enhanced the images on the radiographs, it was not needed to locate or size the defects. The requirement for digitization of all radiographs was dropped, but it would still remain an option to evaluate suspicious regions on the radiographs.

All cylinders were radiographed prior to bonding the end rings. The films were read at Lanxide using an optical magnifier and a light box. None of the cylinders showed definitive flaws. Due to the size of the film and the length of the cylinders, all films overlapped in the center third of the cylinders. Features on one film could be checked against the mating surface of the overlapping film to confirm the presence of a flaw. Two low-material density flaws measuring about 0.030 inch were detected outside the overlap region on cylinder LAN 004 and reported. However, both flaws appeared identical to film-related flaws seen in other cylinder radiographs and probably were film artifacts.

PRESSURE TESTING

Test Setup

Three types of test assemblies were tested. They differed in the type of end closure used (hemispherical or flat) and the type of titanium end cap used.

Hemispherical end closures were planned for use in cyclic tests while flat end plates were planned for use in implosion tests, these being more rugged and, therefore, more capable of withstanding the force of the implosion at high pressure making them reusable. At program initiation, it was not planned that the cylinders would be cycled above 12,000 psi. The machined hemispherical ends were calculated not to provide enough buckling resistance above 12,000 psi, especially with low-modulus materials such as $SiC/Al_2O_3/Al$. For this reason, all cyclic tests run above 12,000 psi were run using flat end plates.

The differences in the two titanium end cap designs are in the external seal. The NRaD Mod 1, Type 2 end caps have a lip on the OD. During cylinder assembly, a silicon sealant is applied to this lip. The NRaD Mod 1, Type 1 end caps do not have such a lip. Type 1 end caps were originally intended for use in proof and implosion tests; Type 2 end caps were originally intended for cyclic tests because they were believed to ensure a better seal under repeated pressurization.

The three types of assemblies can be summarized as follows:

Assembly	End Cap	End Closure
Type I	Type 2	Hemispherical
Type II	Type 2	Flat Plate
Type III	Type 1	Flat Plate

Test assembly Type I is shown in figure 20. NRaD Mod 1, Type 2 end caps (figure 21) are epoxy bonded to the ends of the ceramic cylinder using the procedure described in note 4 of figure 20. A 0.010-inch-thick manila paper gasket (figure 22) ensures a minimum 0.010-inch thickness of epoxy on the bearing interface between the ceramic and the titanium.

Cylinders LAN 001 through LAN 006 were bonded onto the smooth, machined ceramic surface finish. However, test personnel noticed extrusion of the epoxy on the inner diameter of the cylinder on some of the cylinders after pressure testing. So, it was decided that a better bond between the titanium and the ceramic could be achieved if the

ceramic surface to which the end caps would be bonded were grit blasted prior to bonding. The bond surfaces on cylinders LAN 007 through LAN 012 were prepared by the following grit-blasting procedure.

Cylinder ends were cleaned with a suitable solvent. Then, the bearing surfaces of the cylinders were masked using industrial grade duct tape to ensure that the smooth bearing surfaces of the cylinders would not be subjected to grit blasting. The cylinder was placed into a Pro-Finish Model PF-3648 grit blaster manufactured by Empire Abrasive Equipment Co., 2101 W. Cabot Blvd., Langhorn, PA. Norton MCA-1360 abrasive grit (100 grit) was used in the blaster. Air pressure was set to 60 psi and the cylinder ends were grit blasted from a distance of approximately 6 to 8 inches in a smooth sweeping motion. Spraying was continued until the shiny machined ceramic developed a light frosted appearance.

In test assembly Type I, the cylindrical assembly is closed at both ends by titanium hemispheres (figure 23). The assembly is made watertight by a surface seal using a nitrile O-ring for which there is an O-ring gland machined into the titanium end cap. The titanium hemisphere is joined to the titanium cylinder end cap via a V-shaped steel clamp (figure 25).

Each cylinder was instrumented with five CEA-06-250-UT-120 strain-gage rosettes. These were located at the center of the cylinder length and spaced 72 degrees apart. Each of the 1/4-inch, 90-degree rosettes had one leg oriented in the hoop direction and the other in the axial direction. Electrical leads for the strain gages were passed through the pole of the upper hemisphere via a plug (figure 26) held in pace by a washer and nut (figure 27) on the inside of the hemisphere. The bottom hemisphere had a drain plug which could be opened to determine whether there had been any leakage during testing. A cylindrical wooden plug was placed inside the assembly to mitigate the shock of implosion should failure occur.

Figure 29 shows test assembly Type II. This test assembly is identical to test assembly Type I,

except that the cylinder ends are closed by flat steel bulkheads (figure 30) instead of titanium hemispheres.

Figure 31 shows test assembly Type III which uses NRaD Mod 1, Type 1 titanium end caps (figure 32) instead of the Type 2 end caps used in test assembly Type II. Test assembly Types II and III are held together by four 1/2-inch steel tie rods (figure 33). Strain-gage leads are passed through the feed-throughs shown in figure 34. The force of implosion is mitigated by a cylindrical wooden plug (figure 35). Figure 36 is a photograph of a fully machined cylinder with NRaD Mod 1, Type 2 end caps epoxy bonded to it. Figure 37 shows a complete Type II assembly being lowered into a pressure chamber at Southwest Research Institute (SRI), San Antonio, TX, prior to pressurization. All testing was performed at SRI. Figure 38 shows an "as-cast" cylinder, LAN 007, with its green epoxy coating and Mod 1, Type 2 titanium end caps bonded to it.

Pressure Testing

Pressure testing was performed in accordance with the test plan/result summary shown in table 9. Strains were read at 1,000-psi intervals on the first pressurization for each cylinder. When cylinders were to be purposely taken to failure pressure, strains also were read during the second cycle. Acoustic emissions were monitored on cylinders LAN 008 and LAN 009. In test cases where the cylinder withstood all planned pressure testing, at least one end cap was removed using the end cap removal fixture shown in figure 39. The method of end cap removal involves heating up the cylinder end to be removed, which breaks down the epoxy, and then pulling the end cap off the cylinder. Adequate force can be applied to remove the end cap by using the mechanical advantage of turning the nuts on the four 1/2-inch-diameter tie rods. After the end cap was removed, the cylinder was cleaned and taken to Sonic Testing and Engineering, Inc., for pulse-echo ultrasonic inspection to determine the presence and extent of internal circumferential cracking. What follows is a brief summary of the pressure testing.

Cylinder **LAN 001** was proof tested to 12,000 psi and inspected. There was no damage, and no leaks were detected. Strains were read at 1,000-psi intervals and plotted (figure 40). The proof test was followed by 2,000 cycles to 12,000 psi, which the cylinder withstood without any visible damage. After completion of testing, one cylinder end cap was removed, dye-penetrant was applied, but no cracking was visible on the bearing surface. Pulse-echo ultrasonic inspection did show internal circumferential cracking along the entire circumference of the cylinder. Figure 41 shows the C-scan of one end of the cylinder. The pulse-echo ultrasonic inspection was performed by Sonic Testing and Engineering using a 3/8-inch diameter, 3-inch focal length, 10-MHz transducer. Circumferential scans were taken at 0.050-inch interval spacing. Inspection showed that cracks did not extend more than 0.75 inch from the bearing surface.

Cylinder **LAN 002** was proof tested and cycled to 12,500-psi pressure. The cylinder failed during pressurization number 1,968. Figure 42 shows the plotted strain gage data. Figure 43 shows the cylinder end cap remains.

Cylinder **LAN 003** was proof tested and cycled at 16,000 psi. It completed 464 cycles before the test was terminated due to pressure test equipment problems. Strain data is shown in figure 44. Both end caps were removed from the ends of this cylinder. Pulse-echo ultrasonic inspection showed that one end was entirely free of cracks, while the other end had cracks (figure 45) which did not extend more than 0.50 inch.

Cylinder **LAN 004** was proof tested and cycled to 13,000-psi external pressure. Strain data is shown in figure 46. The cylinder failed on cycle number 801.

Cylinder **LAN 005** was proof tested and cycled to 12,500-psi external pressure. Figure 47 shows the strain data taken during proof cycling. The cylinder withstood 2,902 cycles before testing was terminated. Minor extrusion of epoxy was noted on the ID of one end of the cylinder. It was removed and ultrasonically inspected for internal circumferential cracks. Figure 48 shows the results of that inspection.

Cylinder **LAN 006** was proof tested and pressure cycled at 14,000-psi external pressure. The cylinder failed on cycle number 331. Strain gage data are plotted on figure 49.

Cylinder **LAN 007** was the first of two "as-cast" cylinders to be tested. It was the first cylinder on which the ends were grit blasted before titanium end caps were epoxy bonded to it. This cylinder was proof tested and cycled to 12,500 psi. The cylinder failed on cycle number 531. Strain data are plotted in figure 50. The slope of the strain vs. pressure plots are less steep than for the fully-machined cylinders because of the slightly thicker walls of these cylinders.

Cylinder **LAN 008** was proof tested to 10,000 psi, pressurized to 15,000 psi, and finally pressurized to failure, which occurred at 19,000 psi. Strain data for the first and second cycles are plotted in figures 51 and 52, respectively. Acoustic emissions for all three cycles are plotted in figure 53.

Cylinder **LAN 009** was proof tested and cycled to 15,000-psi external pressure. Strain data from the first and second cycles are plotted in figures 54 and 55, respectively. Acoustic emissions for pressurization numbers 1, 2, and 161 are plotted in figure 56. The cylinder withstood 3,003 cycles to 15,000 psi. Examination of the cylinder after testing revealed a chip on the OD. The chip was approximately 0.5 inch in diameter and less than 0.10 inch deep. One end of the cylinder was ultrasonically inspected after removal of the titanium end cap. Figure 57 shows the results of this inspection. Internal circumferential cracks did not extend more than 0.60 inch.

Cylinder **LAN 010** was proof tested and cycled to 13,000 psi. It withstood 3,001 cycles without any visible damage. Strain data are plotted in figure 58. A pulse-echo C-scan of one end is shown in figure 59. Cracking was found to be minimal, not extending more than 0.20 inch.

Cylinder **LAN 011** was proof tested to 10,000 psi and pressurized to failure, which occurred at 19,000 psi. Strain data are plotted in figures 60 and 61, respectively. Note that hoop strains start

diverging at 18,000-psi external hydrostatic pressure.

Cylinder **LAN 012** was the second and final deliverable "as-cast" cylinder. This cylinder was proof tested and cycled to 12,500 psi. The cylinder withstood 2,004 cycles without any apparent damage. Strain data are plotted in figure 62. The ends of this cylinder were not inspected for internal circumferential cracking. The green epoxy coating had a blistered appearance after testing.

TEST OBSERVATIONS/DISCUSSION

MATERIAL PROPERTIES

Table 8 contains a summary of the average material properties measured on specimens taken from the twelve 90-X-089 cylinders. Tables D-1 through D-24 in appendix D show the same data along with the actual raw data for each batch of test specimens taken from the cylinders.

The mean compressive strength of the twelve cylinders was measured to be 301.2 ksi with a standard deviation of 12.7 ksi. The minimum average compressive strength was measured in cylinder LAN 002 at 269.0 ksi, while the maximum average compressive strength of 321.4 ksi was measured in cylinder LAN 004.

The mean compressive modulus measured was 41.6 Msi, with a standard deviation of 1.6 Msi. A high average modulus of 44.7 was measured in cylinder LAN 003; the low of 38.9 Msi was measured in cylinder LAN 002.

The mean fracture toughness was 7.59 ksi*in$^{1/2}$ with a standard deviation of 0.93 ksi*in$^{1/2}$. The maximum fracture toughness of 8.87 ksi*in$^{1/2}$ was measured in cylinder LAN 005 and the minimum of 5.13 ksi*in$^{1/2}$ was measured in cylinder LAN 008.

The specific gravity of the material stayed fairly constant from cylinder to cylinder. The mean specific gravity was 3.365 gm/cc with a standard deviation of 0.013 gm/cc.

The mean flexural strength of all twelve cylinders was measured to be 56.2 ksi, with a standard devi-

ation of 2.8 ksi. A minimum flexural strength of 48.7 ksi was measured in cylinder LAN 008 and a maximum average flexural strength of 62.4 ksi was measured in cylinder LAN 002.

STRAINS

The strain vs. pressure plots for the twelve cylinders show that strains increased linearly with increasing pressure. With the exception of the two "as-cast" cylinders, strains remained fairly uniform from cylinder to cylinder. The average hoop strain at 10,000-psi external hydrostatic pressure for the ten fully-machined cylinders was 3,159.2 microinch/inch with a standard deviation of only 35.5 microinch/inch. The average axial strain at 10,000-psi external hydrostatic pressure was 936.2 microinch/inch with a standard deviation of 13.8 microinch/inch.

Strains were recorded on the first two pressurizations of cylinders LAN 008, LAN 009, and LAN 011. Data shows that the compressive strains decreased with repeated pressurization.

Strains in cylinder LAN 008 at 10,000-psi external pressure on the first and second pressurizations:

	Hoop Strain (micro-inch/inch)	Axial Strain (micro-inch/inch)	Calculated	
			Compressive Modulus (psi)	Poisson's Ratio (psi)
1st Cycle	3,170.8	939.6	41,880,000	0.239
2nd Cycle	3,033.6	922.2	43,970,000	0.231
Difference	137.2	17.2	2,090,000	0.008

Strains in cylinder LAN 009 at 10,000-psi external pressure on the first and second pressurizations:

	Hoop Strain (micro-inch/inch)	Axial Strain (micro-inch/inch)	Calculated	
			Compressive Modulus (psi)	Poisson's Ratio (psi)
1st Cycle	3,184.0	936.6	41,450,000	0.242
2nd Cycle	2,986.2	919.6	44,770,000	0.227
Difference	197.8	17.0	3,120,000	0.014

Strains in cylinder LAN 011 at 10,000-psi external pressure on the first and second pressurizations:

13

	Hoop Strain (micro-inch/inch)	Axial Strain (micro-inch/inch)	Calculated	
			Compres-sive Modulus (psi)	Poisson's Ratio (psi)
1st Cycle	3,184.0	940.2	41,450,000	0.242
2nd Cycle	3,058.6	934.2	43,650,000	0.230
Difference	140.4	6.0	2,200.000	0.012

This phenomenon was first noticed by Dr. Stachiw in the 6-inch-OD by 9-inch-long cylinders fabricated from the same composition (reference 4). The decrease in the magnitude of the compressive strains is not large, but still significant, and indicates that a compaction process is taking place during the first few pressurizations. Because Dr. Stachiw was the first to observe and describe the compaction of the ceramic under hydrostatic loading, it is referred to in this and other reports as the Stachiw effect. This compaction process affects the computed compressive modulus and Poisson's Ratio of the material. The compressive modulus and Poisson's Ratio in columns four and five of the tables were calculated with the following equations.

A thick-wall stress equation from reference 7 was used to compute the expected stress at 10,000-psi external psi on the ID of the cylinder:

$$\sigma_{axial} = \frac{-qa^2}{a^2-b^2}$$

$$\sigma_{hoop} = \frac{-q2a^2}{a^2-b^2}$$

where q = external pressure
a = outer radius
b = inner radius

Then, the following two equations were solved simultaneously for compressive modulus and Poisson's Ratio:

$$\varepsilon_{axial} = \frac{1}{E}(\sigma_{axial} - \gamma\sigma_{hoop})$$

$$\varepsilon_{hoop} = \frac{1}{E}(\sigma_{hoop} - \gamma\sigma_{axial})$$

where E = compressive (Young's) modulus.

The same calculation was repeated for all ten fully-machined cylinders and the results were summarized (table 10). The average computed compressive modulus was 42.04 Msi with a stan-

dard deviation of 0.52 Msi. These values are well within the range of values measured on specimens taken from the cylinder ends. A maximum compressive modulus of 42.98 Msi was calculated for cylinder LAN 001 and a minimum elastic modulus of 41.45 Msi was calculated for cylinder LAN 011. The mean Poisson's Ratio was calculated to be 0.239 with a standard deviation of 0.004.

The strains measured in the two "as-cast" cylinders, LAN 007 and LAN 012, were considerably lower than those in the fully-machined cylinders. This is probably because these cylinders had a slightly greater wall thickness (approximately 0.120 inch thicker) and, therefore, strained less under equivalent stress.

As stated previously, strains in all cylinders remained linear throughout pressurization. Cylinders LAN 008 and LAN 011 were pressurized to failure; strains remained linear up to about 18,000-psi external hydrostatic pressure. At pressures higher than that, the hoop and axial strains diverge, indicative of the cylinder going slightly out-of-round prior to buckling. The failure pressure of 19,000 psi recorded for both cylinders indicates that the critical pressure is repeatable and validates both hand and computer calculations. Hand calculations were based on equation 15.3 of reference 8 derived for closed-ended housings under uniform external pressure where the ends of the cylinder are assumed to be simply supported. The effective length of the cylinder was calculated as follows:

$$L = 18 + 2(0.09) - 2(0.68) = 16.82$$

where 18 is the cylinder length in inches, 0.09 is the bearing thickness of the titanium end caps, and 0.68 equals the engagement length of the cylinder with the flat steel end closure.

Computer calculations were made using the computer program BOSOR4 (reference 9). BOSOR4 is a structural analysis computer program developed by David Bushnell at Lockheed Missiles and Space Co., Inc., that can be used to predict buckling of complex shells of revolution. The meridian of the shell is modeled using a number of segments with material, geometric, and end-constraint conditions representative of the actual structure. Buckling calculations are based on finite difference energy

minimization and can be computed for a range of circumferential wave numbers. More details concerning stress and bucking calculations can be found in reference 10.

The table below summarizes hand and computer calculations made for two sets of engineering properties: those calculated from cylinder strains on the first cycle and those calculated from strains measured on the second cycle. As one can see, the experimental critical collapse pressure of the cylinders lies above the hand-calculated results and below the computer-calculated results.

Cylinder	Engineering properties used in calculation	Hand-calculated collapse pressure	BOSOR4 collapse pressure
LAN 008	E = 41.88 Msi v = 0.239	17,625 psi	22,837 psi
	E* = 43.97 Msi v* = 0.231	18,449 psi	23,833 psi
LAN 011	E = 41.45 Msi v = 0.242	17,463 psi	22,640 psi
	E* = 44.77 Msi v* = 0.227	18,661 psi	23,858 psi

ACOUSTIC EMISSIONS

Acoustic emissions were monitored on cylinders LAN 008 and LAN 009, and recorded results indicate that emissions drop down to almost zero beyond the third pressurization. This behavior is in accordance with the Kaiser Effect which predicts a decrease in the number of acoustic emissions in a material. The acoustic data would seem to verify the "compaction" effect. Figure 53 shows the acoustic emission data for cylinder LAN 008; the number of acoustic events decreases from 1,800 events while climbing to 10,000 psi for the first time, to approximately 100 events by 10,000 psi on the second cycle, and approximately 8 events by 10,000 psi on the third cycle. Acoustic emissions monitored on cylinder LAN 009 follow a similar trend.

CYCLIC FATIGUE LIFE

Figure 63 is a plot of the external hydrostatic pressure (and nominal membrane stress) vs. the num-

ber of pressurizations to failure, or the number of pressurizations withstood by the test cylinders. Examination of the data shows that any attempt to relate the cyclic performance of the cylinders to the level of stress to which they have been tested would be inconclusive. However, the following findings can be formulated on the basis of data generated in these tests:

1. Three cylinders failed at a relatively low number of cycles when compared with the performance of the other seven cylinders. These cylinders were LAN 004, LAN 006, and LAN 007. Cylinders LAN 004 and LAN 006 had ends which were not sand blasted and were, therefore, probably more susceptible to leaks and/or epoxy extrusion. Cylinder LAN 007 had relatively low fracture toughness, however, LAN 012 had equally low fracture toughness and performed many more cycles than LAN 007. The only material property the three cylinders had in common was that their flexural strength was either close to, or less than, the average flexural strength of the twelve cylinders. It may be that flexural strength is an important material property in this application. Finite-element stress analysis has shown that a tensile stress exists near the bearing surface of the cylinders (references 10, 11, and 12).

2. Pulse-echo C-scans taken of cylinders which withstood all planned testing indicated that none of the internal circumferential cracks extended beyond 0.75-inch axial length. All cylinders which had only one end inspected showed internal circumferential cracking. Cylinder LAN 003, pressurized 464 times to 16,000 psi, was inspected on both ends; spalling was found in only one end. No conclusion can be made which relates the extent of crack growth to the stress applied or to the number of pressure cycles applied.

3. Dye-penetrant inspection of the exposed bearing surfaces did not reveal the internal circumferential cracks.

15

CONCLUSIONS

The four main objectives of this study were met:

1. Demonstrate the ability of Lanxide to scale up the proprietary DIMOX™ process to fabricate 12-inch-OD by 18-inch-long by 0.412-inch-thick ceramic composite cylinders of equal quality to the 6-inch-OD by 9-inch-long by 0.206-inch-thick cylinders previously supplied to NRaD. Determine the uniformity and repeatability of these composite cylinders in a quantity scale-up to twelve cylinders.

   Lanxide was able to fabricate12-inch-OD by 18-inch-long cylinders with material properties that either meet or exceed the properties of the 6-inch-OD by 9-inch-long cylinders previously supplied. Calculations based on strains measured during the testing of the 6-inch-OD by 9-inch-long cylinders resulted in a compressive modulus varying between 40 and 45 Msi and a Poisson's Ratio of approximately 0.23. The compressive strength of the material previously delivered in the 6-inch-OD cylinder was approximately 283,000 psi.

   The 12-inch-OD by 18-inch-long cylinders maintained an average compressive modulus of 41.6 Msi, Poisson's Ratio of 0.239, and a compressive strength of 301.2 psi. The compressive strains in both the 6- and 12-inch-OD cylinders exhibited the Stachiw Effect (i.e., significant permanent deformation of the ceramic composite during the first compressive loading).

   Standard deviations calculated for each of the measured and/or calculated engineering properties were small enough to indicate that the cylinders can be fabricated very uniformly and repeatedly. Radiographic nondestructive inspection of the cylinders indicate that these cylinders can be fabricated free of defects.

2. Determine the structural performance of the cylinders under external hydrostatic pressure loading. This includes critical collapse pressure, cyclic fatigue life, and performance repeatability.

The structural performance of the twelve cylinders turned out to be very good. None of the cylinders failed in a manner which cannot be explained. All twelve passed proof tests to at least 10,000-psi external hydrostatic pressure. Those failures which did occur were caused either by cyclic fatigue or by purposely pressurizing the cylinders to critical collapse pressure. The two cylinders which were purposely pressurized to failure not only failed at identical pressure, 19,000 psi, but failed according to buckling failure predictions made by hand calculations and computerized buckling analysis.

Although tests were inconclusive regarding the relation between the number of pressurizations a cylinder can withstand and the stress level in the cylinder, tests did show that Lanxide's 90-X-089 cylinders can withstand at least 1,000 cycles to 9,000-psi external pressure before failure in the design configuration presented and tested in this report. In fact, it is safe to use a maximum nominal design stress of 182,039 psi in the design of the cylinder if 1,000 pressurizations are to be expected. Pulse-echo ultrasonic inspection of cylinders which withstood cyclic pressurization shows that cracks in those cylinders did not extend more than 0.75 inch, even after 3,003 cycles to 15,000-psi external pressure 218,447 psi maximum membrane stress.

3. Compare the performance of the 90-X-089 cylinders against the baseline composition, AL-600 96-percent alumina ceramic manufactured by WESGO.

   Lanxide 90-X-089 has lower compressive strength and lower compressive modulus than WESGO's AL-600 96-percent alumina ceramic. However, its density is lower, and it has higher fracture toughness and higher flexural strength. The last two properties may account for why the material has a better fatigue life than the 96-percent composition and can, therefore, be designed to higher levels of maximum nominal hoop stress while maintaining a 1,000-pressure-cycle rating. The following table compares the material properties of the two materials.

16

	AL-600 96-percent Al_2O_3	90-X-089
Compressive strength (ksi)	350	301
Compressive modulus (Msi)	47.0	41.6
Flexural strength (ksi)	47.0	56.2
Fracture toughness ($ksi*in^{1/2}$)	2.50	7.59
Specific gravity	3.749	3.365

Table 11 compares the cyclic pressurization performance of the two materials. The 90-X-089 composition performs better than the 96-percent alumina-ceramic composition at all levels of stress. The lower weight of the material allows designs having lower weight-to-displacement (W/D) ratios than 96-percent alumina ceramic. The table below compares the weights of the fully-machined and "as cast" 90-X-089 cylinder assemblies (including titanium end caps). The weight of an alumina-ceramic assembly with identical dimensions is included for comparison. These weights represent the actual cylinder assemblies tested, less the end closures which may be of a variety of designs.

Assembly	Displace- ment in seawater (lbs)	Weight (lbs)	Weight-to- displace- ment ratio
Fully-machined 90-X-089 cylinder	76.9	38.0	0.494
"As-cast" 90-X-089 cylinder	78.2	40.5	0.518
AL-600 96-percent alumina-ceramic cylinder	76.9	42.0	0.546

More optimum W/D ratios are attainable if design stress levels found to be safe after testing of these first twelve cylinders are used. Figure 64 plots the achievable W/D ratio of cylinders fabricated from Lanxide's 90-X-089 and WESGO's AL-600 96-percent alumina ceramic having a length-to-diameter ratio of 1.5 and designed for a cyclic fatigue life of 1,000 pressurizations to design depth. In a 12-inch-OD by 18-inch-long cylindrical

assembly, the difference may account for approximately 2.6 pounds of extra payload capability for the design to 20,000 feet. Whether this difference is worth the difference in cost between the two materials, which approaches an order of magnitude, has to be determined by the project manager.

4. Determine the ability of the DIMOX™ process to produce cylinders close enough to net shape that only the ends of the cylinders require machining without any loss in performance.

Lanxide was able to produce cylinders close enough to net shape that only the ends of the cylinder required machining. The data presented in tables 2, 3, and 4 demonstrates the very low dimensional changes that occur during the DIMOX™ growth process. The growth process did not affect the basic shape of the preforms. The dimensional quality of the final part is basically that of the preform. The key to getting the most reproducible cylinder component (one that requires almost no machining to meet performance specifications) is to produce the silicon-carbide preform to the dimensions and tolerances required in the final cylinder before the infiltration step.

The most direct way of doing this (using the casting methods of the 90-X-089 composition) is to use a precision mold that is rigid and dimensionally stable during the preform freeze cycle. It is clear that the fiberglass/rubber mold used for this program was not dimensionally stable enough to cast preforms that are round within 0.010 to 0.020 inch. Fabricating mold elements out of different material, such as metal or graphite-reinforced epoxy composite, may be all that is required to yield a dimensionally stable mold.

One of the two "as-cast" cylinders failed at a lower number of cycles than three other cylinders tested at the same level of stress (182,039-psi nominal hoop stress). Two of these cylinders were fully machined, and the third was the other "as-cast" cylinder. "As cast" cylinder, LAN 007, failed after 531 cycles to 12,500-psi external pressure; the second "as-cast" cylinder withstood 2,004

cycles to the same test pressure. The difference cannot be explained easily as both cylinders had relatively low fracture toughness.

Although 85-percent less surface area requires grinding, the cost savings in grinding is not reduced by 85 percent. An estimated $2,000 can be saved by going from the fully-machined design to the "as-cast" design—a mere 10-percent reduction in price. The weight penalty is minimal. The cost savings are not more substantial because the majority of the labor required to grind the component is in setting up the grinding machine and aligning it properly. The actual grinding of the component can be performed unattended.

Although the cost savings for monocoque hulls is not as substantial as originally anticipated, the DIMOX™ process still has other advantages. The uniqueness of the DIMOX™ process' near-net-shape capability lends itself to geometries that are not practical with traditional ceramic processing. The incorporation of integral ribs on the inside walls of monocoque cylinders provides greatly improved design performance in terms of the W/D ratio. Such ribs can be machined into the inside of the cylinder of iso-pressed parts, but because of the cost of diamond machining, and the quantity of material to be removed, this becomes prohibitively expensive. Green ceramic cylinders can be machined cost effectively, and it is possible to machine internal ribs in a green cylinder. However, traditional processing of ceramics involves substantial dimensional changes in the part during sintering, resulting in very large shrinkage factors (typically 15 percent or greater). Geometries with large differences in wall thickness, such as a cylinder with internal ribs, are predicted to have residual stresses between the thinner wall and the thick wall due to their variable shrinkage factors.

Since the DIMOX™ process uses sediment casting to form the green preform, soft rubber molds can be used to form integral ribs with no difficulty. The matrix infiltration process is essentially free of any dimensional changes in the preform. There is no variable shrinkage

problem in infiltrating green preforms with internal ribs as there is in conventional sintering. The only development work required would be in applying techniques already developed to control the infiltration rate in the thinner region to stop the directed metal-oxidation growth front when it reaches the inside of the thinner wall. This will maintain a smooth surface while the matrix continues to grow through the thicker wall areas to complete the infiltration in those areas.

RECOMMENDATIONS

The following recommendations are made based on the testing performed on the twelve 12-inch-OD by 18-inch-long by 0.412-inch-thick Lanxide 90-X-089 cylinders:

1. Lanxide 90-X-089 is recommended for use in the construction of external pressure housings up to 12-inch-OD by 18-inch-length. Utilization of the composition for cylinders with dimensions greater than this is recommended only after a thorough test and evaluation program.

2. "As-cast" cylinders can be used for deep submergence applications; the weight penalty of using "as-cast" cylinders is negligible, but so are the cost savings associated with using an "as-cast" cylinder instead of a fully-machined cylinder. Therefore, unless delivery schedule is an important factor, one may as well purchase a fully ground cylinder.

3. If Lanxide's 90-X-089 is to be used in an underwater external-pressure application and 1,000 cycles to design depth are expected, the design should be such that the maximum nominal compressive stress does not exceed 182,039 psi. The following are engineering properties to be used for engineering calculations and to be called out on the engineering drawings:

Compressive Strength:	301,000 psi
Compressive Modulus:	41,600,000 psi
Flexural Strength:	56,200 psi
Fracture Toughness:	7.6 ksi*in$^{1/2}$
Specific Gravity:	3.365
Poisson's Ratio:	0.24

Standard finite-element analysis and buckling analysis can be used to analyze pressure-housing designs using 90-X-089.

Furthermore, the cylinder assembly design should incorporate Mod 1, Type 2 end caps bonded in accordance with note 4 in figure 20 to the ceramic surface prepared in accordance with the grit-blasting procedure outlined in this report.

4. Prior to assembly of the cylindrical assembly, the ceramic cylinder should be inspected radiographically. A pulse-echo ultrasonic inspection using a 3/8-inch diameter, 3-inch focal length, and 10 MHz transducer may also be beneficial. The circumferential scanning interval should be 0.010 inch. However, the radiographic inspection represents the minimum required inspection.

5. The cylindrical ceramic housings after placement in service should be periodically nondestructively inspected for presence of circumferential fatigue cracks in the ceramic bearing surfaces on the ends of the cylinder. The frequency of inspections shall depend on the number of dives that the housing performed to 75 percent of its design depth. The frequency of inspections recommended for housings in critical service application is 100 dives, while for noncritical service applications it is 500 dives.

6. In the interest of advancing the state of ceramic fabrication technology, it is strongly recommended that the DIMOX™ process be scaled up to 20-inch-OD by 30-inch-long cylinders and that these cylinders be evaluated by cyclic pressurization. This would help determine whether there are any problems associated with the scale-up to larger cylinder sizes as there appear to be with AL-600 96-percent alumina ceramic manufactured by WESGO (reference 10).

7. Because the 90-X-089 $SiC/Al_2O_3/Al$ composition is not entirely inert to the effects of corrosion, it is strongly recommended that all components, fully-machined and "as-cast," be treated with an epoxy coating such as the one applied by Technicote.

8. Research should be performed to find a method to determine residual stresses in ceramic components by nondestructive means. This may be of special interest with components manufactured by the DIMOX™ process, as there is reason to believe that these components do not have residual stresses in them because of the fabrication techniques. If this is found to be true, the DIMOX™ process will have overcome a problem which has not yet been overcome in the fabrication of the AL-600 96-percent alumina-ceramic components manufactured by WESGO.

REFERENCES

1. Kurkchubasche, R.R., R.P. Johnson, and J. D. Stachiw. 1993. "Application of Ceramic to Large Housings for Underwater Vehicles: Program Outline." NRaD TD 2585 (Oct). NCCOSC RDT&E Division, San Diego, CA.

2. Stachiw, J.D. 1993. "Exploratory Evaluation of Alumina Ceramic Housings for Deep Submergence Service–Third Generation Housings" NRaD TR 1314 (Jun). NCCOSC RDT&E Division, San Diego, CA.

3. Stachiw, J.D. 1990. "Exploratory Evaluation of Alumina Ceramic Housings for Deep Submergence Service: Fourth Generation Housings," NOSC TR 1355 (Jun). Naval Ocean Systems Center, San Diego, CA.

4. Stachiw, J.D., T.J. Henderson, and C.A. Anderson. 1991. "Novel Ceramic Matrix Composites for Deep Submergence Pressure Vessel Applications." NOSC TD 2222 (Oct). NCCOSC RDT&E Division, San Diego, CA.

5. Munz, D.G., J.L. Shannon, and R.T. Bubsey. 1980. "Fracture Toughness Calculations for Maximum Load Four Point Bend Tests of Chevron Notch Specimens," *International Journal of Fracture*, vol. 16, pp. R137–R141.

6. Kurkchubasche, R.R., R.P. Johnson, and J.D. Stachiw. 1993. "Evaluation of Nondestructive Inspection Techniques for Quality Control of Alumina-Ceramic Housing Components," NRaD TR 1588 (Sep). NCCOSC RDT&E Division, San Diego, CA.

7. Roark, R.J. and W.C. Young. 1975. "Formulas for Stress and Strain," Fifth Edition.

8. Bickell, M.B. and Dr. M.C. Ruiz. "Pressure Vessel Design and Analysis," St. Martin's Press.

9. Busnell, D. "BOSOR4 User's Manual," Lockheed Missiles and Space Co., Inc.

10. Johnson, R. P., R. R. Kurkchubasche, and J. D. Stachiw. 1993. "Evaluation of Alumina-Ceramic Housings for Deep Submergence Service: Fifth Generation Housings—Part I," NRaD TR 1584 (Mar). NCCOSC RDT&E Division, San Diego, CA.

11. Johnson, R.P., R.R. Kurkchubasche, and J.D. Stachiw. 1993. "Structural Performance of Cylindrical Pressure Housings of Different Ceramic Compositions Under External Pressure Loading, Part I, Isostatically Pressed Alumina Ceramic," NRaD TR 1590 (Aug). NCCOSC RDT&E Division, San Diego, CA.

12. R. P. Johnson, R. R. Kurkchubashe, and J. D. Stachiw. 1993. "Structural Performance of Cylindrical Pressure Housings of Different Ceramic Compositions Under External Pressure Loading: Part II, Zirconia Toughened Alumina Ceramic," NRaD TR 1593 (Dec). NCCOSC RDT&E Division, San Diego, CA.

13. R. R. Kurkchubasche, R. P. Johnson, and J. D. Stachiw. 1994. "Structural Performance of Cylindrical Pressure Housings of Different Ceramic Compositions Under External Pressure Loading: Part III, Sintered Reaction Bonded Silicon Nitride Ceramic," NRaD TR 1592 (June). NCCOSC RDT&E Division, San Diego, CA.

14. Johnson, R.P., R.R. Kurkchubasche, and J.D. Stachiw. 1993. "Design and Structural Analysis of Alumina-Ceramic Housings for Deep Submergence Service: Fifth Generation Housings," NRaD TR 1583 (Mar). NCCOSC RDT&E Division, San Diego, CA.

15. Stachiw, J.D., R.P. Johnson, and R.R. Kurkchubasche. 1993. "Evaluation of Scale-Model Ceramic Pressure Housing for Deep Submergence Service: Fifth Generation Housings," NRaD TR 1582 (Mar). NCCOSC RDT&E Division, San Diego, CA.

GLOSSARY

CVI	chemical vapor infiltration	NDE	nondestructive evaluation
		NOSC	Naval Ocean Systems Center
DIMOX™	Lanxide's directed metal oxidation (process)	OD	outside diameter
		SiC	silicon carbide
		SRI	Southwest Research Institute
ID	inside diameter	UUV	unmanned underwater vehicle
L	Length	W/D	weight to displacement
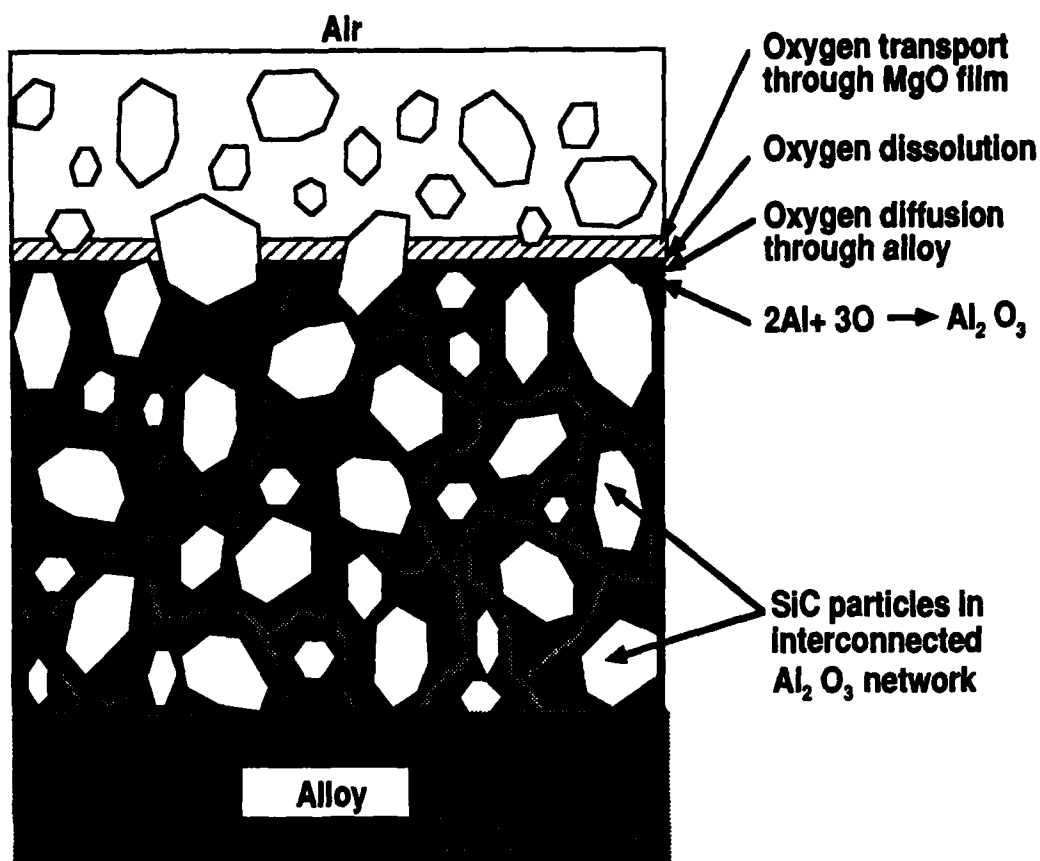
Figure 1. Illustration of the growth mechanism for the formation of alumina-ceramic composites via the DIMOX™ process.

Preform Production

- Slurry Mixing

- Casting

- Vibratory Settling

- Freezing

- Drying

Composite Production

- Barriers & Initiators

Alloy ↓ Oxygen

- DIMOX™ Growth

- Grit Blasting

Post Growth Processing

- Grind to Specification

- NDE

- Coatings

Ship to NCCOSC RDT&E Division
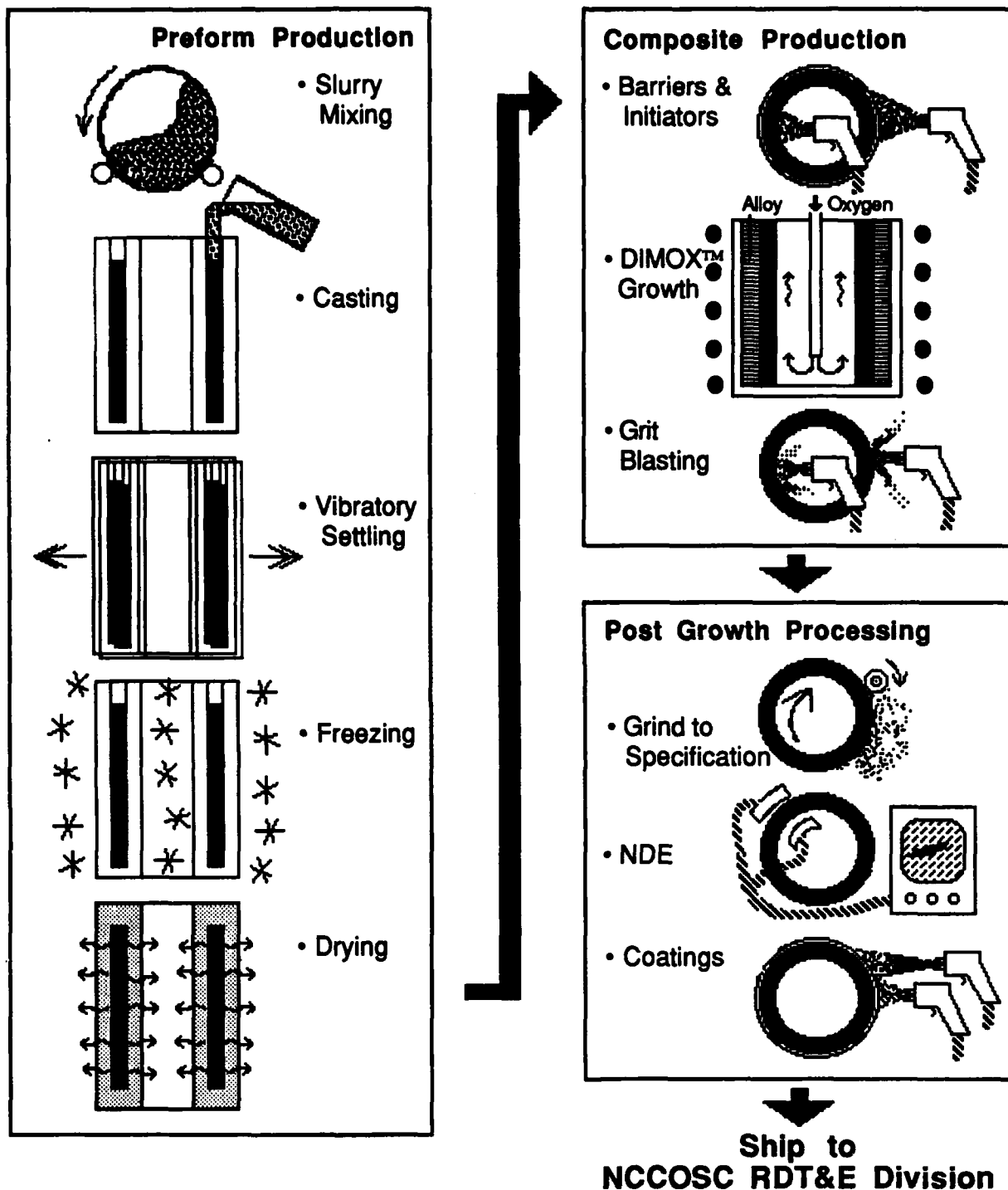
Figure 2. Processing steps to produce a ceramic composite cylinder.
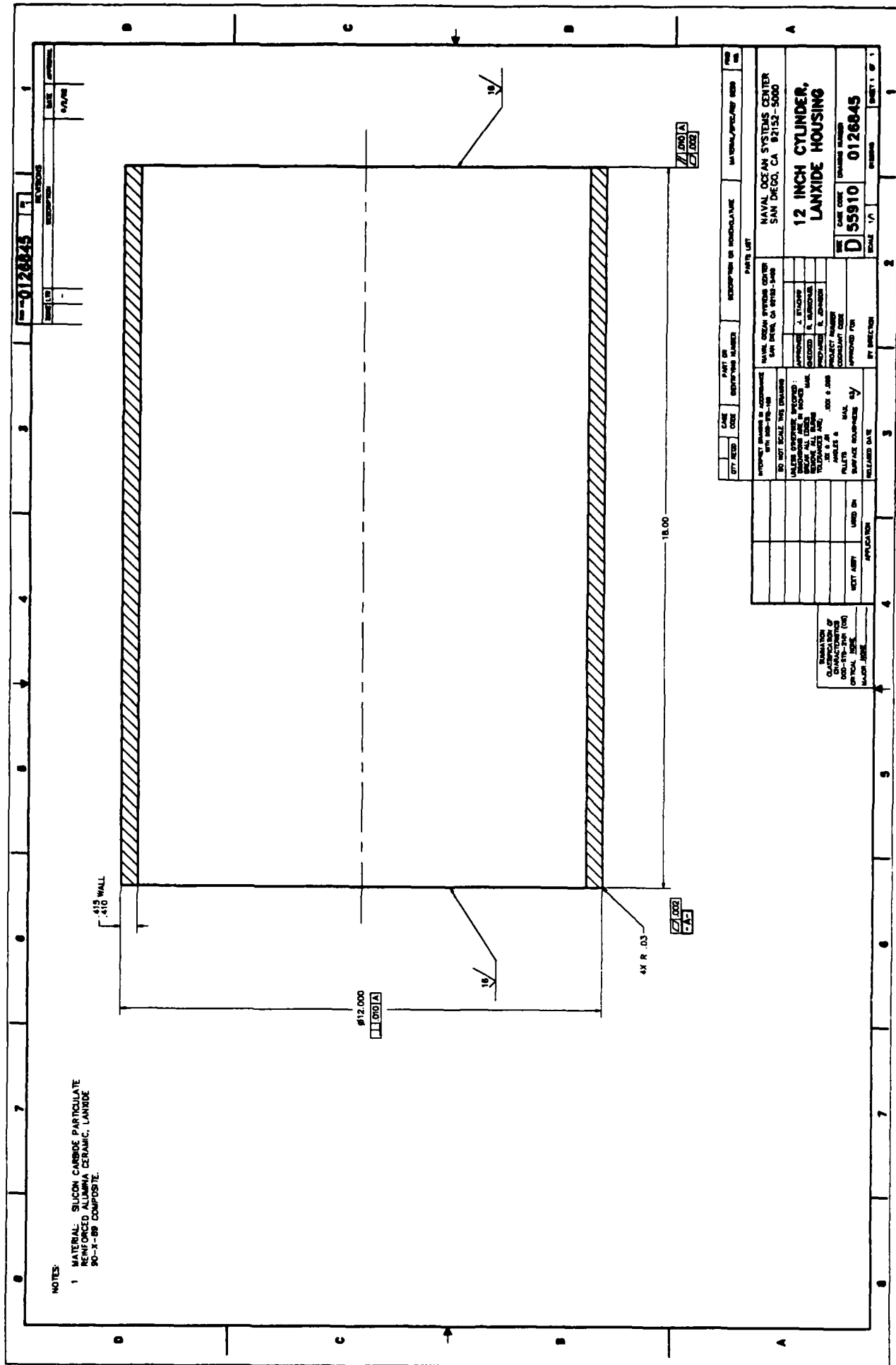
Figure 3. Engineering drawing for fully-ground 12-inch-OD by 18-inch-long SiC/Al$_2$O$_3$/Al composite cylinder.
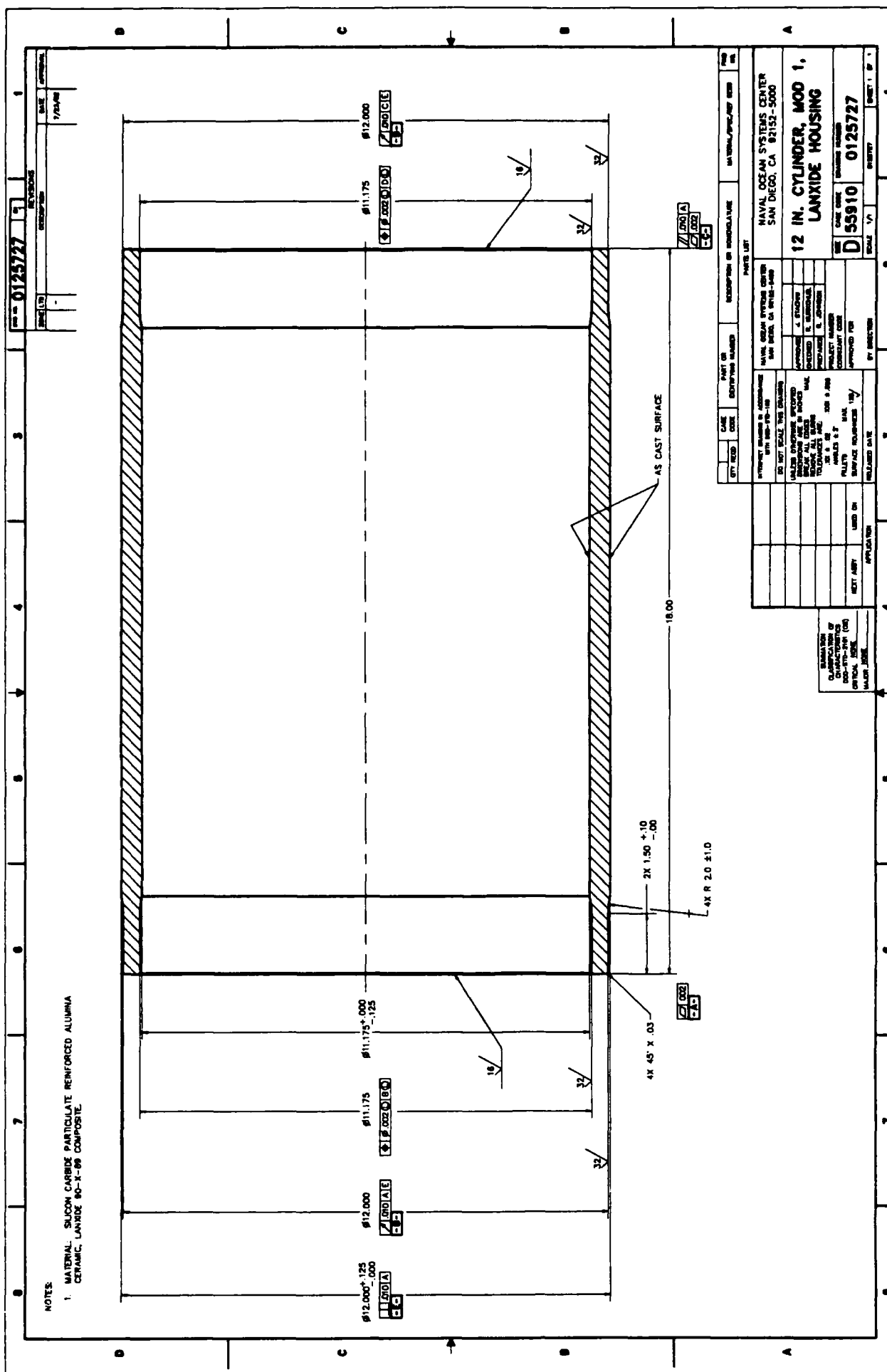
Figure 4. Engineering drawing for "as-cast" 12-inch-OD by 18-inch-long SiC/Al₂O₃/Al composite cylinder.
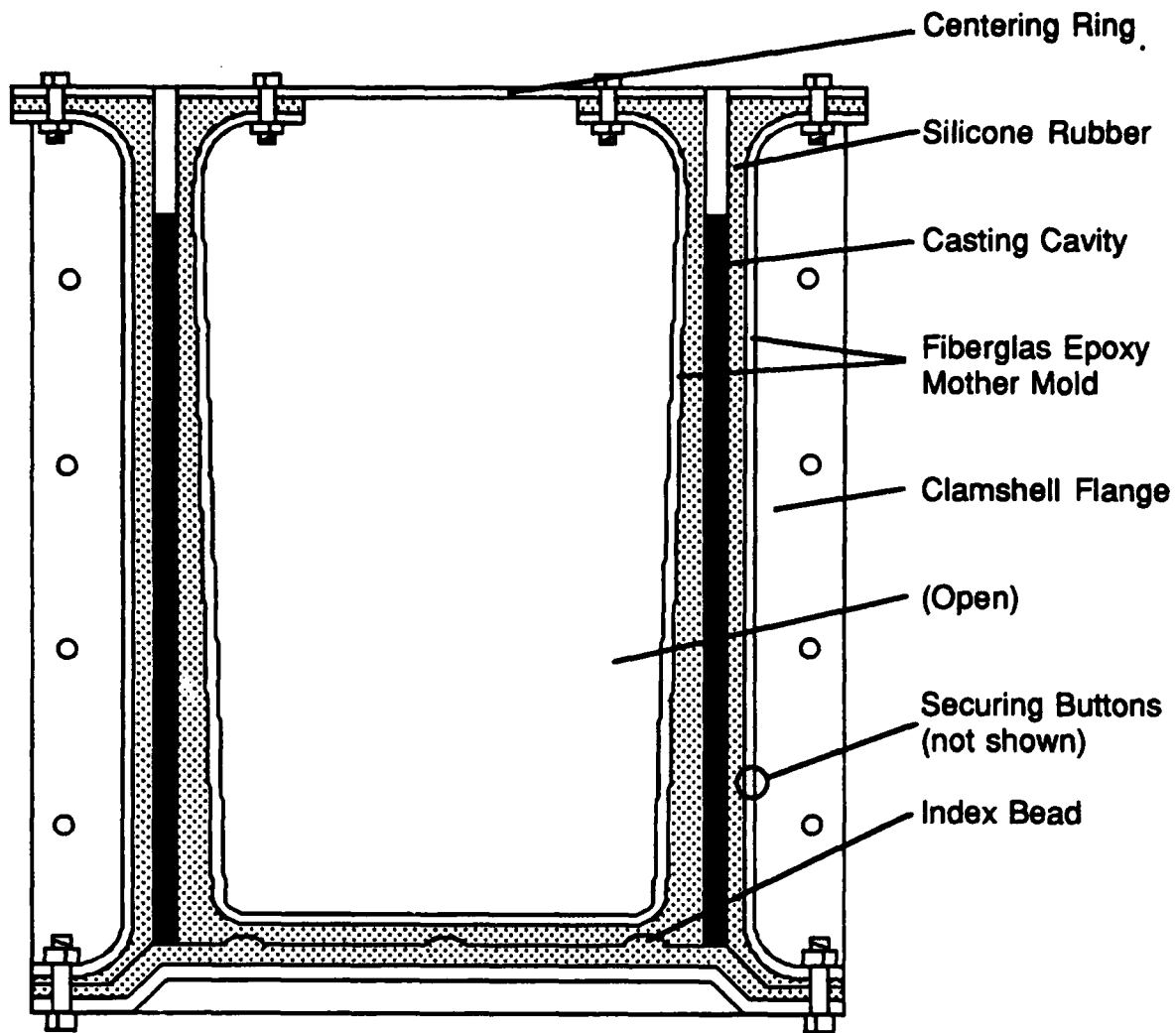
Figure 5. Schematic of mold design to sediment cast cylinder preforms.

Figure 6. Rubber/fiberglass cylinder casting mold.
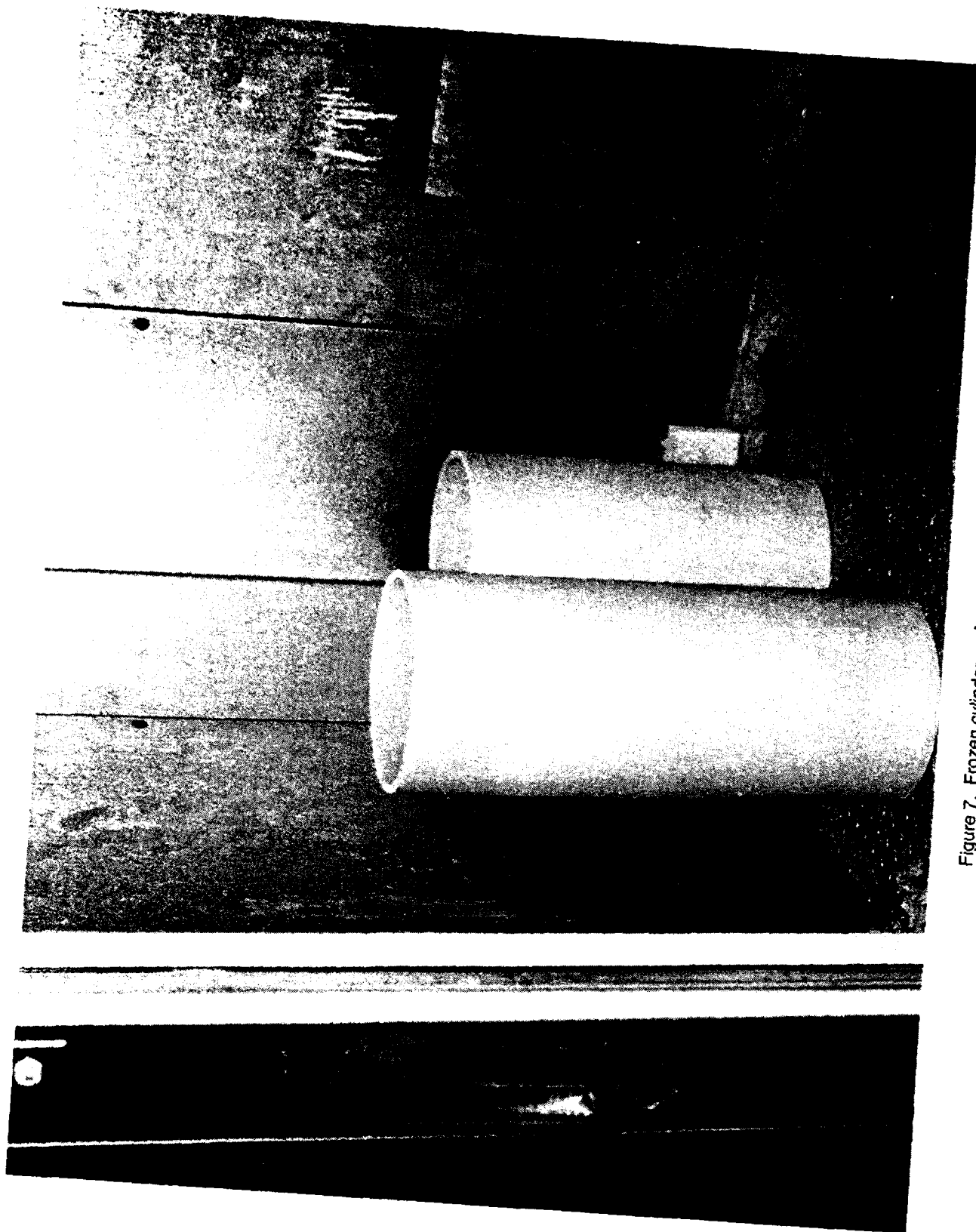
Figure 7. Frozen cylinder preforms after demolding.
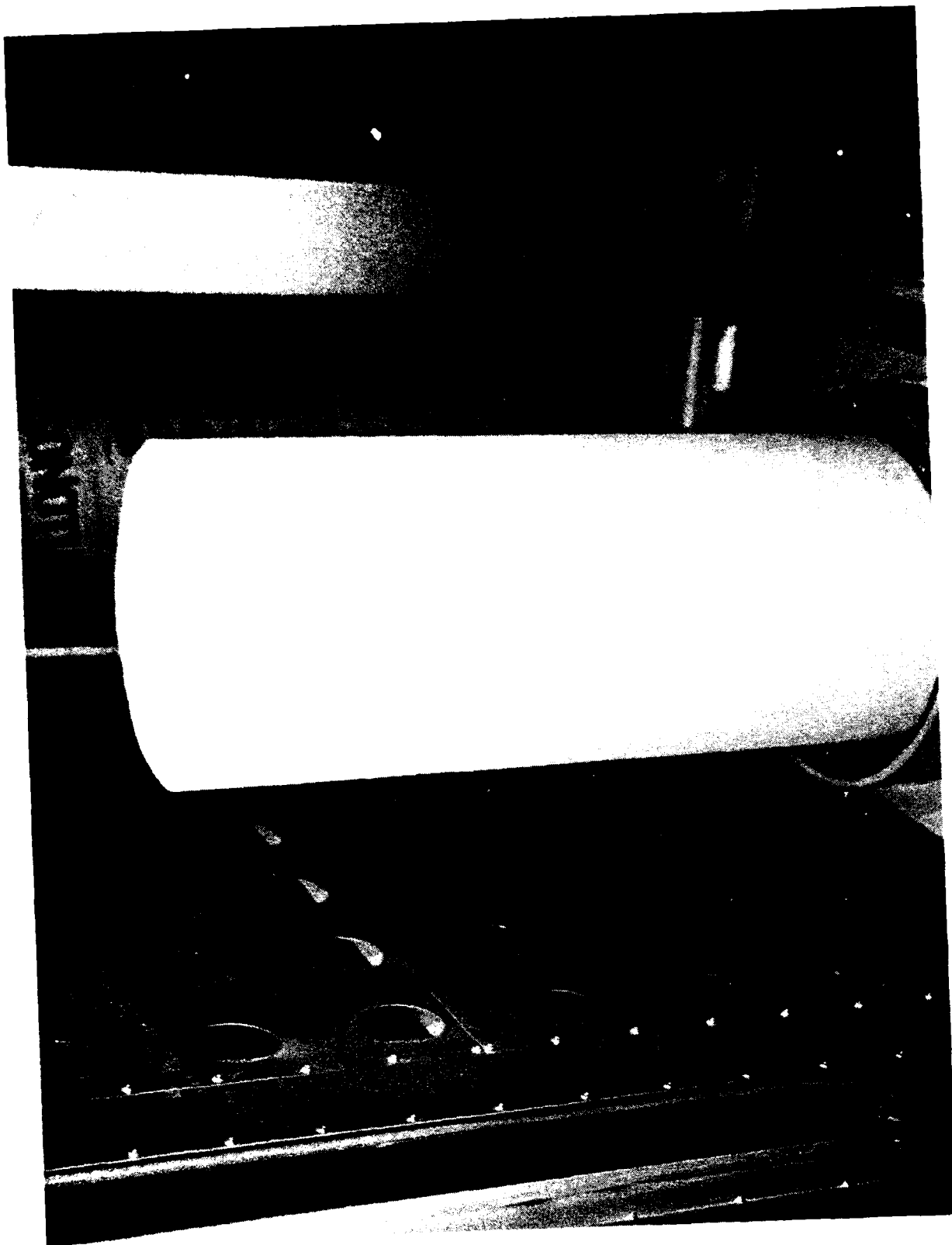
Figure 8. Dried cylinder preform inside dryer.
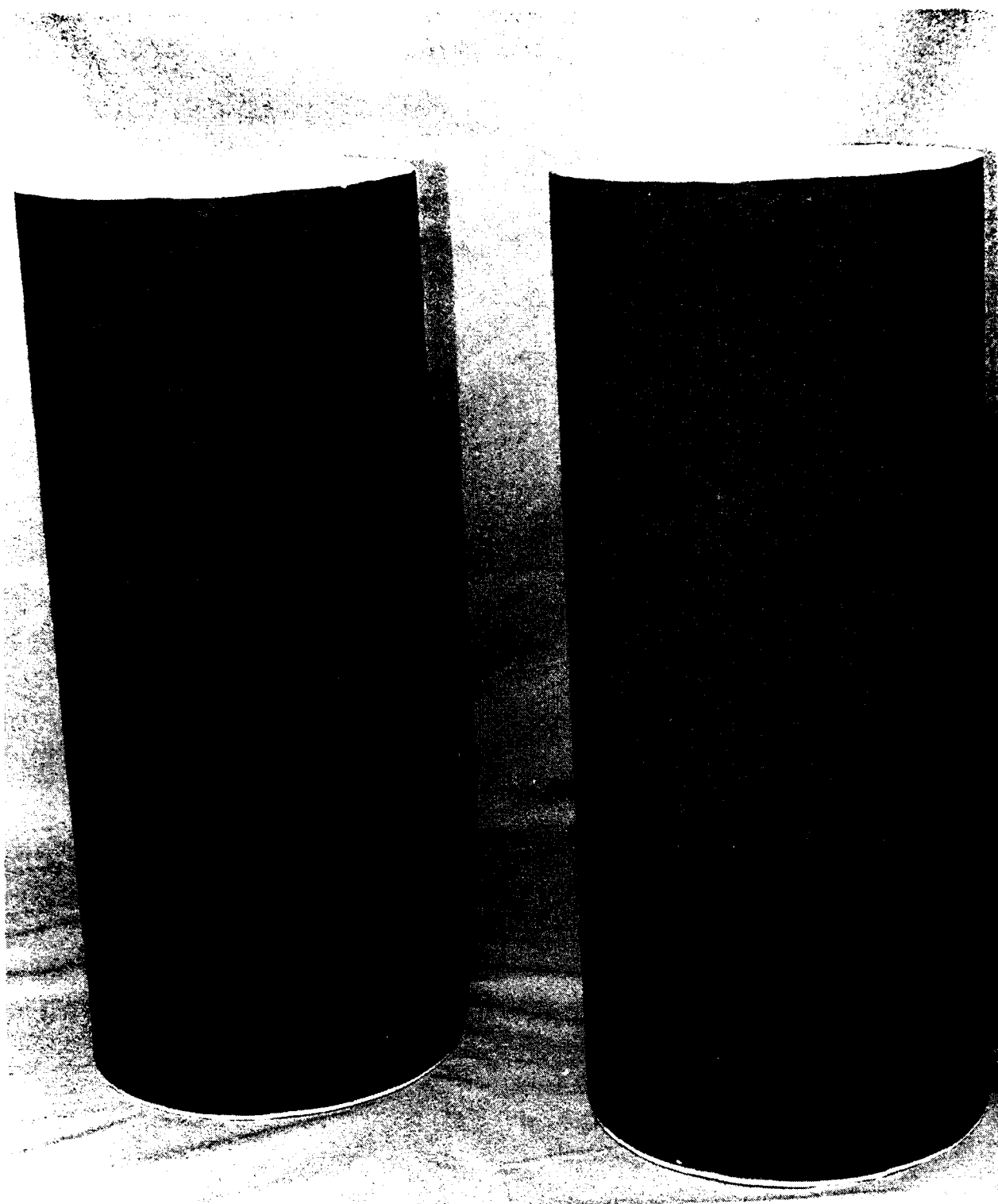
Figure 9. Preforms with barrier and initiation coatings prior to matrix infiltration.
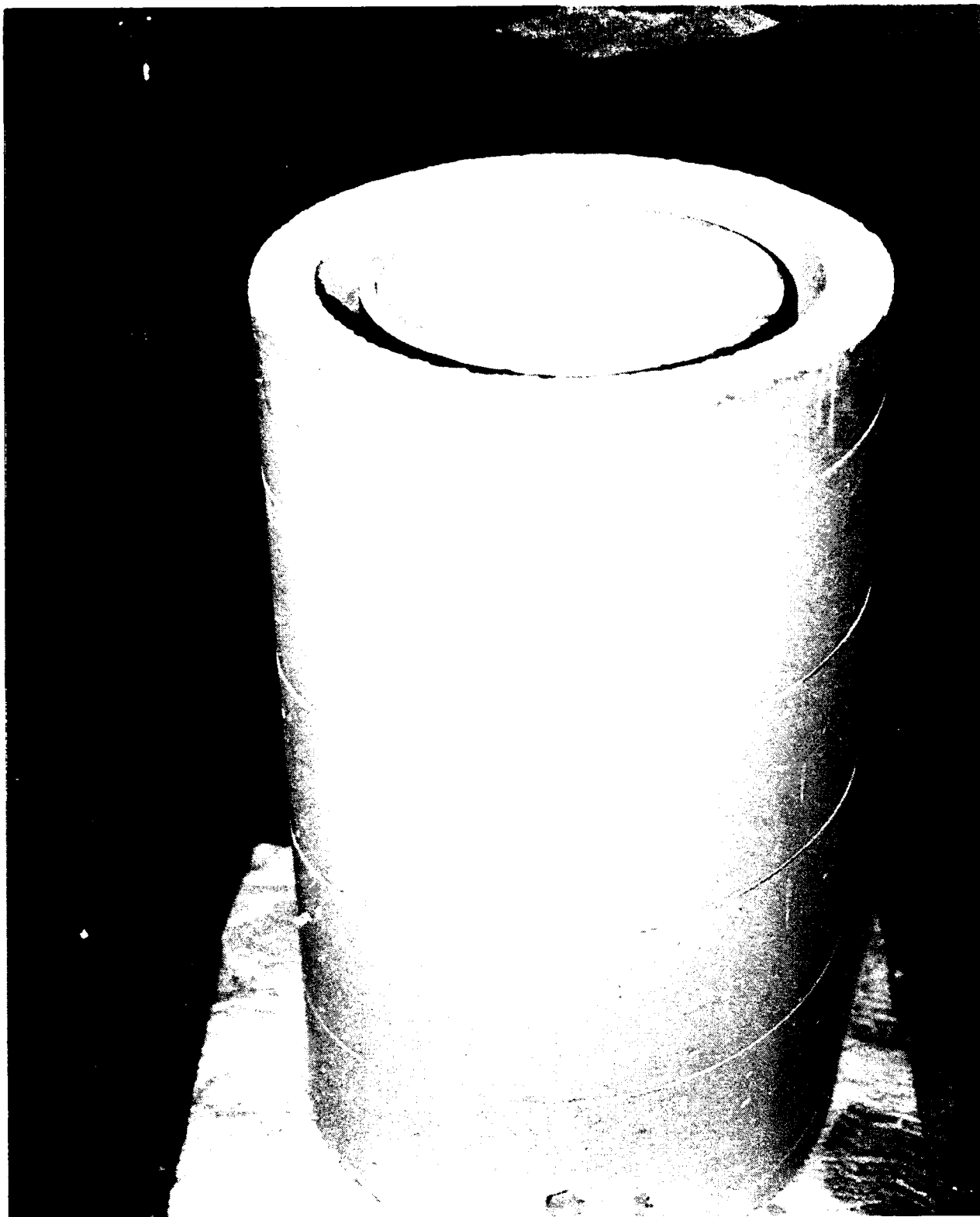
Figure 10. Refractory growth shell with preform inside.
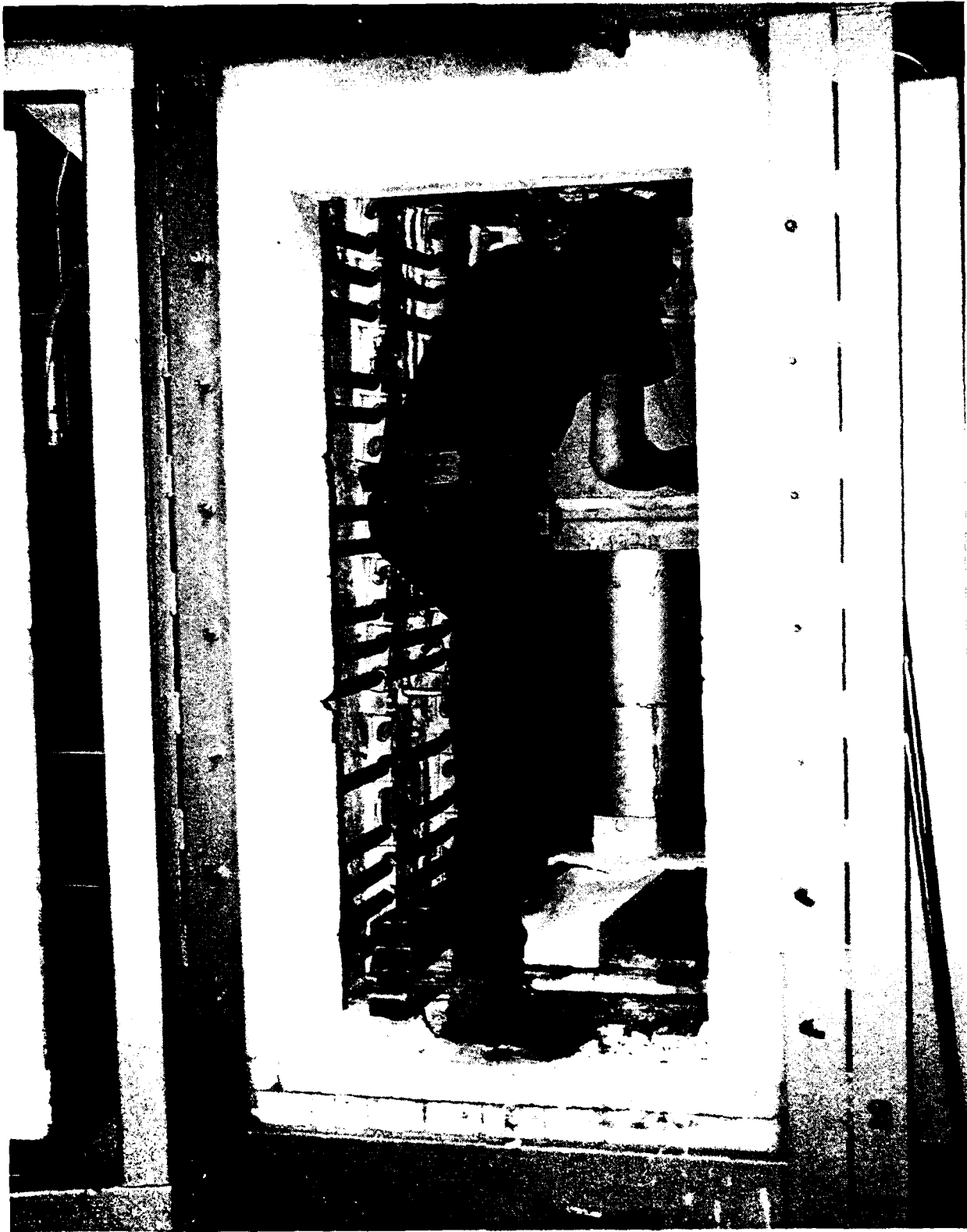
Figure 11. Growth shell being prepared inside the furnace.
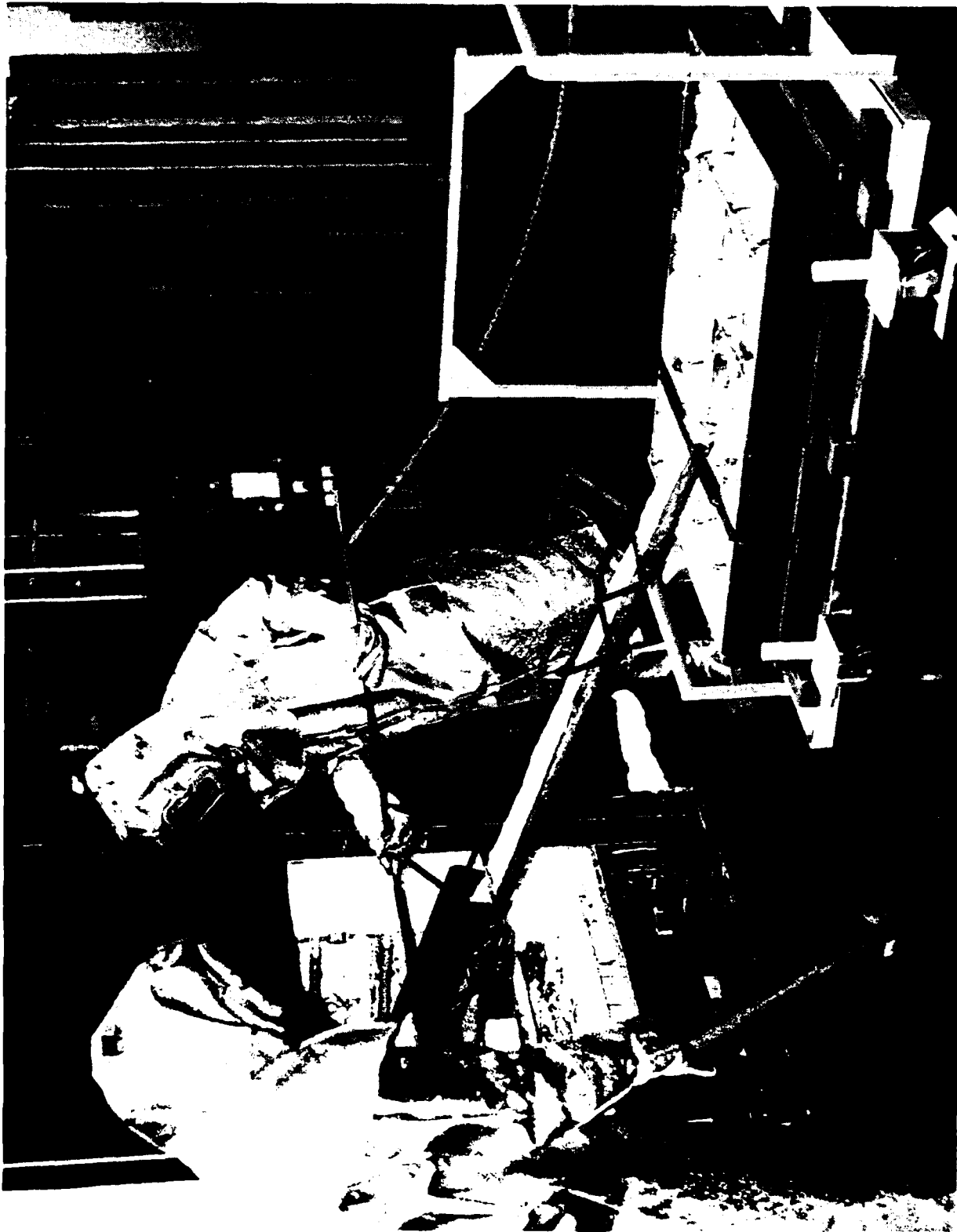
Figure 12. Draining of molten aluminum alloy from growth shells after completion of matrix growth.

Figure 13. Closeup of the draining of molten aluminum alloy from growth shells after completion of matrix growth.

Figure 14. A fully infiltrated cylinder after removal from the refractory shell.
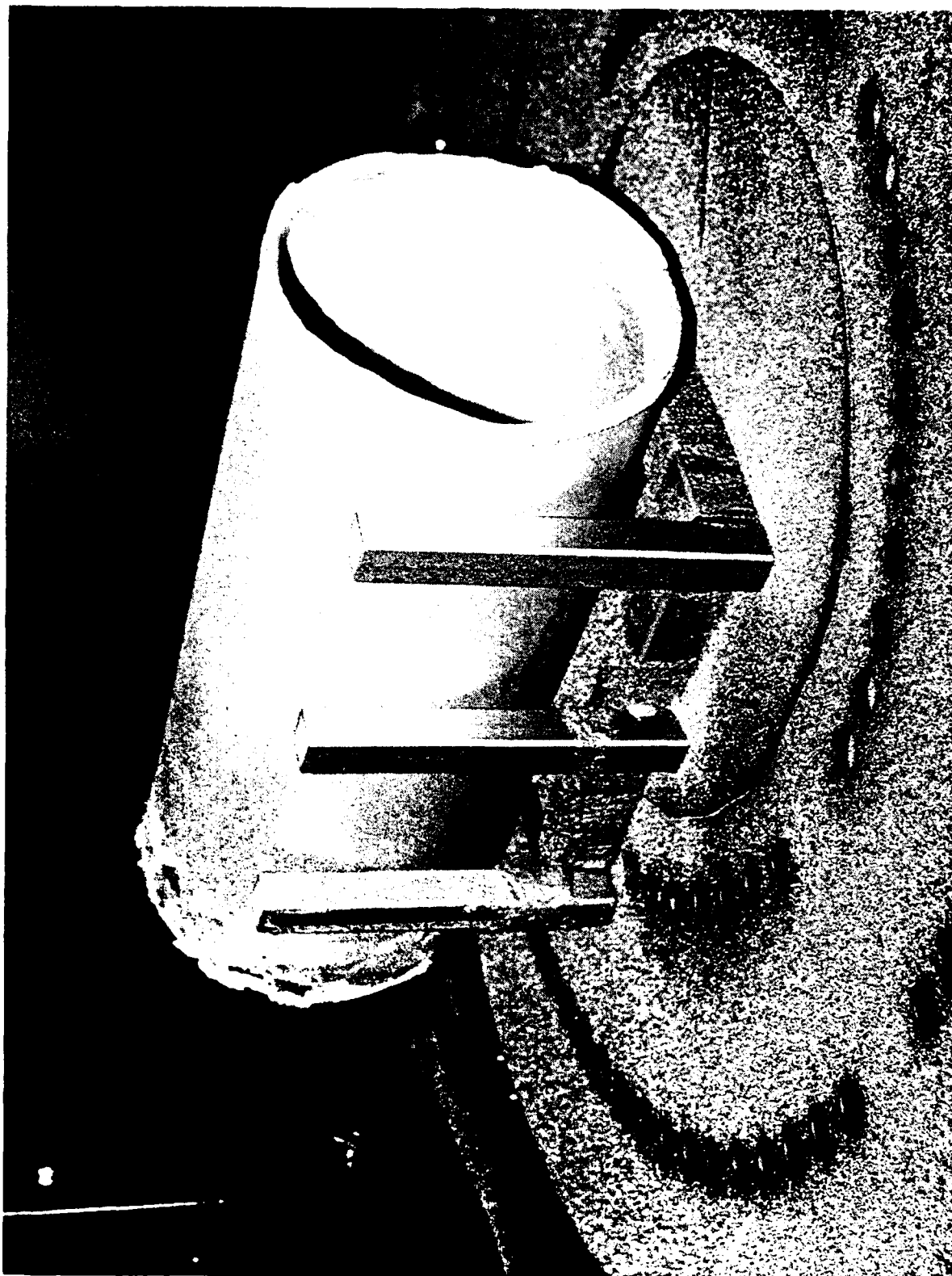
Figure 15. A fully infiltrated cylinder after shot blasting.

LANXIDE

90 - X - 089™
Reinforced Ceramic
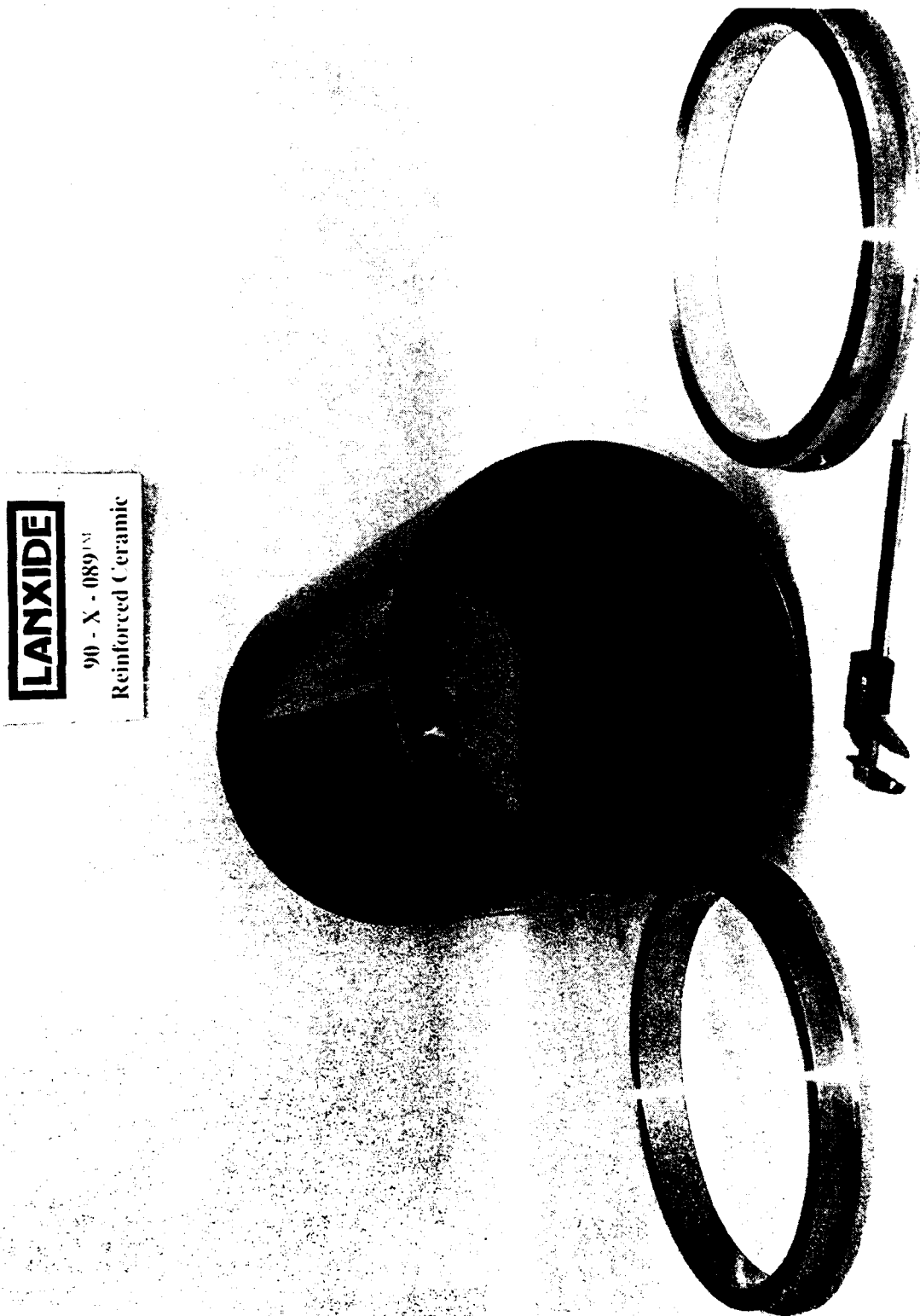
Figure 16. Fully machined SiC/Al$_2$O$_3$/Al composite cylinder with titanium end caps prior to bonding.
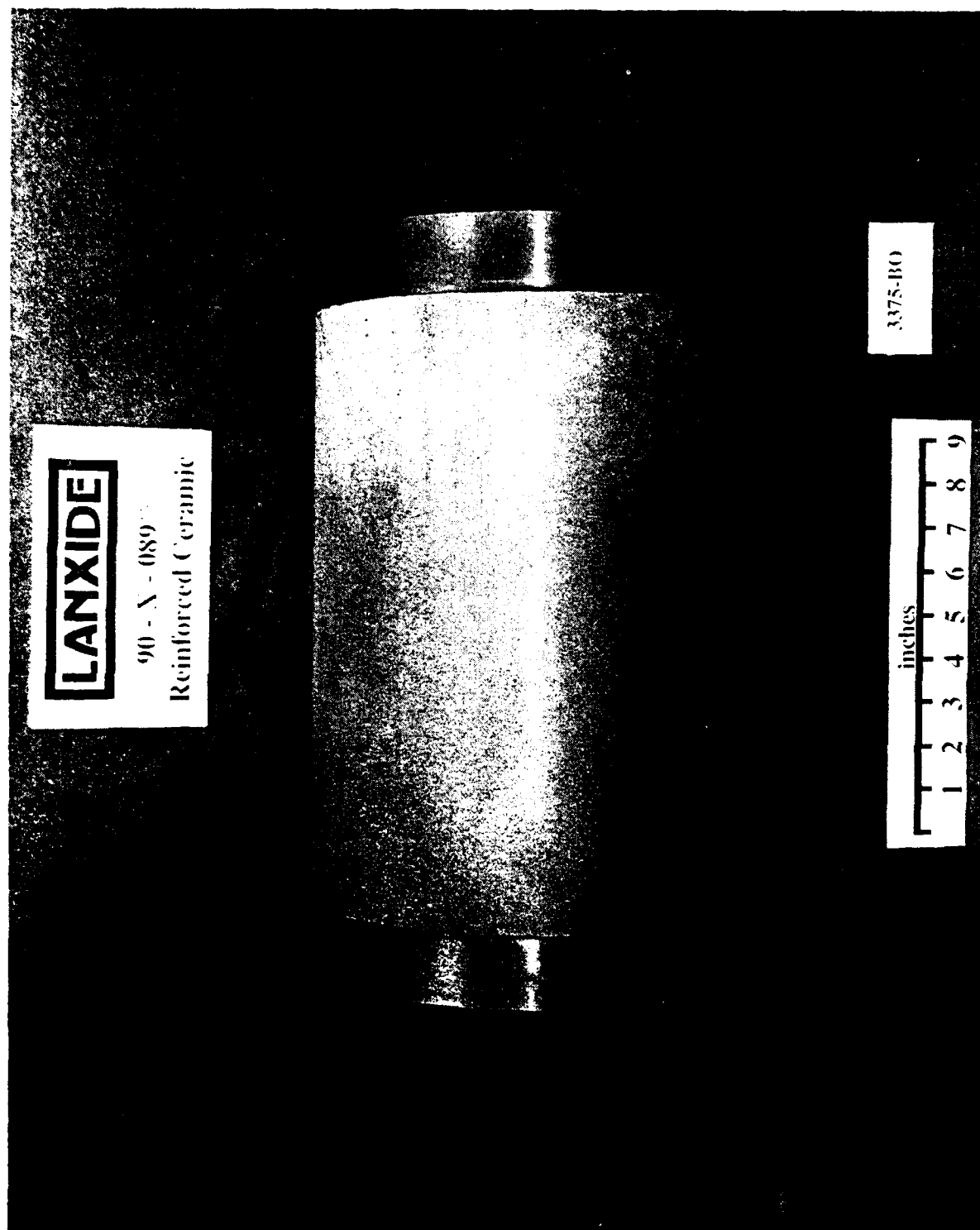
Figure 17. "As-cast" cylinder. Only the ends and the bearing surfaces of this cylinder have been machined.
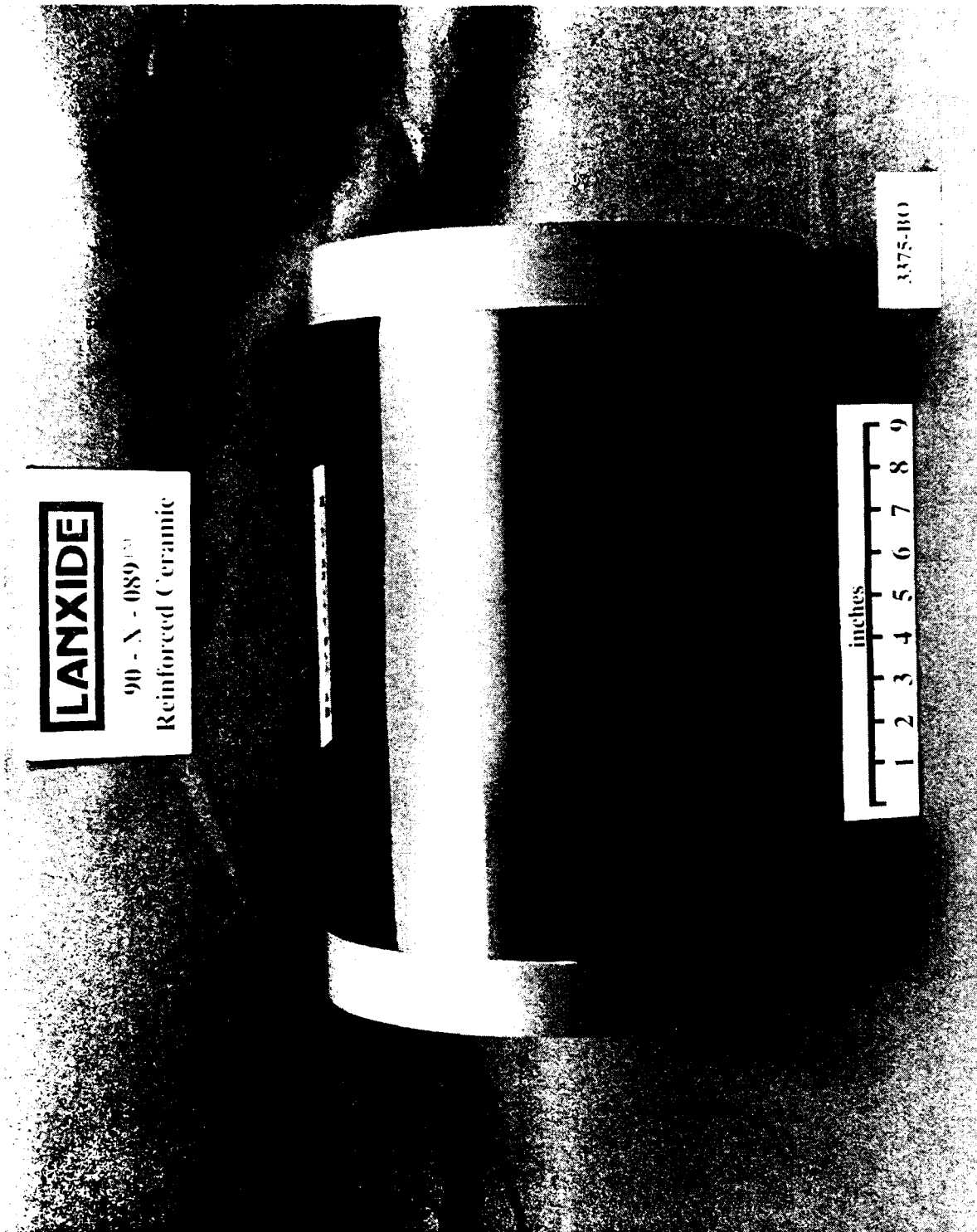
Figure 18. "As-cast" cylinder with Technicote,epoxy coating per WS22351, Rev C.

39
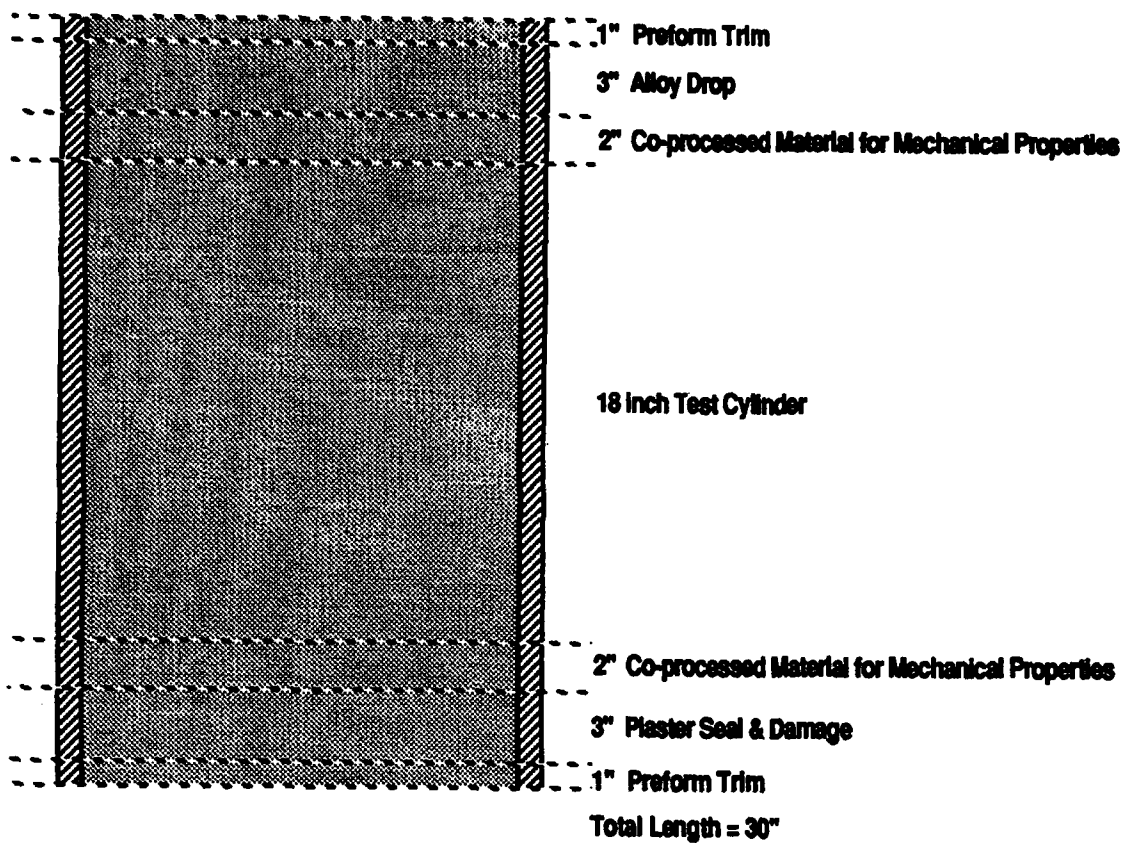
Figure 19. Schematic of preform and the location of the co-processed rings that were removed for material characterization.

NOTES

⚠ A. ASSEMBLY SHALL BE USED TO PERFORM CYCLIC TESTING ON THE FOLLOWING COMPONENTS:

   A. 55910-D128945 LANXIDE HOUSING 12 INCH CYLINDER

   B. 55910-D128912 ZTA HOUSING 12 INCH CYLINDER

   C. 55910-D128915 ALUMINA HOUSING 12 INCH CYLINDER

   D. 55910-D128917 SILICON NITRIDE HOUSING 12 INCH CYLINDER

   E. 55910-D128923 ROTATIONALLY CAST ALUMINA HOUSING 12 INCH CYLINDER

⚠ O-RING (ITEM 12) MAY BE PURCHASED FROM:

   PARKER SEAL GROUP
   O-RING DIVISION
   2360 PALUMBO DRIVE
   P.O. BOX 11751
   LEXINGTON, KY 40512
   (606) 269-2351

⚠ 3. EPOXY RESIN AND HARDENER (ITEMS 17 & 18), PASA JELL 107 (ITEM 19) AND RELEASE AGENT (ITEM 22) MAY BE PURCHASED FROM:

   YALE ENTERPRISES
   4055 PACIFIC HIGHWAY
   SAN DIEGO, CA 92110
   (619) 299-7710

4. CYLINDER ENDCAP (ITEM 6) BONDING PROCEDURE:

   A. WIPE THE INTERIOR OF THE CYLINDER ENDCAP (ITEM 6) WITH METHYL ETHYL KETONE UNTIL PAPER TOWEL SHOWS NO FURTHER DISCOLORATION.

   B. PASSIVATE THE INTERIOR OF THE CYLINDER ENDCAP BY APPLYING A LAYER OF PASA JELL 107 (ITEM 19) AND ALLOWING IT TO ETCH THE TITANIUM SURFACE FOR 30 MINUTES. RINSE OFF INTERIOR OF CYLINDER ENDCAP AND ALLOW SURFACES OF TITANIUM TO AIR DRY. AIR DRYING CAN BE ACCELERATED WITH A FORCED AIR HEATER.

   C. LAY THE CYLINDER ENDCAP FLAT WITH ITS O-RING GLAND FACING DOWN ON THE HORIZONTAL WORKING SURFACE. MIX 100 PARTS EPOXY RESIN (ITEM 17) WITH 70 PARTS HARDENER (ITEM 18) AND POUR A .12 INCH DEEP LAYER IN THE INTERIOR OF THE CYLINDER ENDCAP.

   D. PLACE THE SPACER (ITEM 3) ON TOP OF THE EPOXY LAYER AND PRESS IT DOWN THRU THE EPOXY MIXTURE TO THE BOTTOM OF THE CYLINDER ENDCAP USING A CLEAN TOOL.

   F. POUR ADDITIONAL EPOXY MIXTURE INTO THE BOTTOM OF THE CYLINDER ENDCAP UNTIL THE DEPTH OF THE EPOXY MIXTURE REACHES .50 INCHES.

   F. WIPE THE ENDS OF THE 12 INCH CYLINDER (ITEM 1) WITH METHYL ETHYL KETONE UNTIL PAPER TOWEL SHOWS NO FURTHER DISCOLORATION.

   G. LOWER THE END OF THE 12 INCH CYLINDER INTO THE CYLINDER ENDCAP PARTIALLY FILLED WITH THE EPOXY MIXTURE SO THAT THE 12 INCH CYLINDER IS CENTERED WITHIN THE CYLINDER ENDCAP. ALLOW THE 12 INCH CYLINDER TO SETTLE EVENLY INTO THE CYLINDER ENDCAP UNTIL THE 12 INCH CYLINDER COMES TO REST ON THE SPACER AT THE BOTTOM OF THE CYLINDER ENDCAP. ADDITIONAL WEIGHT UP TO 50 LBS CAN BE PLACED ON TOP OF THE 12 INCH CYLINDER TO HELP IT SETTLE EVENLY THRU THE EPOXY MIXTURE. CARE SHOULD BE TAKEN TO ASSURE THE 12 INCH CYLINDER REMAINS CENTERED WITHIN THE CYLINDER ENDCAP AND THE CENTERLINE OF THE 12 INCH CYLINDER STAYS PERPENDICULAR TO THE WORKING SURFACE THROUGHOUT THE BONDING PROCEDURE.

   H. WIPE OFF ANY SURPLUS EPOXY MIXTURE FROM THE EXTERIOR OF THE CYLINDER ENDCAP THAT EXTRUDED OUT DURING THE BONDING PROCEDURE. LEAVE THE BONDED ASSEMBLY AND ANY SETTLING WEIGHT USED UNDISTURBED FOR AT LEAST 24 HOURS TO ALLOW THE EPOXY MIXTURE TO BEGIN TO CURE. ONCE THIS INITIAL 24 HOUR PERIOD HAS PASSED, ANY EXCESS EPOXY MIXTURE REMAINING ON THE EXTERIOR OF THE CYLINDER ENDCAP SHOULD BE COMPLETELY REMOVED. APPLICATION OF A THIN COAT OF RELEASE AGENT (ITEM 22) TO THE EXTERIOR SURFACES OF THE CYLINDER ENDCAP PRIOR TO BONDING THE CERAMIC CYLINDER MAY BE USED TO HELP CLEANUP THE EXTERIOR OF THE CYLINDER ENDCAP. DO NOT ALLOW RELEASE AGENT ON OR NEAR ANY BONDING SURFACES.

   I. REPEAT THIS BONDING PROCEDURE FOR THE REMAINING ENDCAP AND OPPOSITE END OF THE 12 INCH CYLINDER.

5. APPLY A LIGHT FILM OF SILICONE COMPOUND (ITEM 20) TO O-RINGS (ITEMS 2 & 12) PRIOR TO ASSEMBLY.

⚠ 6. APPLY A BEAD OF RTV (ITEM 21) IN LOCATIONS SHOWN.

7. ALL ELECTRIC STRAIN GAUGES ARE 90° RECTANGULAR ROSETTES. ALL STRAIN GAUGES SHALL BE MOUNTED WITH ONE LEG ORIENTATED IN THE HOOP DIRECTION. ALL GAUGES IS TO BE WATERPROOFED. GAUGE SIZE SHALL BE 1/4.

8. PRESSURE TESTING SHALL BE PERFORMED IN TAP WATER AT AMBIENT ROOM TEMPERATURE AND SHALL CONSIST OF AT A MINIMUM THE FOLLOWING TESTS:

   A. PRESSURIZE TO 10,000 PSI AT AN APPROXIMATE RATE OF 1000 PSI PER MINUTE READING THE STRAINS AT 1000 PSI INTERVALS. AFTER 60 MINUTES AT A SUSTAINED PRESSURE OF 10,000 PSI RECORD ALL STRAINS AND DEPRESSURIZE TO 0 PSI AT AN APPROXIMATE RATE OF 10,000 PSI PER MINUTE. AFTER DEPRESSURIZATION RECORD ALL RESIDUAL STRAINS.

   B. PRESSURE CYCLE FROM 50 PSI TO A MAXIMUM OF 13,000 PSI AS INSTRUCTED BY NRaD. MAINTAIN PEAK PRESSURE FOR A DURATION OF ONE MINUTE FOR EACH CYCLE. PRESSURIZATION AND DEPRESSURIZATION RATES SHALL NOT EXCEED A RATE OF 10,000 PSI PER MINUTE.

9. PRESSURE TEST DOCUMENTATION SHALL CONSIST OF THE FOLLOWING:

   A. COMPUTER PRINTOUT OF ALL STRAINS RECORDED FOR INITIAL PROOF TEST TO 10,000 PSI.

   B. STRIP CHARTS WITH PRESSURE HISTORIES FOR EACH PRESSURIZATION.

PARTS LIST

FIND NO.	QTY REQD	CAGE CODE	PART OR IDENTIFYING NUMBER	DESCRIPTION OR NOMENCLATURE	MATERIAL/SPEC/ZONE
22	AR			DEVCON LIQUID RELEASE AGENT	MIL-A-46146
21	AR			ADHESIVE-SEALANTS, RTV	
20	AR			SILICONE COMPOUND	MIL-S-8660
19	AR			PASA JELL 107	
18	AR			CIBA GEIGY 283 HARDENER	
17	AR			CIBA GEIGY 6010 EPOXY RESIN	
16					
15					
14	2		MS51972-10	NUT, HEX, CRES, 1.000-12UNF-28	
13					
12	2		2-218	O-RING	
11	2		SK9402-087	WOOD PLUG, HEMISPHERE, 12 INCH	
10	1		SK9402-077-3	PLUG, HEMISPHERE, 12 INCH	
9	1		SK9402-077-1	PLUG, HEMISPHERE, 12 INCH	
8	2		SK9402-088	WASHER, HEMISPHERE, 12 IN	
7	2		SK9402-086	CLAMP BAND, HEMISPHERE, 12 INCH	
6	2		SK9402-087	END CAP, MOD 1, TYPE 2, 12 IN CYL	
5					
4	2		SK9402-084	HEMISPHERE, 12 INCH	
3	2		SK9402-082	SPACER, 12 INCH CYLINDER	
2	2		SK9402-045	O-RING, END CAP, MOD 1, 12 IN CYL	
1	1			12 INCH CYLINDER	

REVISIONS

SYM	DESCRIPTION	DATE	APPROVED
		1/4/88	
2	REMOVE ITEM 6, CHANGE ITEM 10	3/28/88	
3	ADD SHEET 3	9/1/88	
3	UPDATE NOTE 8, DRAWING TITLE	1/17/89	

NAVAL COMMAND, CONTROL AND OCEAN SURVEILLANCE CENTER
RESEARCH, DEVELOPMENT, TEST AND EVALUATION DIVISION
SAN DIEGO, CA 92152-5000

TEST ASSEMBLY 1, 12 INCH CYLINDER

SIZE	CAGE CODE	DRAWING NUMBER
D	55910	SK9402-070

SHEET 1 OF 3

Figure 20. 12-inch cylinder test assembly, Type 1 configuration, Sheet 1.

Figure 20. 12-inch cylinder test assembly, Type I configuration, Sheet 2.

VIEW A-A

(14.12 MAX)

(.250-18NPT)

Figure 20. 12-inch cylinder test assembly, Type I configuration, Sheet 3.

Figure 21. 12-inch cylinder Mod 1, Type 2 end-cap joint ring.

44

Figure 22. 12-inch cylinder spacer.

45

Figure 23. 12-inch hemisphere.

46

Figure 24. 12-inch cylinder Mod 1 end-cap joint ring O-ring.

Figure 25. 12-inch hemisphere clamp band.

48

Figure 26. 12-inch hemisphere plug.

49

Figure 27. 12-inch hemisphere washer.

Figure 28. 12-inch hemisphere wooden plug.

Figure 29. 12-inch cylinder test assembly, Type II configuration, Sheet 1.

PARTS LIST

ITEM	QTY REQD	CAGE CODE	PART OR IDENTIFYING NUMBER	DESCRIPTION OR NOMENCLATURE	MATERIAL/SPEC/NOTE
22	AR			ADHESIVE-SEALANTS, RTV	MIL-A-46146
21	AR			DEVCON LIQUID RELEASE AGENT	
20	AR			SILICONE COMPOUND	MIL-S-8660
19	AR			PASA JELL 107	
18	AR			CIBA GEIGY 283 HARDENER	
17	AR			CIBA GEIGY 6010 EPOXY RESIN	
16	8		MS51971-5	NUT, HEX, CRES, .500-13UNC-2B	
15	8		MS35338-143	WASHER, LOCK, CRES, Ø.500 NOM	
14	8		MS15795-816	WASHER, FLT, CRES, Ø.531 ID	
13					
12	1		2-218	O-RING	
11					
10	1		SK9402-086	WOOD PLUG, FLAT END PLATE, 12 INCH	
9					
8	4		SK9402-084	TIE ROD	
7	1		SK9402-085	FEED THRU, FLAT END PLATE, 12 INCH	
6	2		SK9402-082	SPACER, 12 INCH CYLINDER	
5	2		SK9402-087	END CAP, MOD 1, TYPE 2, 12 IN. CYL	
4	2		SK9402-045	O-RING, END CAP, MOD 1, 12 IN. CYL	
3	1		SK9402-043-2	FLAT END PLATE, 12 INCH	
2	1		SK9402-043-1	FLAT END PLATE, 12 INCH	
1	1			12 INCH CYLINDER	

NOTES:

1. ASSEMBLY SHALL BE USED TO PERFORM AN IMPLOSION TEST ON THE FOLLOWING COMPONENTS:

   A. 55910-0128845 LANXIDE HOUSING 12 INCH CYLINDER
   B. 55910-0128812 ZTA HOUSING 12 INCH CYLINDER
   C. 55910-0128815 ALUMINA HOUSING 12 INCH CYLINDER
   D. 55910-0128817 SILICON NITRIDE HOUSING 12 INCH CYLINDER
   E. 55910-0128823 ROTATED FULLY CAST ALUMINA HOUSING 12 INCH CYLINDER

2. O-RING (ITEM 12) MAY BE PURCHASED FROM:

   PARKER SEAL GROUP
   O-RING DIVISION
   2360 PALUMBO DRIVE
   P.O. BOX 11751
   LEXINGTON, KY 40512
   (606) 269-2351

3. EPOXY RESIN AND HARDENER (ITEMS 17 & 18), PASA JELL 107 (ITEM 19), AND RELEASE AGENT (ITEM 21) MAY BE PURCHASED FROM:

   YALE ENTERPRISES
   4055 PACIFIC HIGHWAY
   SAN DIEGO, CA 92110
   (619) 299-7710

4. CYLINDER ENDCAP (ITEM 5) BONDING PROCEDURE:

   A. WIPE THE INTERIOR OF THE CYLINDER ENDCAP (ITEM 5) WITH METHYL ETHYL KETONE UNTIL PAPER TOWEL SHOWS NO FURTHER DISCOLORATION.

   B. PASSIVATE THE INTERIOR OF THE CYLINDER ENDCAP BY APPLYING A LAYER OF PASA JELL 107 (ITEM 19) AND ALLOWING IT TO ETCH THE TITANIUM SURFACE FOR 30 MINUTES. RINSE OFF INTERIOR OF CYLINDER ENDCAP AND ALLOW SURFACES OF TITANIUM TO AIR DRY. AIR DRYING CAN BE ACCELERATED WITH A FORCED AIR HEATER.

   C. LAY THE CYLINDER ENDCAP FLAT WITH ITS O-RING GLAND FACING DOWN ON THE HORIZONTAL WORKING SURFACE. MIX 100 PARTS EPOXY RESIN (ITEM 17) WITH 70 PARTS HARDENER (ITEM 18) AND POUR A .12 INCH DEEP LAYER IN THE INTERIOR OF THE CYLINDER ENDCAP.

   D. PLACE THE SPACER (ITEM 6) ON TOP OF THE EPOXY LAYER AND PRESS IT DOWN THRU THE EPOXY MIXTURE TO THE BOTTOM OF THE CYLINDER ENDCAP USING A CLEAN TOOL.

   E. POUR ADDITIONAL EPOXY MIXTURE INTO THE BOTTOM OF THE CYLINDER ENDCAP UNTIL THE DEPTH OF THE EPOXY MIXTURE REACHES .50 INCHES.

   F. WIPE THE ENDS OF THE 12 INCH CYLINDER (ITEM 1) WITH METHYL ETHYL KETONE UNTIL PAPER TOWEL SHOWS NO FURTHER DISCOLORATION.

   G. LOWER THE END OF THE 12 INCH CYLINDER INTO THE CYLINDER ENDCAP PARTIALLY FILLED WITH THE EPOXY MIXTURE SO THAT THE 12 INCH CYLINDER IS CENTERED WITHIN THE CYLINDER ENDCAP. ALLOW THE 12 INCH CYLINDER TO SETTLE EVENLY INTO THE CYLINDER ENDCAP UNTIL THE 12 INCH CYLINDER COMES TO REST ON THE SPACER AT THE BOTTOM OF THE CYLINDER ENDCAP. ADDITIONAL WEIGHT UP TO 50 LBS CAN BE PLACED ON TOP OF THE 12 INCH CYLINDER TO HELP IT SETTLE EVENLY THRU THE EPOXY MIXTURE. CARE SHOULD BE TAKEN TO ASSURE THE 12 INCH CYLINDER REMAINS CENTERED WITHIN THE CYLINDER ENDCAP AND THE CENTERLINE OF THE 12 INCH CYLINDER STAYS PERPENDICULAR TO THE WORKING SURFACE THROUGHOUT THE BONDING PROCEDURE.

   H. WIPE OFF ANY SURPLUS EPOXY MIXTURE FROM THE EXTERIOR OF THE CYLINDER ENDCAP THAT EXTRUDED OUT DURING THE BONDING PROCEDURE. LEAVE THE BONDED ASSEMBLY AND ANY SETTLING WEIGHTS USED UNDISTURBED FOR AT LEAST 24 HOURS TO ALLOW THE EPOXY MIXTURE TO BEGIN TO CURE. ONCE THIS INITIAL 24 HOUR PERIOD HAS PASSED, ANY EXCESS EPOXY MIXTURE REMAINING ON THE EXTERIOR OF THE CYLINDER ENDCAP SHOULD BE COMPLETELY REMOVED. APPLICATION OF A THIN COAT OF RELEASE AGENT (ITEM 21) TO THE EXTERIOR SURFACES OF THE CYLINDER ENDCAP PRIOR TO BONDING THE CERAMIC CYLINDER MAY BE USED TO HELP CLEANUP THE EXTERIOR OF THE CYLINDER ENDCAP. DO NOT ALLOW RELEASE AGENT ON OR NEAR ANY BONDING SURFACES.

   I. REPEAT THIS BONDING PROCEDURE FOR THE REMAINING ENDCAP AND OPPOSITE END OF THE 12 INCH CYLINDER.

5. APPLY A LIGHT FILM OF SILICONE COMPOUND (ITEM 20) TO O-RINGS (ITEMS 4 & 12) PRIOR TO ASSEMBLY. APPLY A BEAD OF RTV (ITEM 22) IN LOCATIONS SHOWN.

6. ALL ELECTRIC STRAIN GAUGES ARE 60° RECTANGULAR ROSETTES. ALL STRAIN GAUGES SHALL BE MOUNTED WITH ONE LEG ORIENTATED IN THE HOOP DIRECTION. ALL GAUGES TO BE WATERPROOFED. GAUGE SIZE SHALL BE 1/4.

7. PRESSURE TESTING SHALL BE PERFORMED IN TAP WATER AT AMBIENT ROOM TEMPERATURE AND SHALL CONSIST OF THE FOLLOWING TESTS:

   A. PRESSURIZE TO 10,000 PSI AT AN APPROXIMATE RATE OF 1000 PSI PER MINUTE READING THE STRAINS AT 1000 PSI INTERVALS. AFTER 80 MINUTES AT A SUSTAINED PRESSURE OF 10,000 PSI RECORD ALL STRAINS AND DEPRESSURIZE TO 0 PSI AT AN APPROXIMATE RATE OF 10,000 PSI PER MINUTE. AFTER DEPRESSURIZATION RECORD ALL RESIDUAL STRAINS.

   B. PRESSURE CYCLE FROM 50 PSI TO A MAXIMUM OF 18,000 PSI AS INSTRUCTED BY NRaD. MAINTAIN PEAK PRESSURE FOR A DURATION OF ONE MINUTE FOR EACH CYCLE. PRESSURIZATION AND DEPRESSURIZATION RATES SHALL NOT EXCEED A RATE OF 10,000 PSI PER MINUTE.

8. PRESSURE TEST DOCUMENTATION SHALL CONSIST OF THE FOLLOWING:

   A. COMPUTER PRINTOUT OF ALL STRAINS RECORDED FOR INITIAL PROOF TEST TO 10,000 PSI AND IMPLOSION TEST.

   B. STRIP CHART WITH PRESSURE HISTORY FOR IMPLOSION TEST.

52

Figure 29. 12-inch cylinder test assembly, Type II configuration, Sheet 2.

53

Figure 30. 12-inch flat end plate.

54

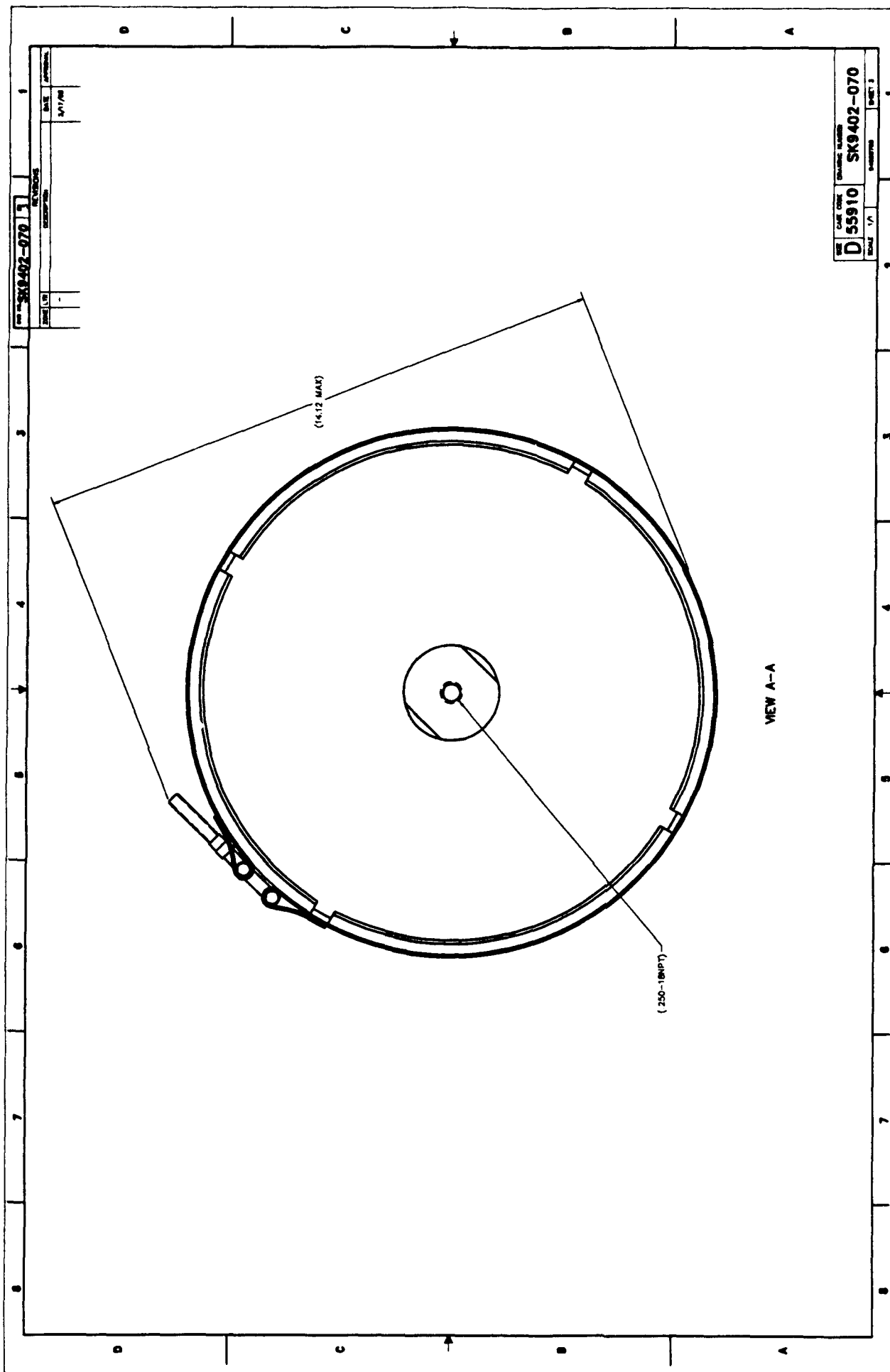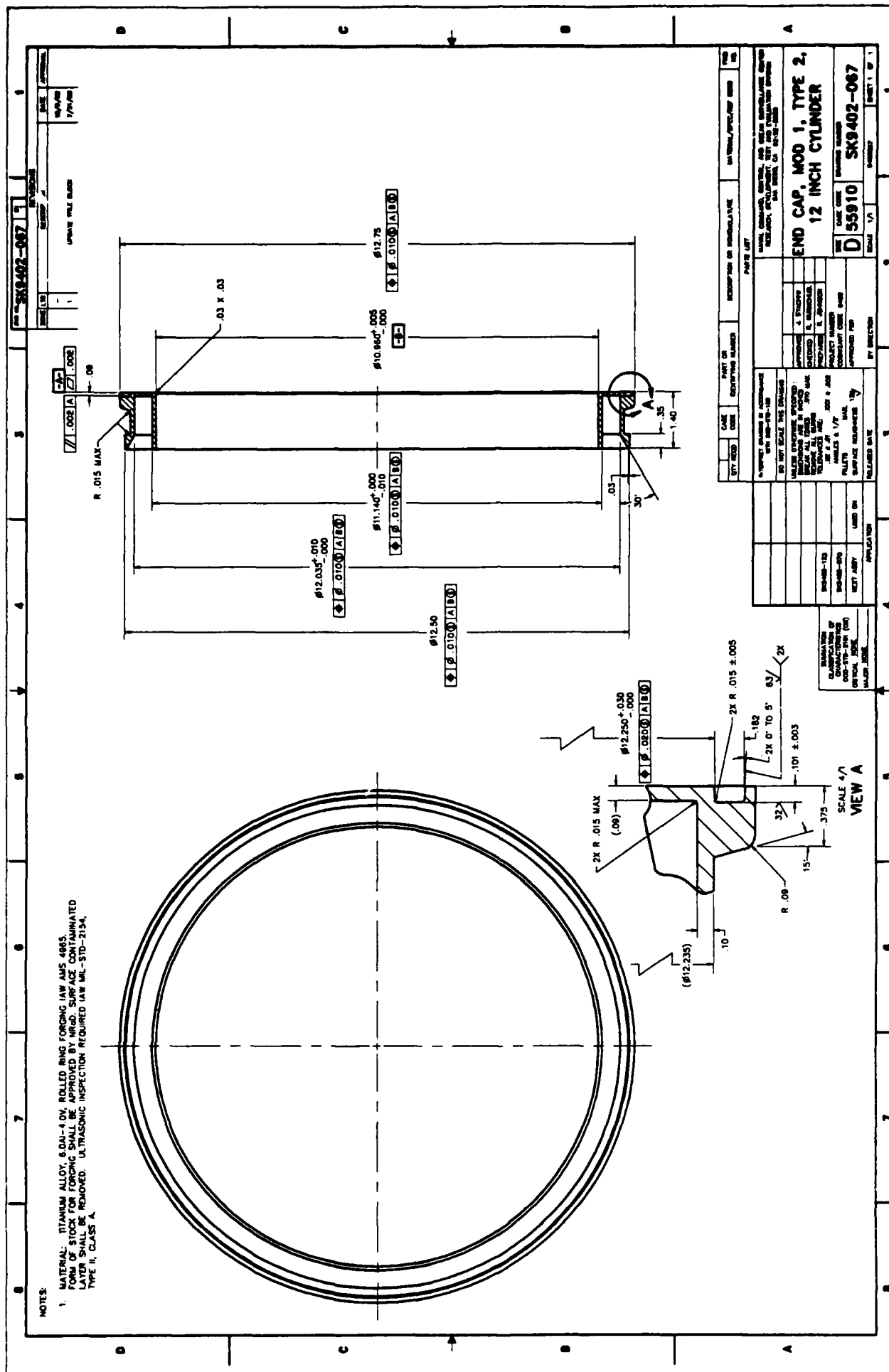Figure 31. 12-inch cylinder test assembly, Type III configuration, Sheet 1.

Figure 31. 12-inch cylinder test assembly, Type III configuration, Sheet 2.

56

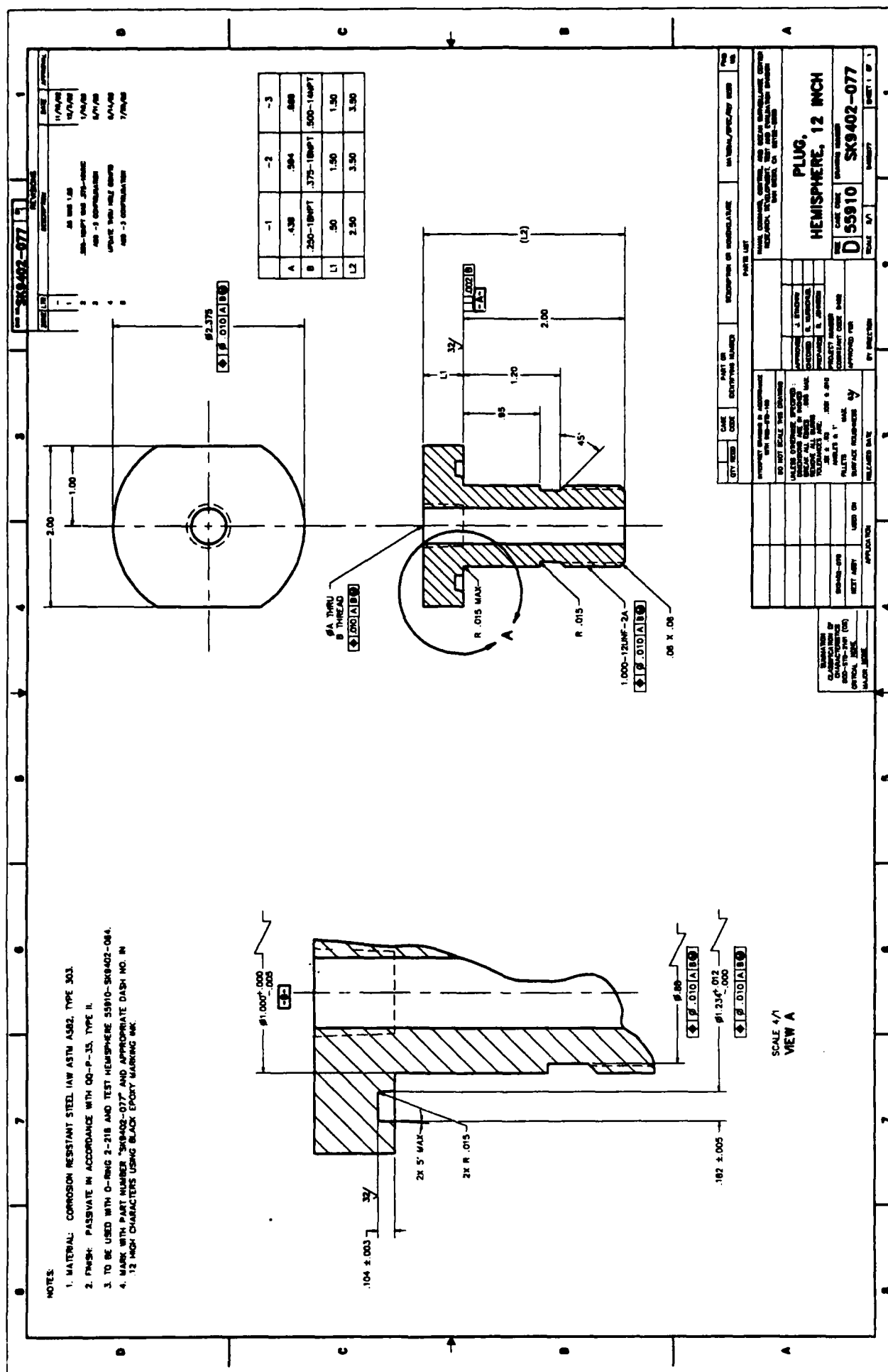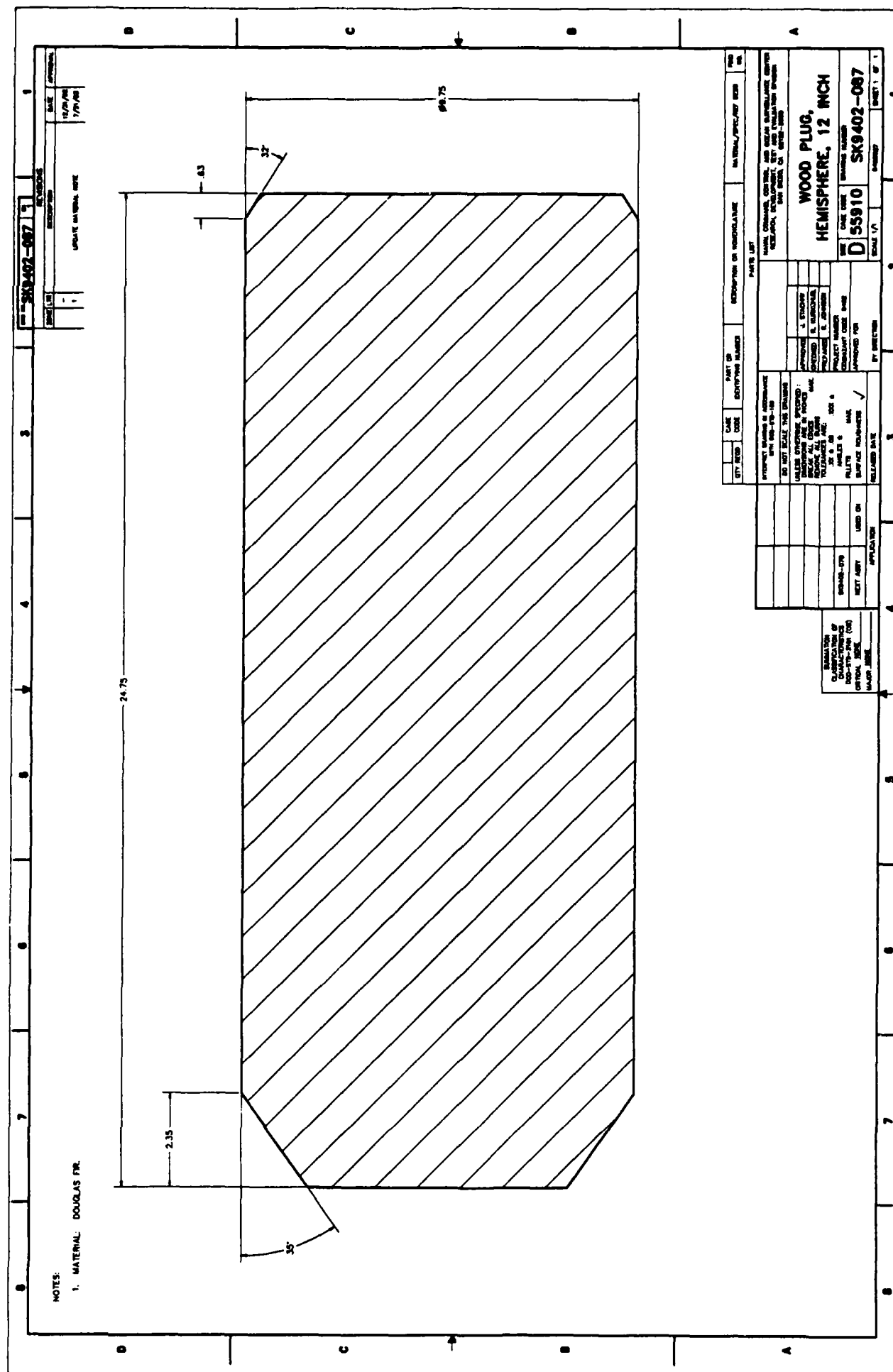Figure 32. 12-inch cylinder Mod 1, Type 1 end-cap joint ring.

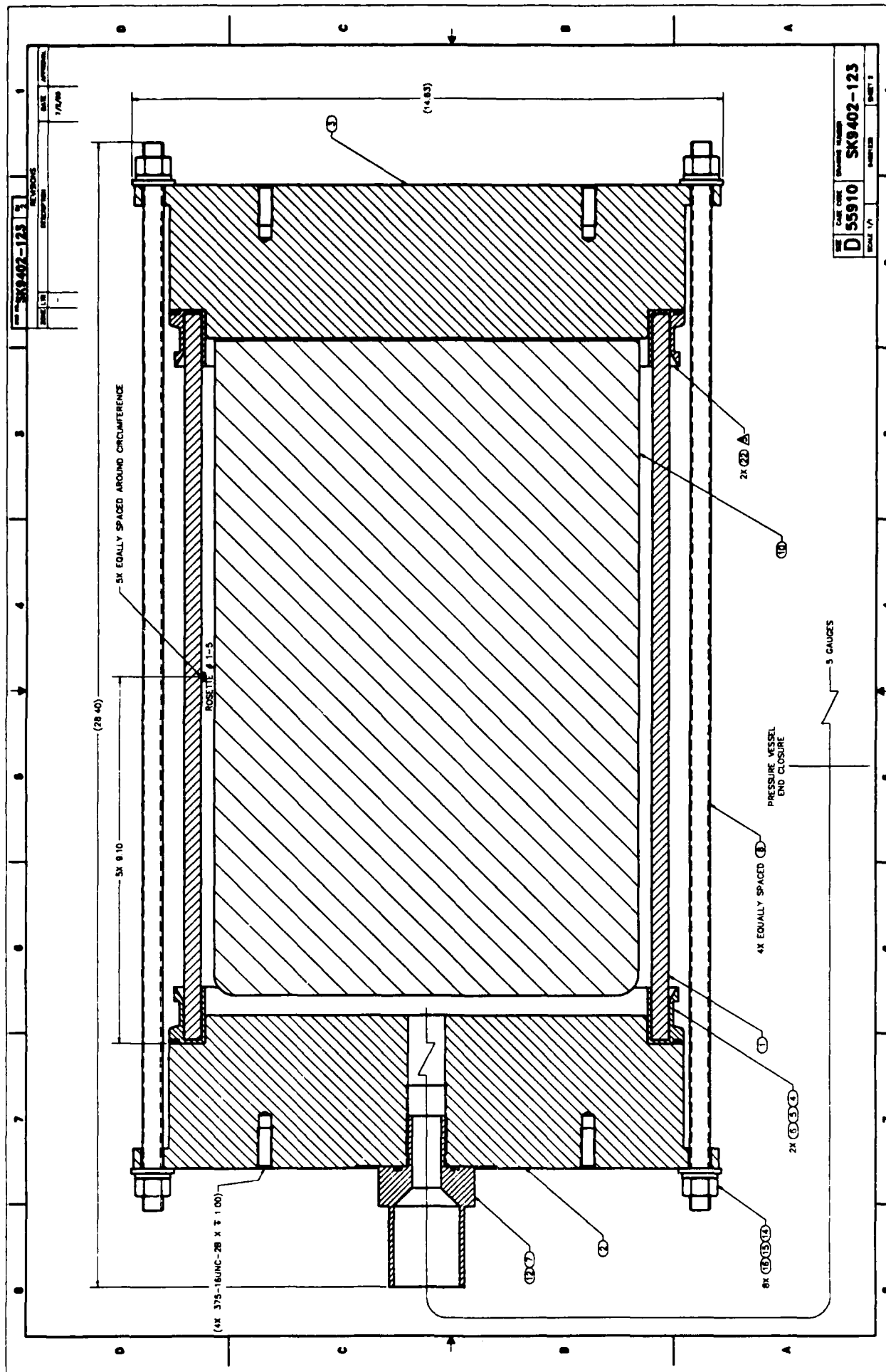Figure 33. 12-inch flat end-plate tie rod.

Figure 34. 12-inch flat end-plate feed through.
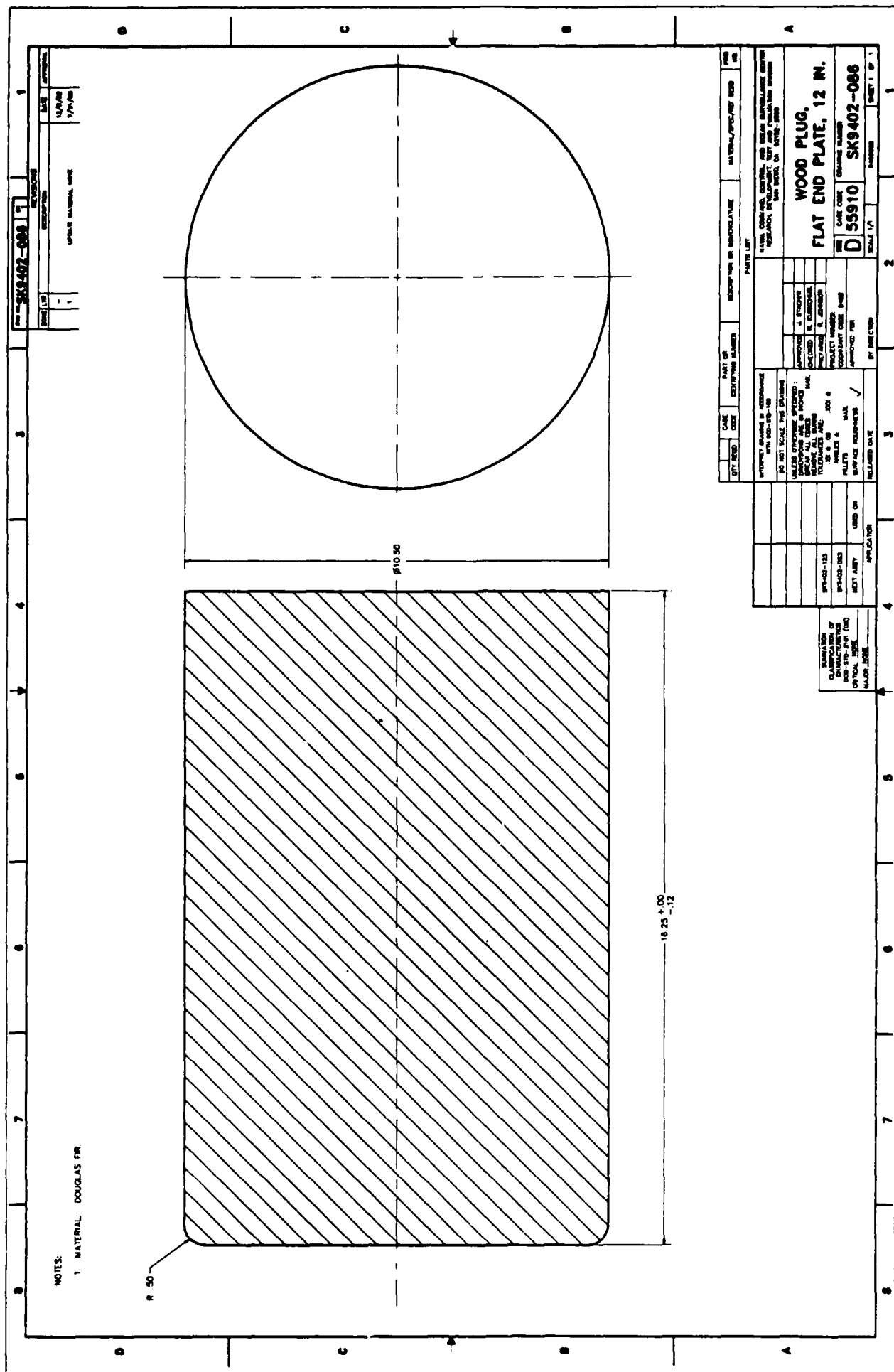
Figure 35. 12-inch flat end-plate wooden plug.

LANXIDE

90 - X - 089
Reinforced Ceramic

Figure 36. Fully machined cylinder with Type 2 titanium end caps bonded in place.
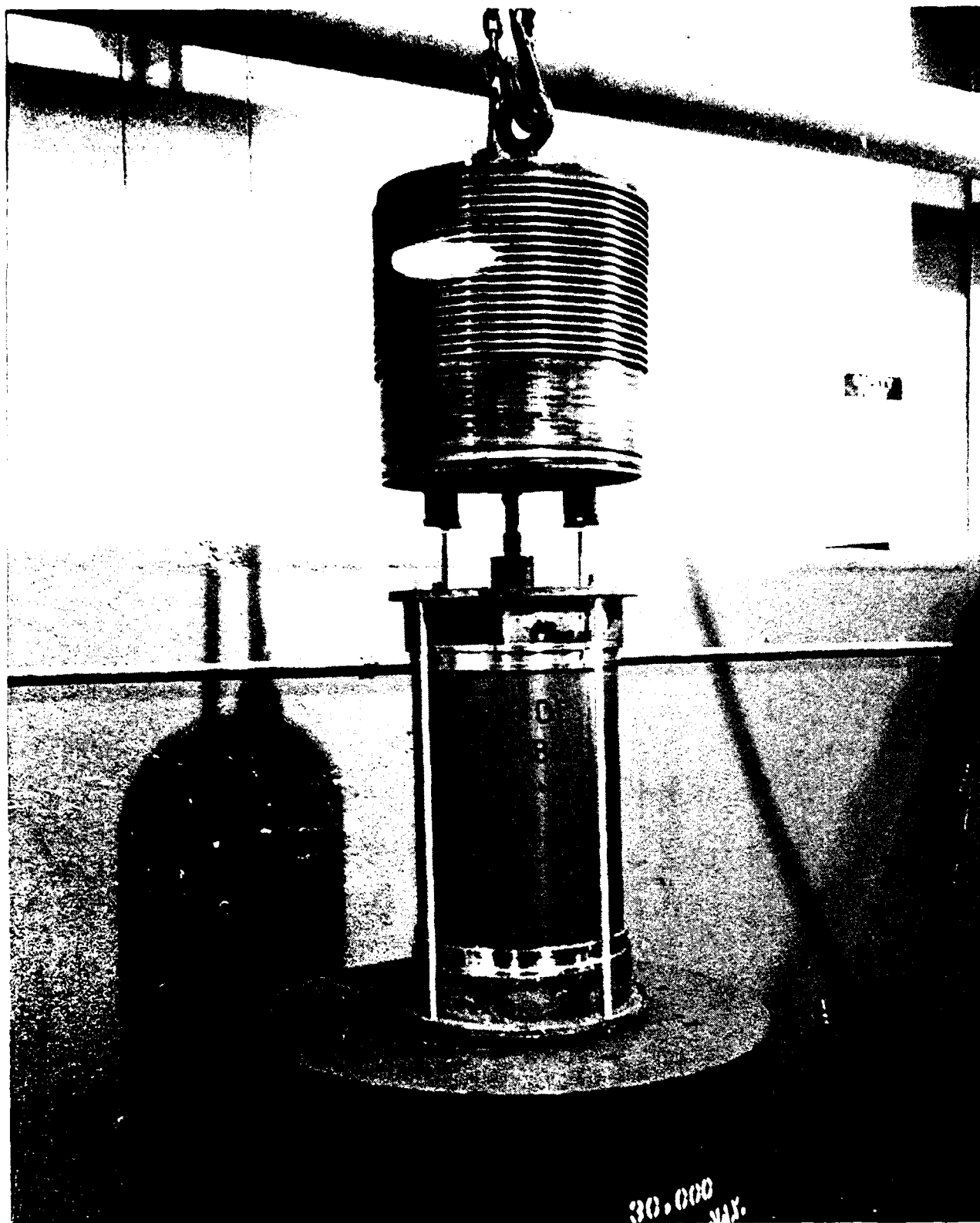
Figure 37. Type II test assembly being lowered into pressure chamber.
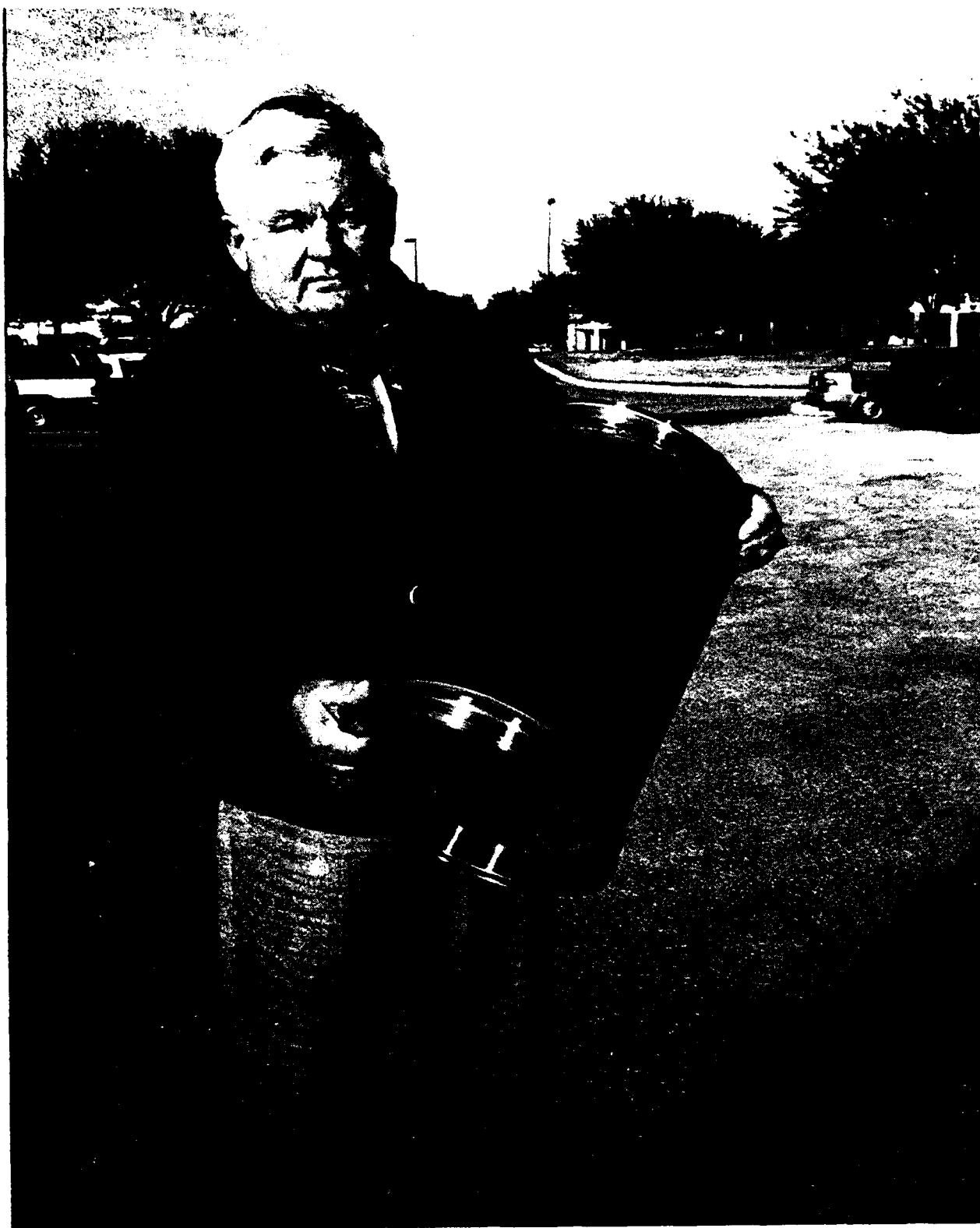
Figure 38. "As-cast" cylinder with green epoxy coating, prior to testing.

Figure 39. Fixture used to remove titanium end caps from ceramic cylinders for crack inspection after pressure testing.
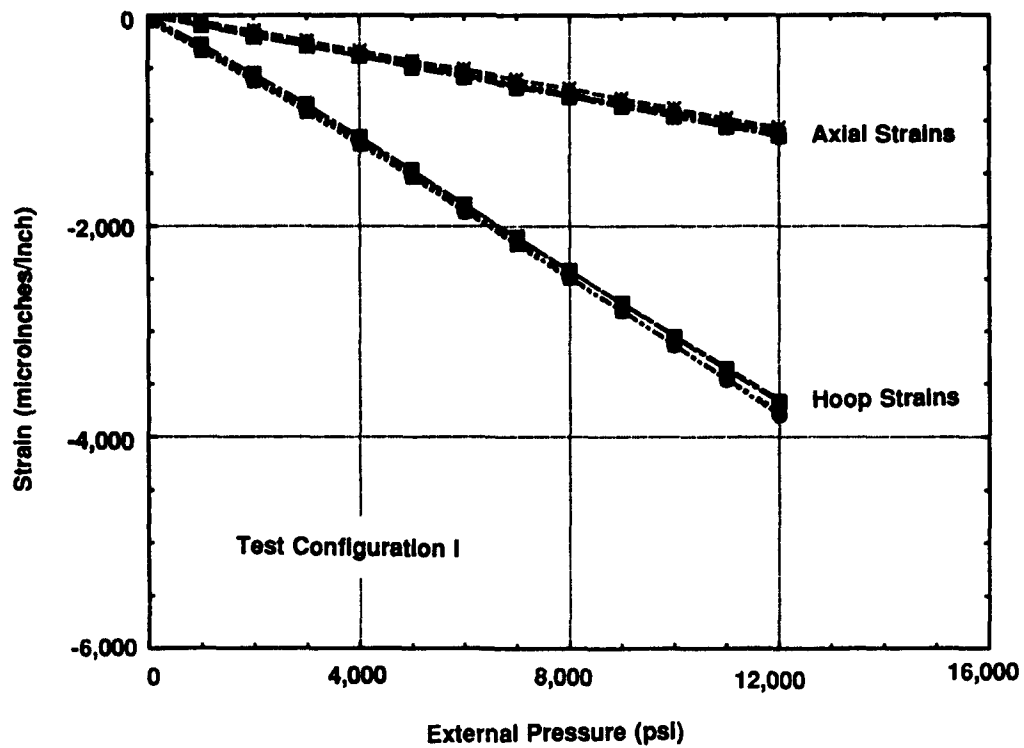
Figure 40. Pressure vs. strain plot for cylinder LAN 001.
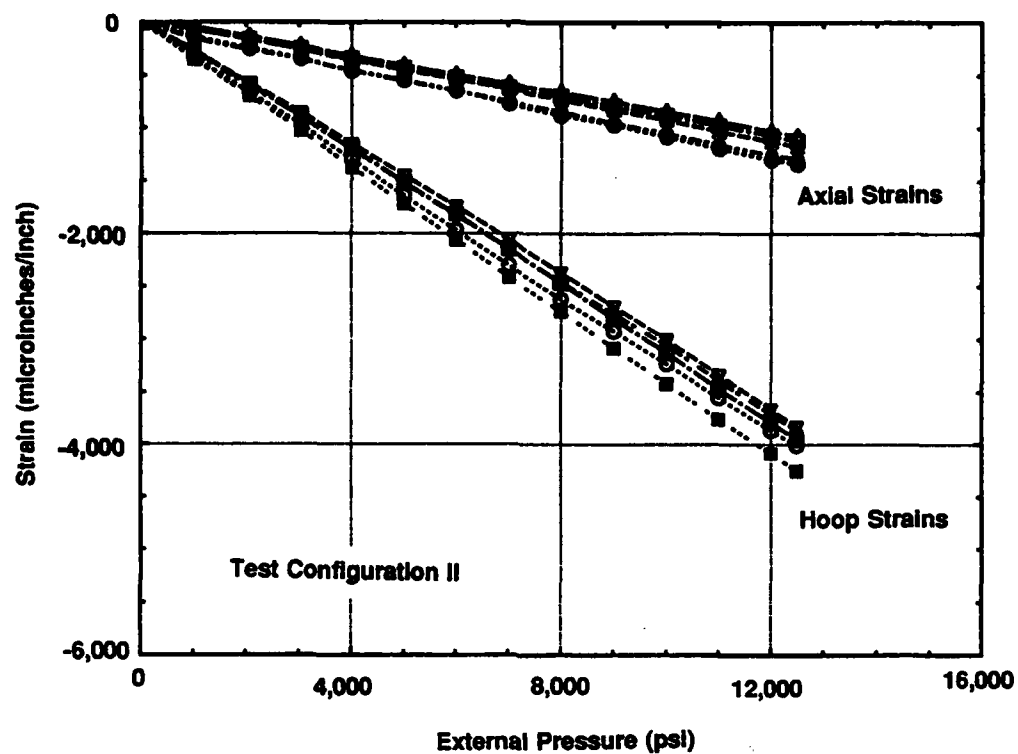
Figure 42. Pressure vs. strain plot for cylinder LAN 002.
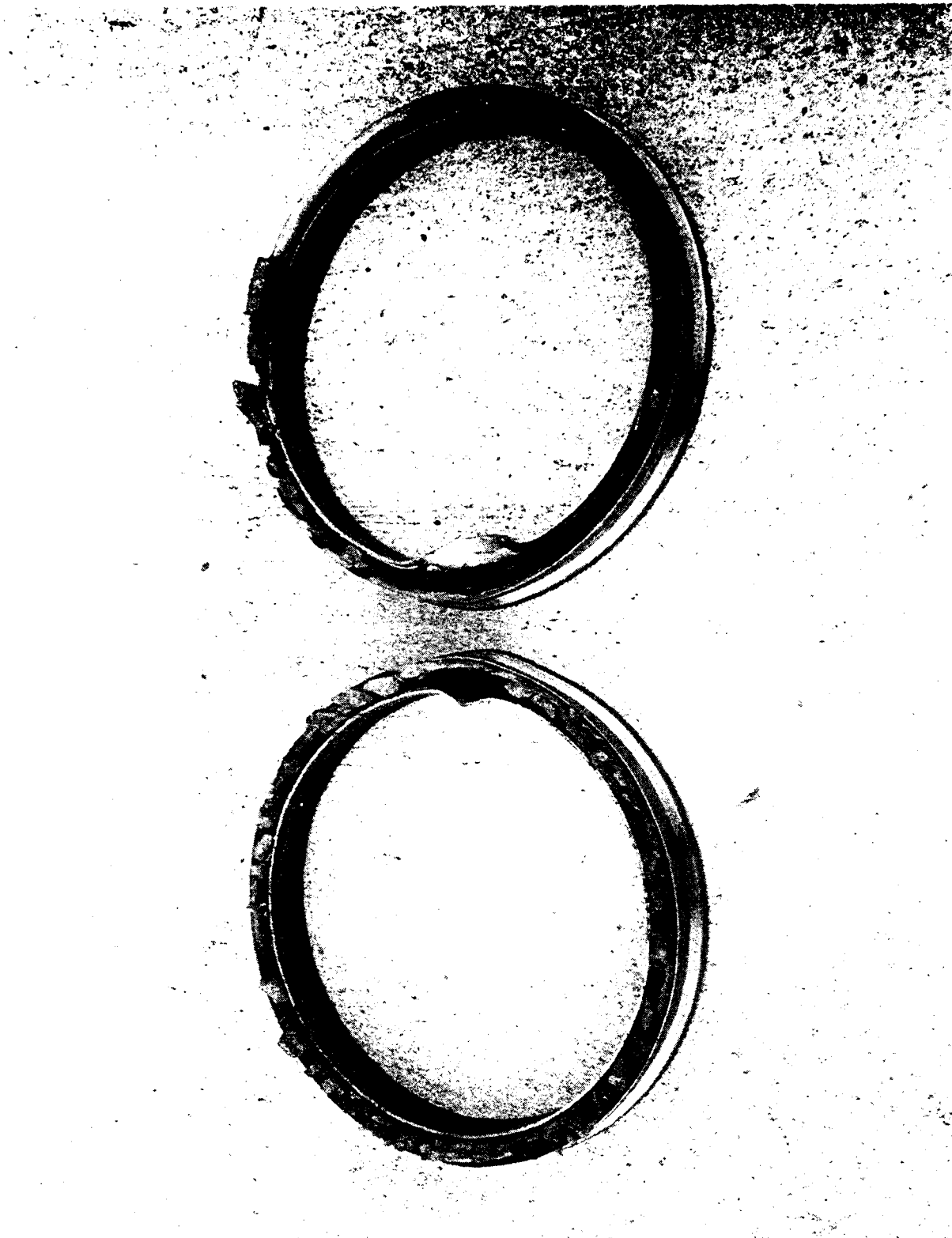
Figure 43. End cap remains of failed cylinder LAN 002.
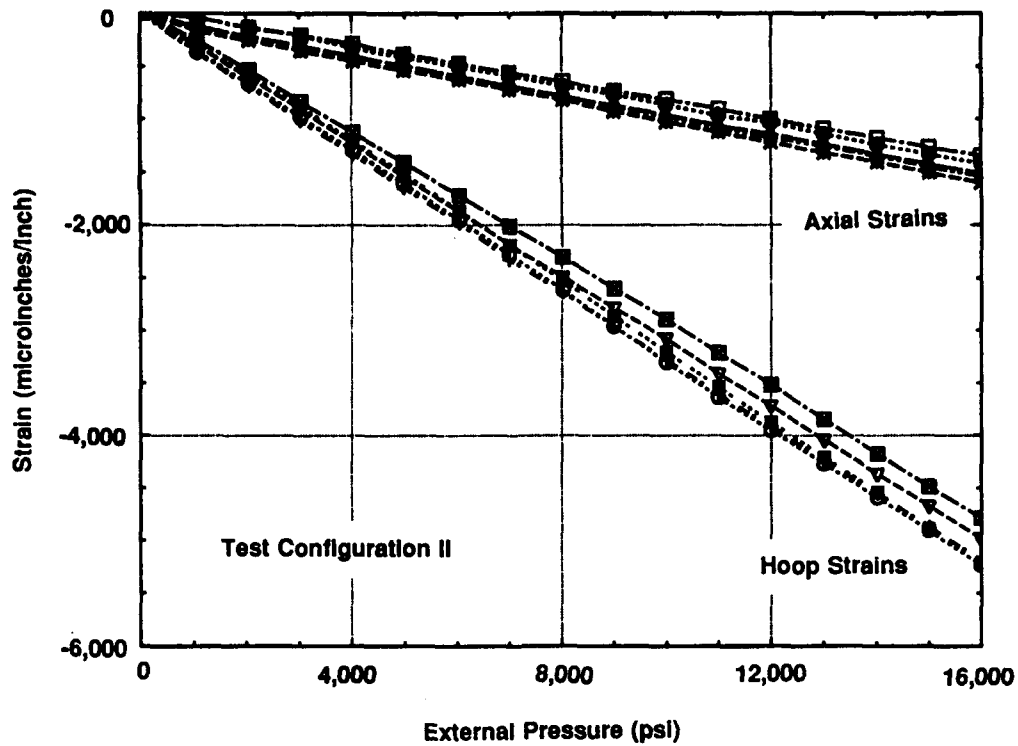
Figure 44. Pressure vs. strain plot for cylinder LAN 003.

CIRCUMFERENCE

BEARING SURFACE   0°

BEARING SURFACE   90°

BEARING SURFACE   180°

BEARING SURFACE   270°

BEARING SURFACE   315°

45°

135°

225°

Figure 1. Pulse core Co-...   of ...
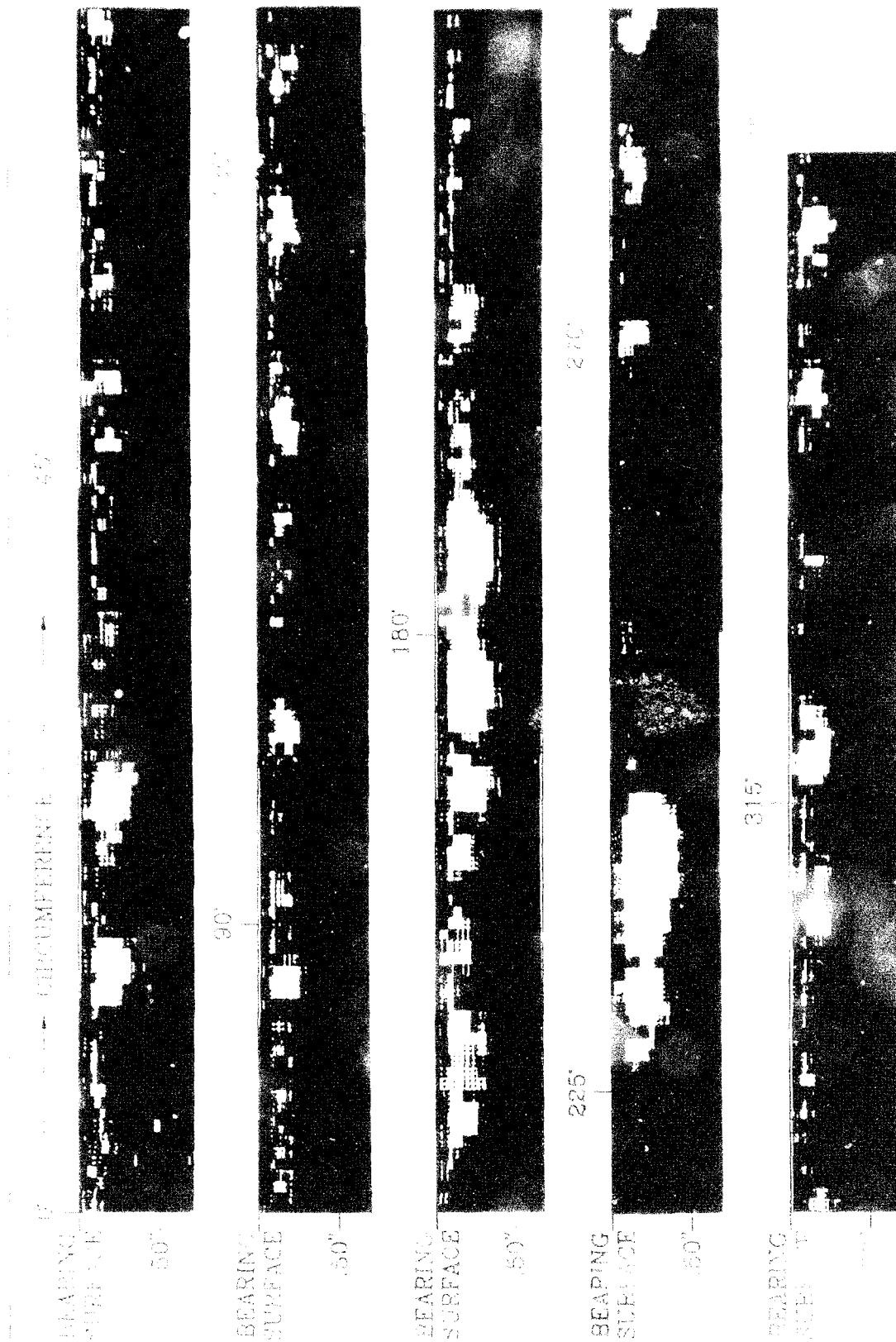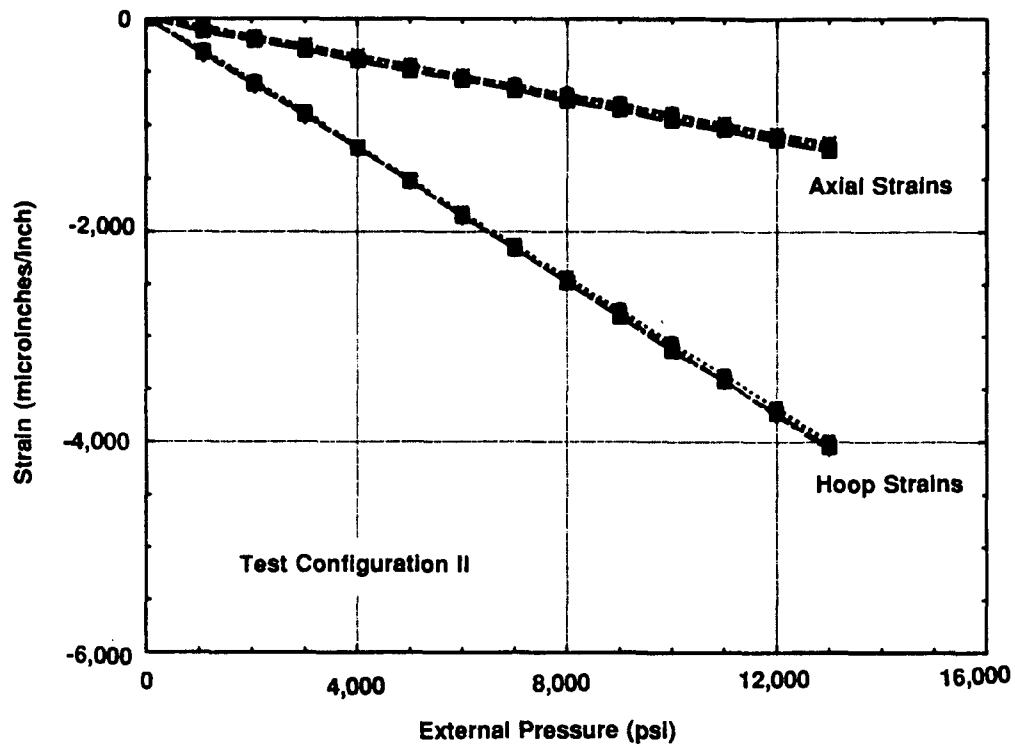
Figure 46. Pressure vs. strain plot for cylinder LAN 004.
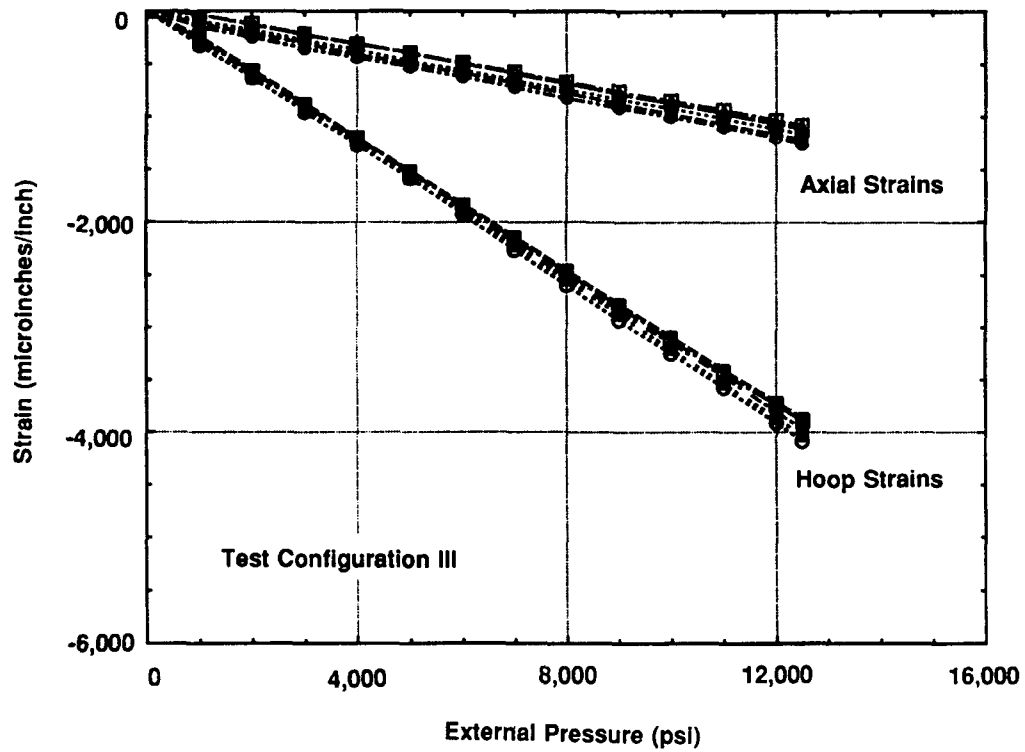
Figure 47. Pressure vs. strain plot for cylinder LAN 005.
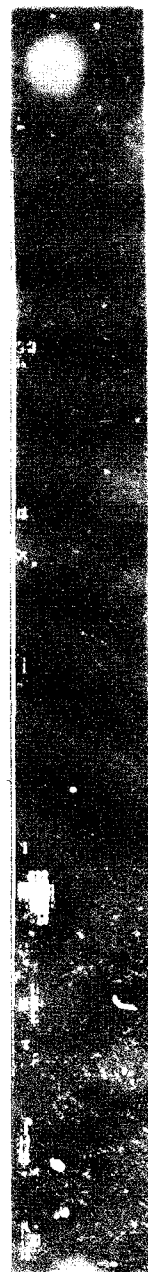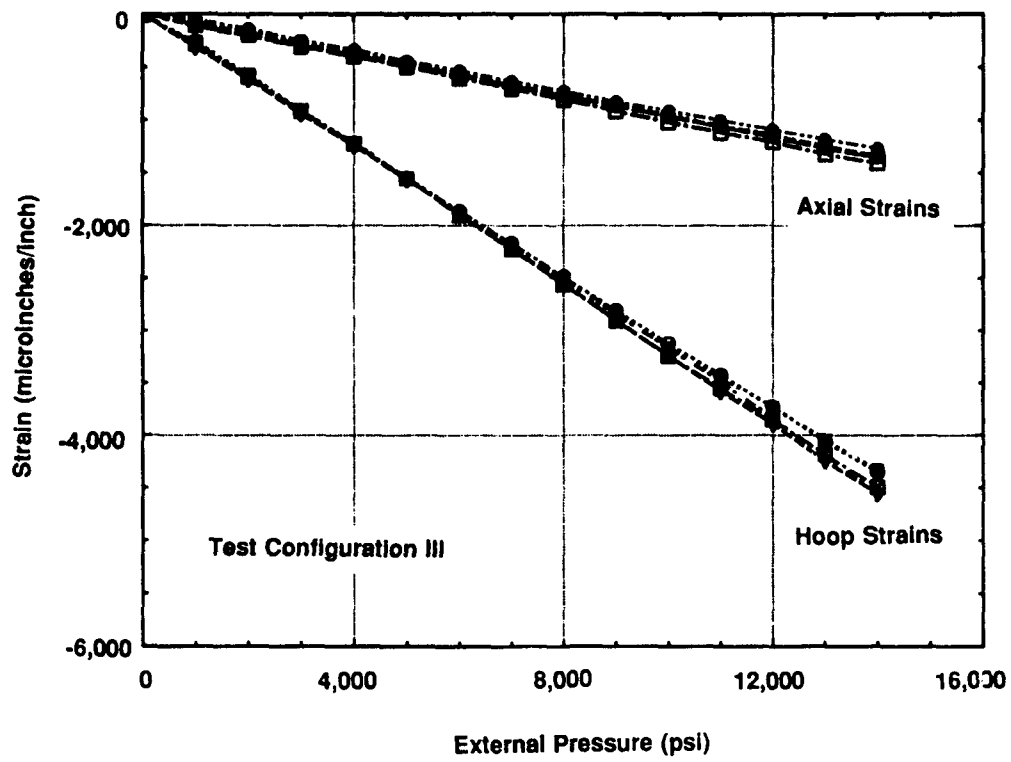
Figure 49. Pressure vs. strain plot for cylinder LAN 006.
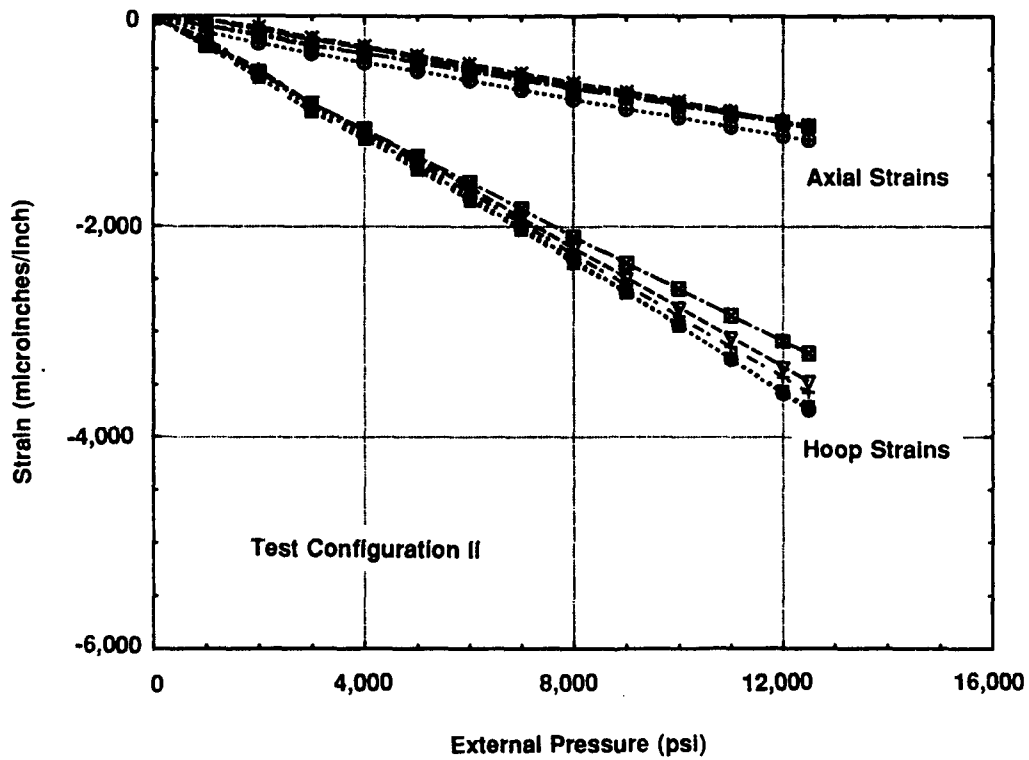
Figure 50. Pressure vs. strain plot for cylinder LAN 007.

73
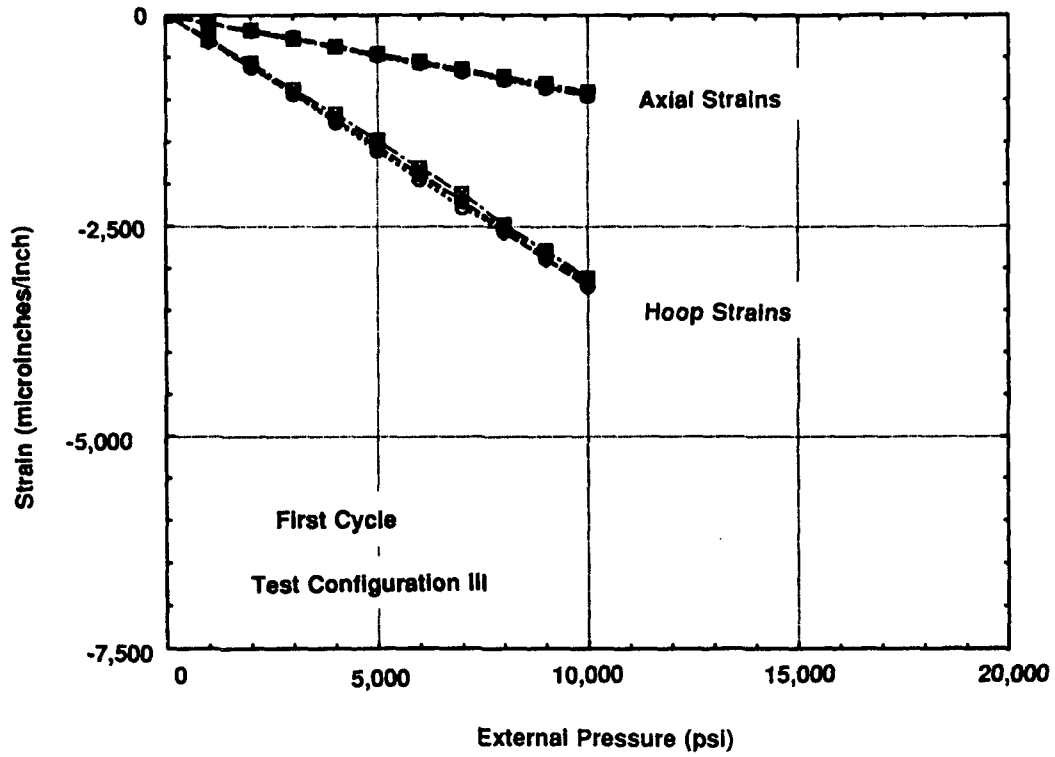
Figure 51. Pressure vs. strain plot for the first pressurization of cylinder LAN 008.
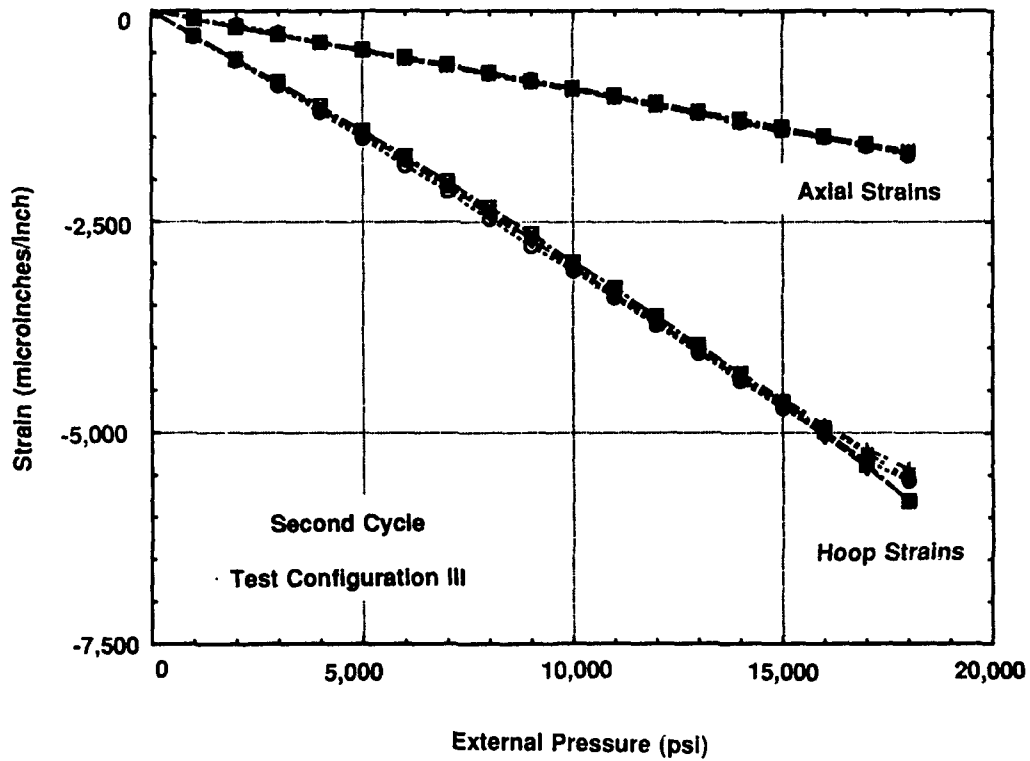
Figure 52. Pressure vs. strain plot for the second pressurization of cylinder LAN 008.

74
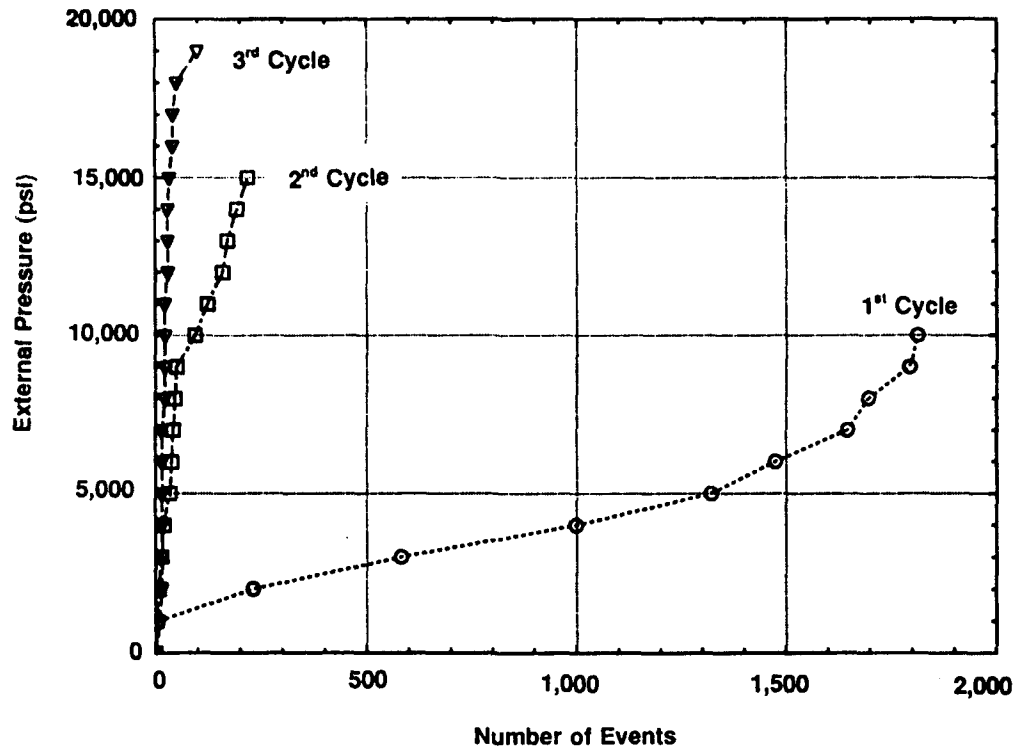
Figure 53. Acoustic emissions for first, second, and third pressurizations of cylinder LAN 008.
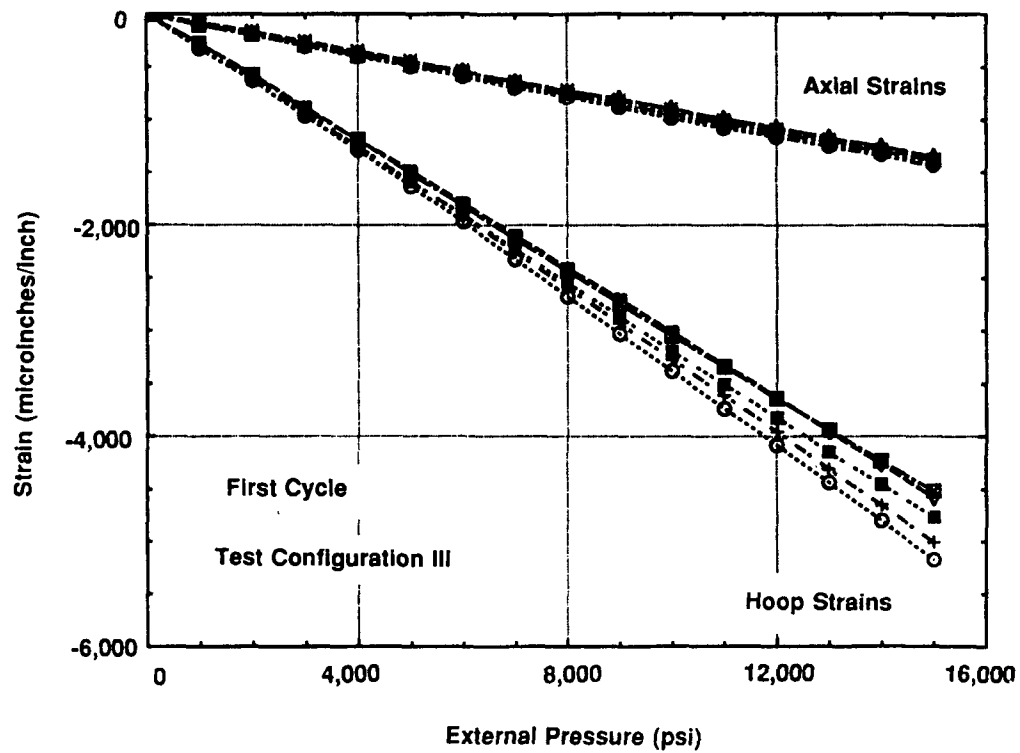
Figure 54. Pressure vs. strain plot for the first pressurization of cylinder LAN 009.
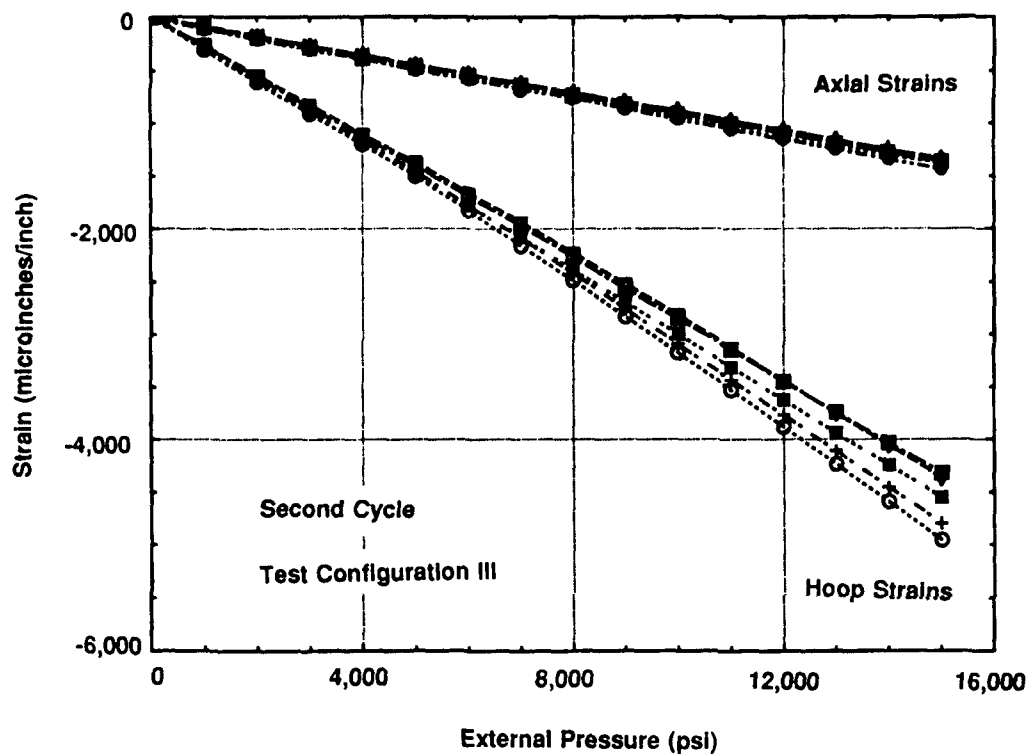
Figure 55. Pressure vs. strain plot for the second pressurization of cylinder LAN 009.
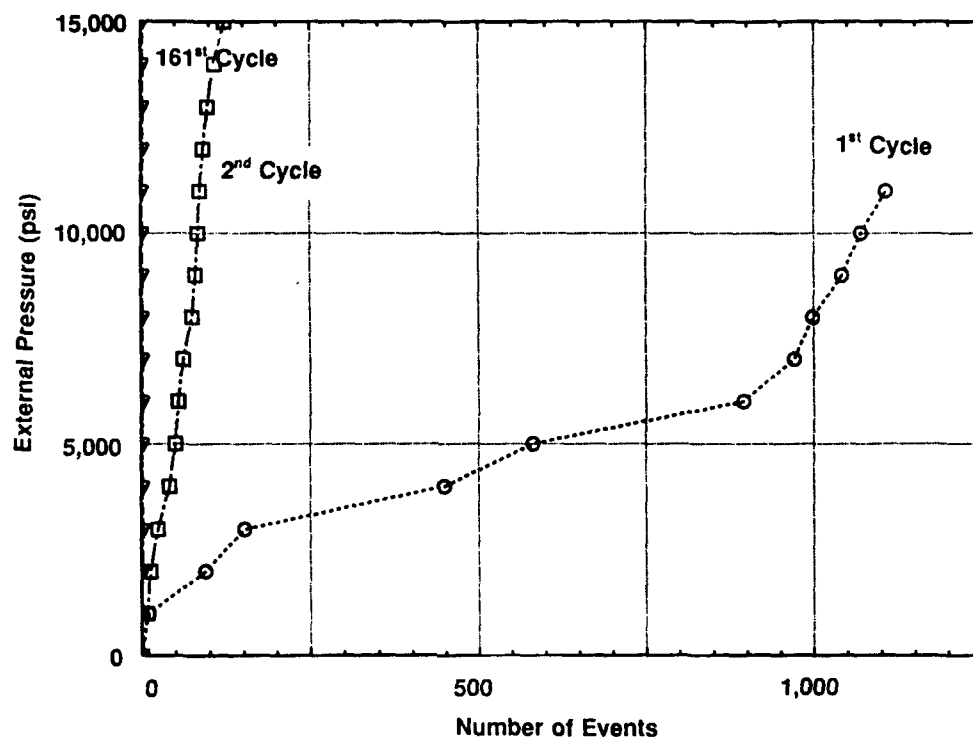
Figure 56. Acoustic emissions for first, second, and 161st pressurizations of cylinder LAN 009.

76
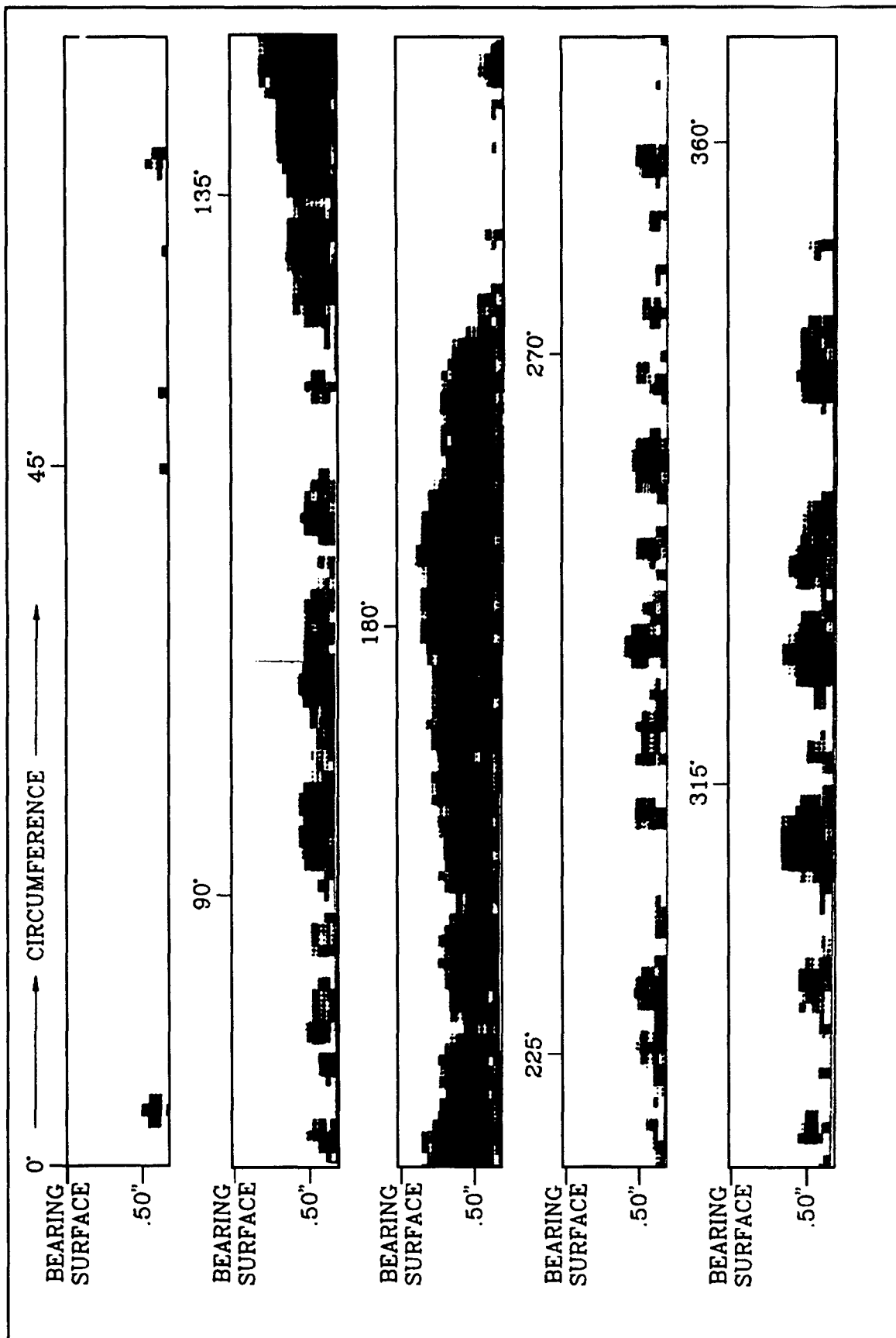
Figure. 57. Pulse-echo C-scan of one end of cylinder LAN 009.
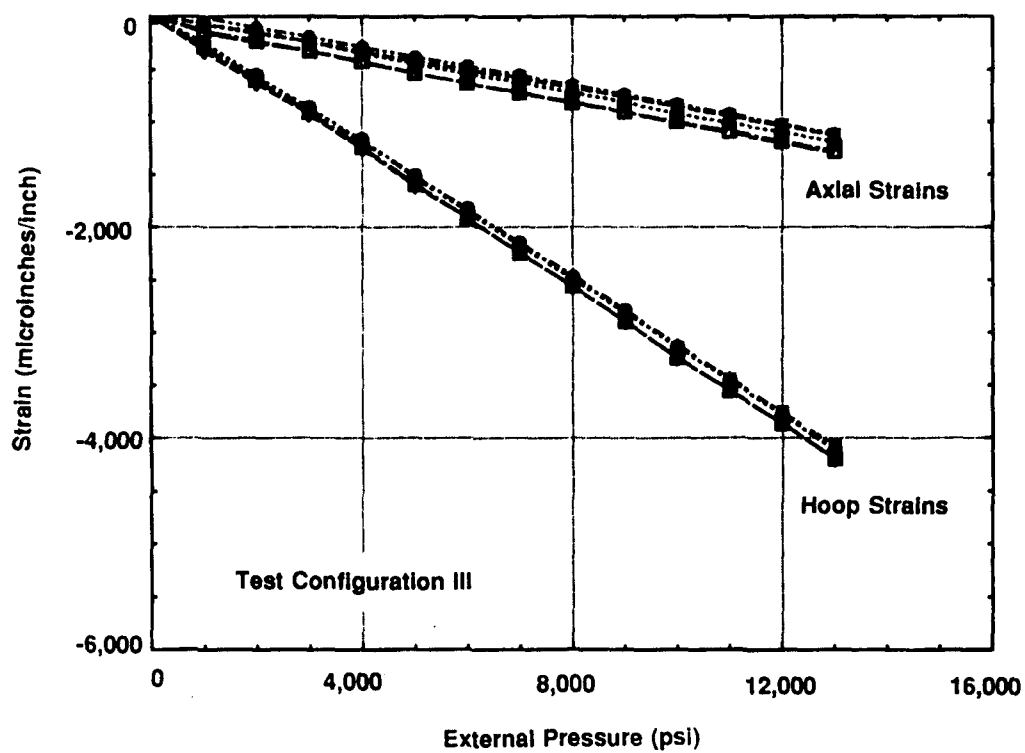
Figure 58. Pressure vs. strain plot for cylinder LAN 010.
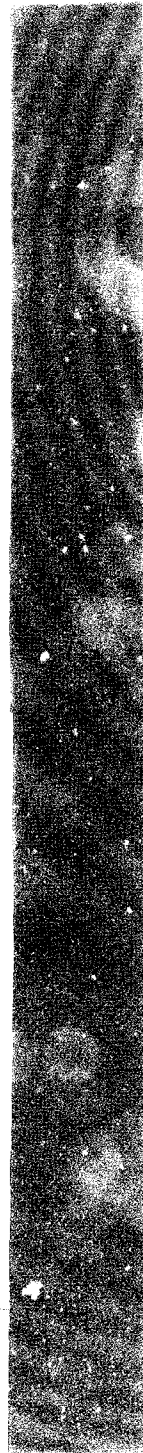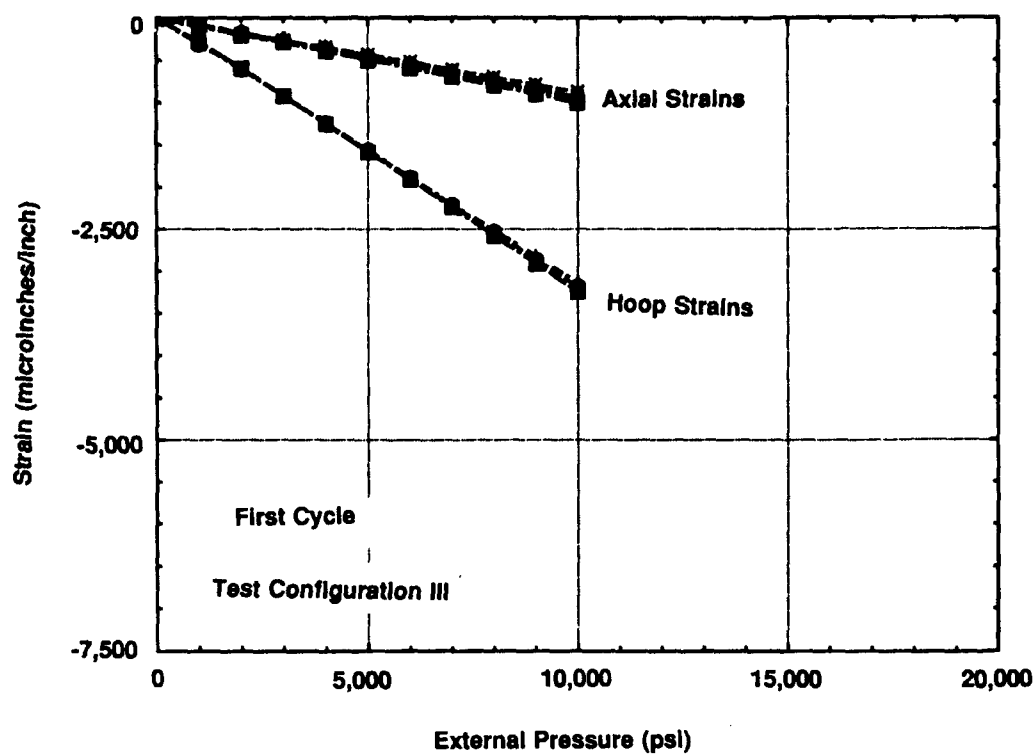
Figure 60. Pressure vs. strain plot for the first pressurization of cylinder LAN 011.
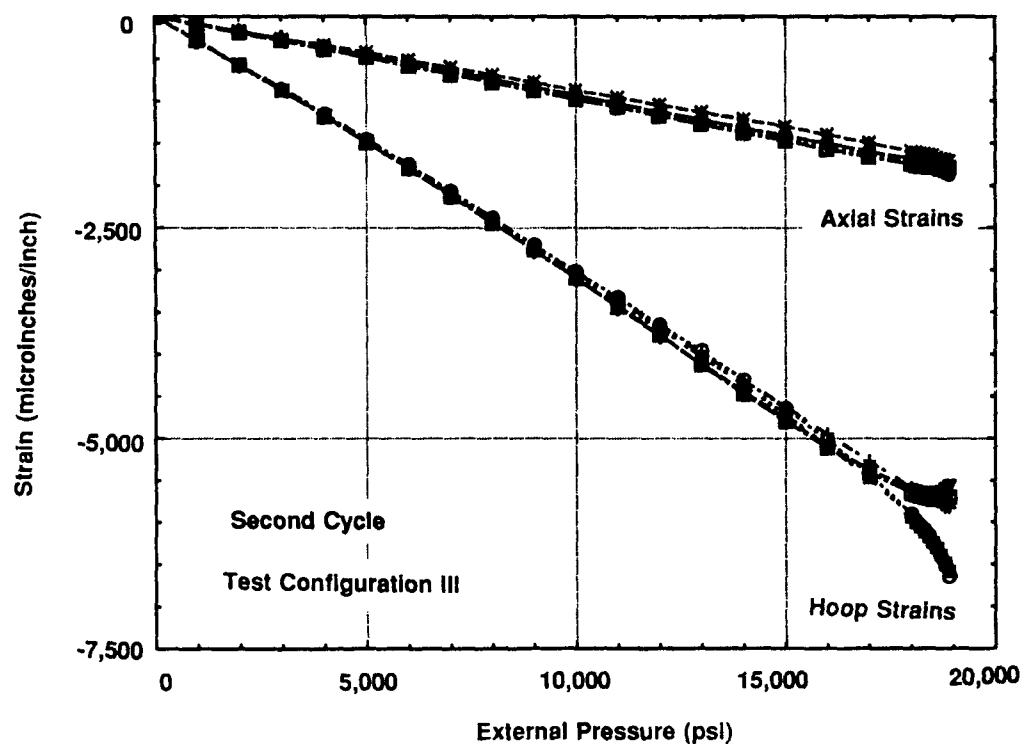
Figure 61. Pressure vs. strain plot for the second pressurization of cylinder LAN 011.
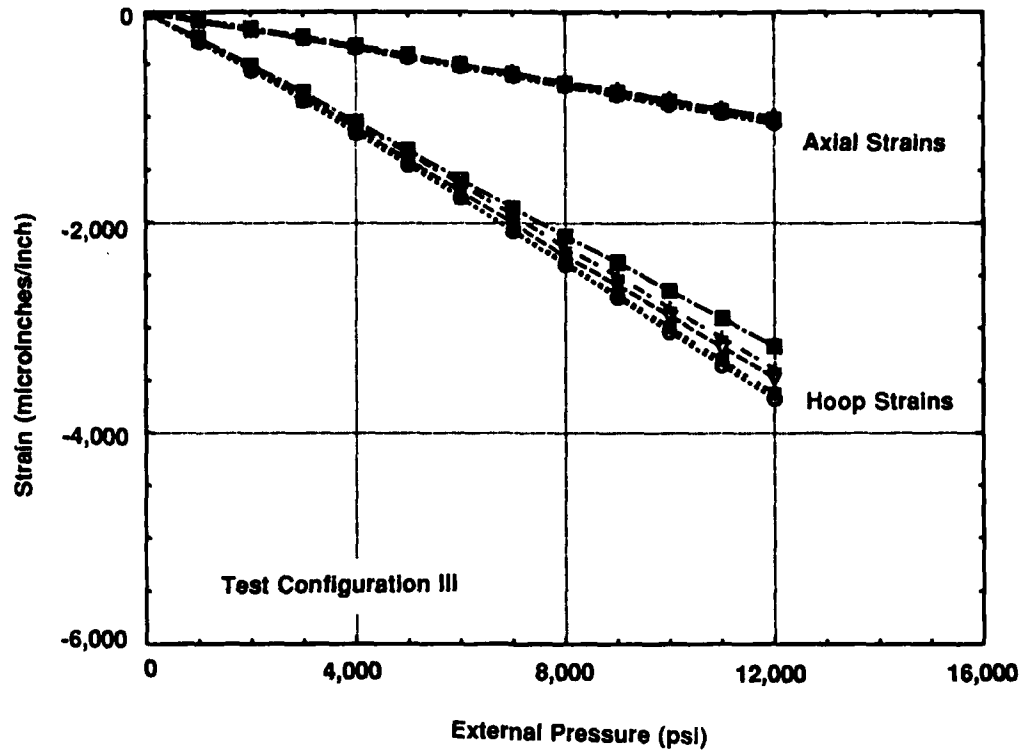
Figure 62. Pressure vs. strain plot for cylinder LAN 012.
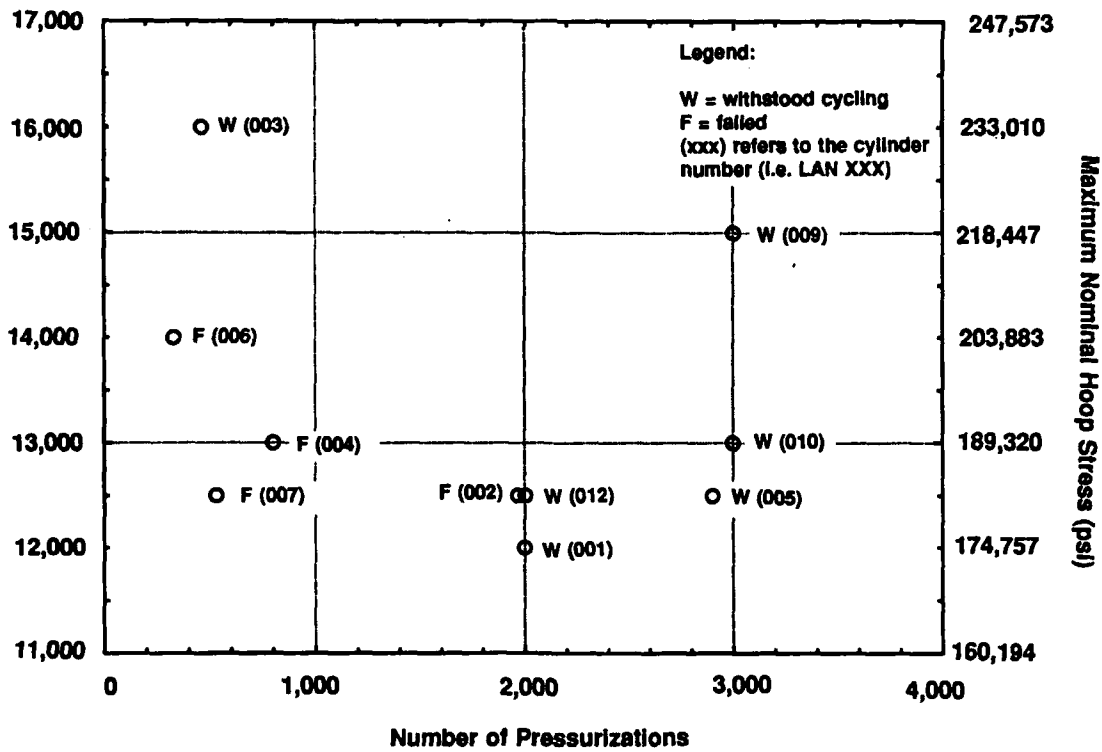
Figure 63. Number of pressurizations to failure, or pressurizations withstood vs. external hydrostatic pressure applied and maximum nominal membrane stress.
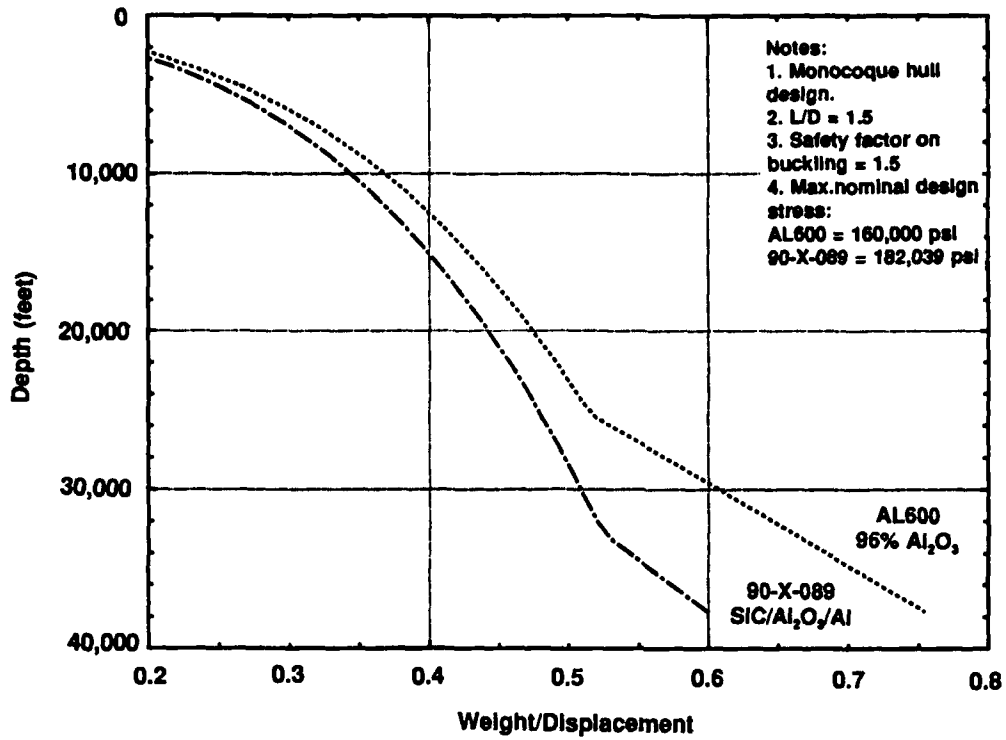
Figure 64. W/D ratio vs. depth curves for AL-600 96-percent alumina-ceramic and Lanxide 90-X-089 cylinders.

82

Table 1. Properties of several SiC/Al$_2$O$_3$/Al composites grown by the DIMOX™ process.

Property	COMPOSITION		
	90-X-089	91-X-1037	90-X-1007
Flexural Strength MPa (ksi)	383 56	179 26	476 69
Fracture Toughness MPa-m$^{1/2}$ (ksi·in$^{1/2}$)	7.9 7.2	5.5 5.0	6.6 6.0
Compressive Strength MPa (ksi)	2,075 301	ND	ND
Modulus of Elasticity GPa (Msi)	303 44	391 57	341 49
Bulk Density g/cc	3.37	3.30	3.43
Thermal Conductivity W/m-K (BUT/h-ft-°F)	105 60	140 80	88 50
Thermal Expansion ppm/°C (ppm/°F)	5.9 calc'd 3.3 calc'd	6.0 3.3	7.0 3.9
Carbide Loading vol%	52	73	51
Residual Metal vol%	18	6	11

Table 2. Dimensional analysis of three cylinder preforms.

CYLINDER	Inside Diameter (mean of six)		Outside Diameter (mean of six)	
	Max Axis	Min Axis	Max Axis	Min Axis
BL	11.204	11.107	12.139	12.018
BM	11.186	11.121	12.129	12.068
BO	11.157	11.098	NA	NA
Tolerance*	±0.024	±0.012	±0.005	±0.025

Table 3. Dimensional analysis of eleven grown cylinders.

CYLINDER	Inside Diameter (mean of six)		Outside Diameter (mean of six)	
	Max Axis	Min Axis	Max Axis	Min Axis
AY	11.163	11.076	12.099	12.037
AZ	11.165	11.077	12.099	12.050
BA	11.173	11.082	12.130	12.016
BB	11.164	11.087	12.110	12.028
BC	11.176	11.075	12.102	12.042
BD	11.158	11.080	12.105	12.035
BE	11.157	11.085	12.111	12.044
BJ	11.182	11.069	12.121	12.026
BL	11.178	11.079	12.137	12.016
BM	11.172	11.099	12.111	12.061
BO	11.164	11.092	NA	NA
MAX	11.182	11.099	12.137	12.061
MIN	11.157	11.069	12.099	12.016
MEAN	11.168	11.082	12.113	12.036
RANGE	0.025	0.030	0.038	0.045
TOLERANCE*	0.013	0.015	0.019	0.023
Std. Dev.	0.008	0.008	0.013	0.014

Table 4. Dimensional changes during growth for three cylinders.

CYLINDER	Inside Diameter	(78 each)	Outside Diameter	(78 each)
	Mean Δ ID	Std Deviation	Mean Δ ID	Std Deviation
BL	-0.022	0.012	0.004	0.010
BM	-0.018	0.006	-0.007	0.006
BO	0.000	0.006	N A	N A
MAX	0.011 (of 234)	—	0.024 (of 156)	—
MIN	-0.060 (of 234)	—	-0.031 (of 156)	—
MEAN	-0.013 (of 234)	—	-0.002 (of 156)	—
Std. Dev.	0.013 (of 234)	—	0.010 (of 156)	—

Table 5. Dimensional changes occurring during the growth of cylinder 3375-BL.

OD DIMENSIONS - PART 3375-BL — Dimensions of Grown Part minus Dried Preform

LENGTH (in 3" increments)

15° increments Around Circumference in CCW direction from index mark. (0° at row 1, 180° at row 13)

		TOP 1	2	3	4	BOTTOM 5	6	mean	range
0°	1	0.007	0.015	0.020	0.013	0.011	0.024	0.015	0.017
	2	0.002	0.013	0.013	0.014	0.010	0.017	0.012	0.015
	3	-0.010	0.008	0.007	0.004	-0.001	0.009	0.003	0.019
	4	-0.012	0.000	0.001	0.010	0.003	-0.001	0.000	0.022
	5	-0.017	0.000	-0.006	-0.005	0.004	0.007	-0.003	0.024
	6	-0.011	0.000	-0.003	-0.009	0.001	-0.001	-0.004	0.012
	7	-0.010	0.006	0.001	-0.009	-0.031	-0.011	-0.009	0.037
	8	-0.010	0.000	0.002	-0.012	-0.007	-0.014	-0.007	0.016
	9	-0.002	0.010	0.021	-0.007	-0.006	-0.012	0.001	0.033
	10	0.007	0.012	0.004	0.000	0.000	-0.003	0.003	0.015
	11	0.013	0.017	0.010	0.009	0.009	0.009	0.011	0.008
	12	0.015	0.009	0.010	0.008	0.016	0.019	0.013	0.011
180°	13	0.010	0.010	0.009	0.012	0.010	0.017	0.011	0.008
	mean	-0.001	0.008	0.007	0.002	0.001	0.005	0.004	avg of all
	max	0.015	0.017	0.021	0.014	0.016	0.024	0.024	max of all
	min	-0.017	0.000	-0.006	-0.012	-0.031	-0.014	-0.031	min of all
	range	0.032	0.017	0.027	0.026	0.047	0.038	0.010	std dev
								0.055	range of all

ID DIMENSIONS   PART 3375-BL — Dimensions of Grown Part minus Dried Preform

LENGTH (in 3" increments)

15° increments Around Circumference in CCW direction from index mark. (0° at row 1, 180° at row 13)

		TOP 1	2	3	4	BOTTOM 5	6	mean	range
0°	1	-0.012	-0.010	-0.015	-0.012	-0.020	-0.020	-0.015	0.010
	2	-0.011	-0.011	-0.012	-0.019	-0.022	-0.024	-0.017	0.013
	3	-0.016	-0.012	-0.010	-0.016	-0.030	-0.029	-0.019	0.020
	4	-0.022	-0.015	-0.020	-0.015	-0.025	-0.019	-0.019	0.010
	5	-0.042	-0.030	-0.025	-0.029	-0.033	-0.014	-0.029	0.028
	6	-0.057	-0.060	-0.043	-0.026	-0.033	-0.034	-0.042	0.034
	7	-0.038	-0.044	-0.027	-0.029	-0.024	-0.033	-0.033	0.020
	8	-0.032	-0.036	-0.036	-0.032	-0.014	-0.020	-0.028	0.022
	9	-0.031	-0.024	-0.026	-0.025	-0.016	-0.019	-0.024	0.015
	10	-0.015	-0.013	-0.018	-0.028	-0.029	-0.023	-0.021	0.016
	11	-0.003	-0.014	-0.022	-0.019	-0.023	-0.029	-0.018	0.026
	12	0.009	-0.008	-0.021	-0.017	-0.022	-0.021	-0.013	0.031
180°	13	0.002	-0.002	-0.011	-0.009	-0.022	-0.021	-0.011	0.024
	mean	-0.021	-0.021	-0.022	-0.021	-0.024	-0.024	-0.022	avg of all
	max	0.009	-0.002	-0.010	-0.009	-0.014	-0.014	0.009	max of all
	min	-0.057	-0.060	-0.043	-0.032	-0.033	-0.034	-0.060	min of all
	range	0.066	0.058	0.033	0.023	0.019	0.020	0.012	std dev
								0.069	range of all

Table 6. Dimensional changes occurring during the growth of cylinder 3375-BM.

OD DIMENSIONS - PART 3375-BM — Dimensions of Grown Part minus Dried Preform

LENGTH (in 3" increments)

		TOP				BOTTOM			
		1	2	3	4	5	6	mean	range
0°	1	0.005	-0.004	-0.002	-0.012	-0.005	-0.012	-0.005	0.017
	2	0.004	-0.005	0.002	-0.012	0.003	-0.012	-0.003	0.016
	3	0.001	-0.004	-0.001	-0.007	-0.001	-0.012	-0.004	0.013
15° increments	4	0.001	-0.007	-0.008	-0.001	-0.004	0.000	-0.003	0.009
Around	5	-0.004	-0.008	0.000	-0.008	-0.009	-0.014	-0.007	0.014
Circumference	6	-0.006	-0.015	-0.008	-0.010	-0.014	-0.012	-0.011	0.009
in CCW	7	-0.009	-0.014	-0.006	-0.010	-0.015	-0.015	-0.012	0.009
direction from	8	-0.004	-0.011	-0.009	-0.010	-0.016	-0.018	-0.011	0.014
index mark.	9	0.000	-0.007	-0.008	-0.007	-0.010	-0.018	-0.008	0.018
	10	0.002	-0.005	-0.004	-0.008	-0.018	-0.016	-0.006	0.020
	11	0.003	0.000	-0.002	-0.005	-0.013	-0.013	-0.005	0.016
	12	0.001	0.007	-0.005	0.005	-0.012	-0.018	-0.004	0.025
180°	13	0.001	0.007	-0.010	-0.004	-0.008	-0.011	-0.004	0.018
	mean	0.000	-0.005	-0.005	-0.007	-0.009	-0.013	-0.007	avg of all
	max	0.005	0.007	0.002	0.005	0.003	0.000	0.007	max of all
	min	-0.009	-0.015	-0.010	-0.012	-0.018	-0.018	-0.018	min of all
	range	0.014	0.022	0.012	0.017	0.021	0.018	0.006	std dev
								0.025	range of all

ID DIMENSIONS   PART 3375-BM — Dimensions of Grown Part minus Dried Preform

LENGTH (in 3" increments)

		TOP				BOTTOM			
		1	2	3	4	5	6	mean	range
0°	1	-0.014	-0.010	-0.016	-0.014	-0.013	-0.023	-0.015	0.013
	2	-0.015	-0.010	-0.012	-0.012	-0.013	-0.018	-0.013	0.008
	3	-0.014	-0.013	-0.012	-0.010	-0.016	-0.024	-0.015	0.014
15° increments	4	-0.013	-0.009	-0.012	-0.013	-0.020	-0.016	-0.014	0.011
Around	5	0.005	0.008	-0.017	-0.015	-0.022	-0.015	-0.009	0.030
Circumference	6	-0.023	-0.021	-0.019	-0.023	-0.024	-0.021	-0.022	0.005
in CCW	7	-0.022	-0.029	-0.022	-0.022	-0.020	-0.019	-0.022	0.010
direction from	8	-0.022	-0.025	-0.023	-0.024	-0.022	-0.024	-0.023	0.003
index mark.	9	-0.024	-0.024	-0.025	-0.020	-0.016	-0.025	-0.022	0.009
	10	-0.025	-0.021	-0.023	-0.017	-0.022	-0.022	-0.022	0.008
	11	-0.016	-0.017	-0.020	-0.024	-0.029	-0.024	-0.022	0.013
	12	-0.014	-0.014	-0.019	-0.017	-0.030	-0.025	-0.020	0.016
180°	13	-0.011	-0.010	-0.018	-0.018	-0.016	-0.021	-0.016	0.011
	mean	-0.016	-0.015	-0.018	-0.018	-0.020	-0.021	-0.018	avg of all
	max	0.005	0.008	-0.012	-0.010	-0.013	-0.015	0.008	max of all
	min	-0.025	-0.029	-0.025	-0.024	-0.030	-0.025	-0.030	min of all
	range	0.030	0.037	0.013	0.014	0.017	0.010	0.006	std dev
								0.038	range of all

Table 7. Dimensional changes occurring during the growth of cylinder 3375-BO.

ID DIMENSIONS		PART 3375-BO					Dimensions of Grown Part minus Dried Preform	
		LENGTH (in 3" increments)						
		TOP				BOTTOM		
		1	2	3	4	5	6	mean	range
0°	1	0.007	0.007	0.006	0.006	0.006	0.006	0.006	0.001
	2	0.008	0.000	0.007	0.004	0.009	0.002	0.005	0.009
	3	0.008	0.005	0.007	0.005	0.011	0.008	0.007	0.006
15° increments	4	0.007	0.007	0.008	0.007	0.007	0.002	0.006	0.006
Around	5	0.003	0.001	-0.001	0.003	0.004	0.001	0.002	0.005
Circumference	6	-0.005	-0.002	-0.006	-0.003	-0.006	-0.007	-0.005	0.005
in CCW	7	-0.006	-0.008	-0.009	-0.008	-0.010	-0.009	-0.008	0.004
direction from	8	-0.007	-0.007	-0.011	-0.010	-0.007	-0.009	-0.008	0.004
index mark.	9	-0.005	-0.005	-0.006	-0.008	-0.005	-0.008	-0.006	0.003
	10	-0.001	-0.001	-0.004	-0.003	-0.004	-0.008	-0.003	0.007
	11	0.001	0.001	-0.002	-0.002	-0.003	-0.006	-0.002	0.007
	12	0.004	0.005	0.004	0.003	-0.002	0.002	0.003	0.007
180°	13	0.008	0.008	0.006	0.009	0.004	0.007	0.007	0.005
	mean	0.002	0.001	0.000	0.000	0.000	-0.001	0.000	avg of all
	max	0.008	0.008	0.008	0.009	0.011	0.008	0.011	max of all
	min	-0.007	-0.008	-0.011	-0.010	-0.010	-0.009	-0.011	min of all
	range	0.015	0.016	0.019	0.019	0.021	0.017	0.006	std dev
								0.022	range of all

Table 8. Summary of average material property data for each deliverable cylinder (English units), Sheet 1.

Cylinder		Flexural Testing Strength (ksi)	Compression Testing Strength (ksi)	Compression Testing MOE (Msi)	Toughness (Ksi•in$^{1/2}$)	Density (lb/in^3)	Metal (v%)	Filler (v%)	Matrix (v%)	Porosity (v%)
LAN 001	TOP	56.0 ± 0.9	297.6 ± 12.2	40.2 ± 0.1	8.14 ± 0.80	0.1218	18.55	52.73	28.37	0.34
	BOTTOM	55.8 ± 4.2	305.3 ± 6.2	42.9 ± 3.0	8.17 ± 0.55	0.1240	19.84	52.58	27.37	0.21
LAN 002	TOP	62.4 ± 2.6	283.8 ± 12.6	42.5 ± 3.2	8.21 ± 0.82	0.1220	18.46	48.86	32.10	0.58
	BOTTOM	60.6 ± 3.0	269.0 ± 13.3	38.9 ± 0.7	8.19 ± 0.82	0.1220	18.98	49.66	31.10	0.27
LAN 003	TOP	53.7 ± 3.5	301.5 ± 9.7	43.8 ± 3.2	7.28 ± 0.3	0.1216	20.24	52.05	27.57	0.14
	BOTTOM	58.5 ± 2.9	303.1 ± 3.3	44.7 ± 4.1	7.21 ± 1.3	0.1212	20.72	53.82	25.34	0.12
LAN 004	TOP	57.1 ± 3.3	306.9 ± 6.8	41.5 ± 0.1	8.21 ± 0.7	0.1217	18.53	53.82	27.57	0.08
	BOTTOM	54.2 ± 4.5	321.4 ± 4.6	43.1 ± 0.4	7.33 ± 0.5	0.1201	17.53	52.77	29.57	0.13
LAN 005	TOP	57.6 ± 2.5	312.4 ± 6.7	42.4 ± 2.9	8.31 ± 1.0	0.1215	18.73	54.26	26.88	0.12
	BOTTOM	52.9 ± 4.2	300.9 ± 2.5	41.6 ± 3.9	8.87 ± 0.9	0.1215	19.96	52.33	27.58	0.13
LAN 006	TOP	55.8 ± 3.0	319.1 ± 20.5	43.9 ± 2.3	7.89 ± 0.64	0.1217	19.14	51.22	29.47	0.17
	BOTTOM	56.3 ± 3.3	307.5 ± 6.4	41.3 ± 3.5	8.61 ± 1.09	0.1216	18.04	54.81	27.05	0.11
LAN 007	TOP	53.4 ± 3.5	285.6 ± 13.5	39.9 ± 3.2	6.19 ± 0.3	0.1224	19.28	51.97	28.28	0.48
	BOTTOM	54.0 ± 3.2	288.9 ± 5.6	42.2 ± 3.6	6.32 ± 0.6	0.1214	18.94	51.?	29.37	0.36
LAN 008	TOP	59.3 ± 1.0	306.9 ± 13.0	41.2 ± 1.3	6.50 ± 0.4	0.1218	19.26	5(..	30.22	0.24
	BOTTOM	48.7 ± 9.7	286.0 ± 24.0	41.5 ± 1.7	5.13 ± 1.0	0.1217	17.15		31.08	0.44
LAN 009	TOP	57.1 ± 3.6	318.4 ± 8.4	42.6 ± 0.7	8.17 ± 0.8	0.1213	16.39		26.63	0.24
	BOTTOM	57.7 ± 2.2	307.3 ± 6.5	41.2 ± 0.1	8.19 ± 0.9	0.1212	18.88	54.48	26.47	0.17
LAN 010	TOP	59.5 ± 2.6	310.5 ± 9.0	41.6 ± 0.4	7.64 ± 0.9	0.1218	16.81	55.84	26.97	0.39
	BOTTOM	55.0 ± 2.5	292.3 ± 6.7	39.6 ± 0.0	7.79 ± 0.9	0.1212	16.99	52.28	29.86	0.87
LAN 011	TOP	55.3 ± 5.1	312.4 ± 10.6	40.6 ± 0.9	7.78 ± 0.5	0.1217	17.55	50.61	31.21	0.62
	BOTTOM	55.5 ± 2.5	299.9 ± 3.8	39.2 ± 0.1	8.57 ± 0.6	0.1216	20.06	48.66	31.03	0.25
LAN 012	TOP	57.7 ± 2.8	301.1 ± 10.0	43.7 ± 2.8	7.19 ± 0.5	0.1212	13.85	46.78	38.61	0.76
	BOTTOM	55.7 ± 5.8	290.2 ± 10.2	39.2 ± 0.9	6.2 ± 1.3	0.1209	12.15	46.67	40.33	0.86
	Mean Of All	56.3 ± 2.9	301.2 ± 12.6	41.6 ± 1.6	7.59 ± 0.9	0.1215 ± 0.0004	18.17	51.91	29.58	0.34

Table 8. Summary of average material property data for each deliverable cylinder (S.I. units), Sheet 2.

Cylinder		Flexural Testing Strength (MPa)	Compression Testing		Toughness (MPa·m$^{1/2}$)	Density (g/cc)
			Strength (MPa)	MOE (GPa)		
LAN 001	TOP	386 ± 6	2052 ± 84	296 ± 21	8.95 ± 0.9	3.374
	BOTTOM	385 ± 29	2105 ± 43	277 ± 1	8.98 ± 0.6	3.364
LAN 002	TOP	430 ± 18	1957 ± 87	293 ± 22	9.02 ± 0.9	3.381
	BOTTOM	418 ± 21	1855 ± 92	268 ± 5	9.00 ± 0.9	3.379
LAN 003	TOP	370 ± 24	2079 ± 67	302 ± 22	8.00 ± 0.3	3.369
	BOTTOM	403 ± 20	2090 ± 23	308 ± 28	7.92 ± 1.4	3.360
LAN 004	TOP	394 ± 23	2116 ± 47	286 ± 1	9.02 ± 0.8	3.371
	BOTTOM	374 ± 31	2116 ± 32	297 ± 3	8.06 ± 0.6	3.326
LAN 005	TOP	397 ± 17	2154 ± 46	292 ± 20	9.13 ± 1.1	3.367
	BOTTOM	365 ± 29	2075 ± 17	287 ± 27	9.75 ± 1.0	3.367
LAN 006	TOP	385 ± 21	2200 ± 41	303 ± 16	8.67 ± 0.7	3.372
	BOTTOM	388 ± 23	2120 ± 44	285 ± 24	9.46 ± 1.2	3.368
LAN 007	TOP	368 ± 24	1969 ± 93	275 ± 22	6.81 ± 0.3	3.390
	BOTTOM	372 ± 22	1992 ± 41	291 ± 25	6.94 ± 0.7	3.363
LAN 008	TOP	409 ± 7	2116 ± 89	284 ± 9	7.41 ± 0.4	3.374
	BOTTOM	336 ± 67	1975 ± 167	286 ± 12	5.64 ± 1.1	3.344
LAN 009	TOP	394 ± 25	2195 ± 58	294 ± 5	8.98 ± 0.9	3.359
	BOTTOM	398 ± 15	2119 ± 45	284 ± 1	9.00 ± 0.9	3.358
LAN 010	TOP	410 ± 18	2141 ± 62	287 ± 3	8.39 ± 0.9	3.376
	BOTTOM	379 ± 17	2015 ± 46	273 ± 1	8.56 ± 0.9	3.357
LAN 011	TOP	381 ± 35	2154 ± 73	280 ± 6	8.55 ± 0.5	3.370
	BOTTOM	383 ± 17	2068 ± 26	270 ± 1	9.42 ± 0.7	3.368
LAN 012	TOP	398 ± 19	2076 ± 69	301 ± 19	7.31 ± 0.6	3.358
	BOTTOM	384 ± 40	2001 ± 70	270 ± 6	6.80 ± 1.4	3.349
Mean Of All		388 ± 20	2077 ± 87	287 ± 11	8.35 ± 1.01	3.365 ± 0.013

Table 9. Summary of pressure test plans and results for cylinders LAN 001 through LAN 012, Sheet 1.

Cylinder No.	Test Configuration	Test Plan/Test Result
LAN 001	I	Proof test cylinder to 12,000 psi, read strains. Cycle cylinder to 12,000 psi, stop testing after 2,000 cycles.
		1-proof cycle to 12,000 psi, no damage noted. Cylinder **completed 2,000 cycles to 12,000 psi**, no leaks or damage noted.
LAN 002	II	Proof test cylinder to 12,500 psi, read strains. Cycle cylinder to 12,500 psi, stop testing after 3,000 cycles.
		1-proof cycle to **12,500 psi**, no damage noted. Cylinder **failed on cycle number 1,968** during pressurization.
LAN 003	II	Proof test cylinder to 16,000 psi, read strains. Cycle cylinder to 16,000 psi, stop testing after 500 cycles.
		1-proof cycle to **16,000 psi**, no damage noted. Terminated test with **464 cycles completed.**No failure.
LAN 004	II	Proof test cylinder to 13,000 psi, read strains. Cycle cylinder to 13,000 psi, stop testing after 2,000 cycles.
		1-proof cycle to **13,000 psi**, no damage noted. Cylinder **failed on cycle number 801** during pressurization.
LAN 005	III	Proof test cylinder to 12,500 psi, read strains. Cycle cylinder to 12,500 psi, stop testing after 3,000 cycles.
		1-proof cycle to **12,500 psi**, no damage noted. Cylinder **completed 2,902 cycles**, no damage noted. Test was terminated due to leak in tank.
LAN 006	III	Proof test cylinder to 14,000 psi, read strains. Cycle cylinder to 14,000 psi, stop testing after 1,000 cycles.
		1-proof cycle to **14,000 psi**, no damage noted. Cylinder **failed on cycle number 331** during pressurization.

Table 9. Summary of pressure test plans and results for cylinders LAN 001 through LAN 012, Sheet 2.

Cylinder No.	Test Configuration	Test Plan/Test Result
LAN 007	III "as-cast" sand-blasted ends	Proof test cylinder to 12,500 psi, read strains. Cycle cylinder to 12,500 psi, stop testing after 3,000 cycles.
		1-proof cycle to **12,500 psi**, no damage noted. Cylinder **failed on cycle number 531** during pressurization.
LAN 008	III sand-blasted ends	Proof test cylinder to 10,000 psi. Monitor acoustic emissions. Pressurize cylinder to failure
		1-proof cycle to 10,000 psi. Cylinder **failed at 19,000 psi.**
LAN 009	III sand-blasted ends	Proof test cylinder to 15,000 psi, read strains. Cycle cylinder to 15,000 psi, stop testing after 3,000 cycles.
		2-proof cycles to **15,000 psi**, no damage noted. Cylinder **completed 3,003 cycles**, no damage noted.
LAN 010	III sand-blasted ends	Proof test cylinder to 13,000 psi, read strains. Cycle cylinder to 13,000 psi, stop testing after 3,000 cycles.
		1-proof cycle to **13,000 psi**, no damage noted. Cylinder **completed 3,001 cycles**, no damage noted.
LAN 011	III sand-blasted ends	Proof test cylinder to 10,000 psi, read strains. Then pressurize cylinder to failure, read strains at 1,000 psi intervals to 18,000 psi, then at 100 psi intervals.
		1-proof cycle to 10,000 psi, no damage noted. Cylinder **failed at 19,000 psi** on second cycle.
LAN 012	III "as-cast" sand-blasted ends	Proof test cylinder to 12,500 psi, read strains. Cycle cylinder to 12,500 psi, stop testing after 2,000 cycles.
		1-proof cycle to **12,5000 psi**, no damage noted. Cylinder **completed 2,004 cycles**, no damage noted.

Table 10. Average measured axial and hoop strains, calculated compressive modulus, and Poisson's Ratio.

Cylinder	Strains at 10,000 psi external pressure (microinches/inch)		Calculated Poisson's Ratio	Measured Compressive Modulus (Msi)		Calculated Compressive Modulus (Msi)
	Axial	Hoop		Top	Bottom	
LAN 001	931.4	3097.4	0.235	40.2	42.9	42.98
LAN 002	955.8	3169.0	0.234	42.5	38.9	42.03
LAN 003	929.6	3153.2	0.241	43.8	44.7	42.07
LAN 004	924.2	3096.0	0.237	41.5	43.1	42.94
LAN 005	920.4	3159.0	0.244	42.4	41.6	41.91
LAN 006	961.8	3186.6	0.233	43.9	41.3	41.80
LAN 007	852.0	2817.4	0.233	39.9	42.2	47.28
LAN 008	939.6	3170.8	0.239	41.2	41.5	41.88
LAN 009	936.6	3184.0	0.241	42.6	41.2	41.65
LAN 010	922.2	3177.2	0.245	41.6	39.6	41.64
LAN 011	940.2	3199.0	0.242	40.6	39.2	41.45
LAN012	855.0	2070.2	0.237	43.7	39.2	46.30
Mean*	936.2	3159.2	0.239			42.04
St.Dev.*	13.8	35.5	0.004			0.52

* Note: As-cast cylinders LAN007 and LAN012 were not included in the calculations of the mean and standard deviation.

Table 11. Summary of cyclic pressure testing of Lanxide's 90-X-089 composite and comparison with the performance of AL-600 96-percent Al_2O_3 ceramic manufactured by WESGO.

External hydrostatic pressure (psi)	Maximum nominal hoop stress (psi)	Number of pressurizations	
		Lanxide 90-X-089 SiC/Al_2O_3/Al cylinder	Wesgo AL600 96% Al_2O_3 cylinder
9,000	131,067		withstood 3,000
10,000	145,631		
11,000	160,194		withstood 1,380 failure at 2,969
12,000	174,757	withstood 2,000	failure at 1,065
12,500	182,039	failure at 531 failure at 1,968 withstood 2,004 withstood 2,902	
13,000	189,320	failure at 801 withstood 3,001	failure at 762
14,000	203,883	failure at 331	failure at 214
15,000	218,447	withstood 3,003	failure at 707
16,000	233,010	withstood 464	

APPENDIX A: THE PROTOTYPE 12-INCH-OD BY 12-INCH-LONG SiC/ Al_2O_3/Al CERAMIC COMPOSITE CYLINDER FABRICATED BY LANXIDE CORPORATION

FIGURES

APPENDIX A: THE PROTOTYPE 12-INCH-OD BY 12-INCH-LONG SiC/Al₂O₃/Al CERAMIC COMPOSITE CYLINDER FABRICATED BY LANXIDE CORPORATION

INTRODUCTION

The Navy has a requirement for lightweight pressure housings for its unmanned deep submergence, underwater vehicles. Ceramics appear to be the ideal material for this application. The Naval Command, Control and Ocean Surveillance Center (NCCOSC) RDT&E Division (NRaD) has found that the Lanxide DIMOX™ process appears to be particularly well suited for fabrication of cylinders and hemispheres from SiC/Al₂O₃/Al ceramic composite that provides these components with superior fracture toughness.

To develop the fabrication process for cylinders NOSC[1] awarded a contract in 1990 to Lanxide Corporation. The output of that contract was a series of 6.039-inch-OD by 9-inch-long by 0.206-inch-thick cylinders that subsequently were pressure tested to destruction by NOSC. The test results indicate that the compressive strength of the ceramic composite under biaxial compression is ≧ 326,000 psi and its modulus of elasticity $E=44.5 \times 10^6$ psi. The material was found to exhibit a permanent deformation of 0.025 percent after several loading cycles to −150,000 psi compressive cycles.

Encouraged by the outstanding performance of the Lanxide 90-X-089 ceramic composite 6-inch scale-model cylinders, NRaD awarded a second contract in 1992 for the development of a process for fabrication of 12-inch-OD by 18-inch-long by 0.412-inch-thick cylinders. This test report summarizes the structural performance of the first successful 12-inch-OD cylinder fabricated by the DIMOX™ process from Lanxide 90-X-089 ceramic composite.

This cylinder was fabricated at contractor's expense, and delivered to NRaD prior to award of

---

[1]NRaD was previously Naval Ocean Systems Center (NOSC).

the contract to serve as a proof of contractor's ability to fabricate such cylinders.

CYLINDER DESCRIPTION

The physical characteristics of the cylinder are:

Outside diameter	=	12.03	inches
Length	=	12.0	inches
Thickness	=	0.420	inch
Weight	=	22.52	lbs (10,201 grams)
Density	=	0.122	lbs/in³
Compressive strength	=	315,000	psi

The 12-inch-long cylinder was obtained by cutting away rings from an 18-inch-long cylinder fabricated from Lanxide 90-X-089 (500 grit SiC with a grown aluminum oxide matrix) by the DIMOX™ process. The compressive strength of the ceramic composite in the cylinders was determined by testing of specimens machined from rings removed from both ends of the cylinder.

TEST SETUP

Titanium end caps, type Mod 1, were bonded to both ends of the cylinder with epoxy adhesive (figure A1). The thickness of the epoxy interlayer between the plane ceramic bearing surface and the titanium seat varied from 0.010 to 0.015 inch. The epoxy interlayer was formulated from 100 parts CIBA Geigy 6010 resin and 70 parts CIBA Geigy 283 hardener.

The cylinder was instrumented on the interior surface with rectangular strain gages, type CEA-06-12SWT-350. Gages 1 through 5 were located at 72-degree intervals at midbay, while gages 6 through 10 were located in a single line from midbay to one of the cylinder ends at 0.91-inch intervals.

After strain gage instrumentation, the cylinder was placed on a steel bulkhead that provided the cylinder with axial and radial support. This was followed by inserting a loosely fitting wooden plug into the cylinder for mitigation of shock loading to the pressure vessel generated by implosion of the vessel

(figure A2). Placing a second bulkhead on top of the cylinder and tightening the external tie rods completed the test assembly (figure A3).

After potting of strain gage leads into bulkhead penetrators screwed into the steel bulkhead and the pressure vessel cover, the test assembly was lowered into the pressure vessel (figure A4). Locking the pressure vessel cover completed preparations for testing.

TEST PROCEDURE

The pressure inside the vessel was raised at 1,000-psi intervals to 10,000 psi, and the strains were recorded. After a one-minute hold, the vessel was depressurized and the strains were read again. The pressurization was repeated 20 times and the strains were recorded. After the 20th pressurization, the strain recording equipment was disconnected and the pressure cycling from 50 to 10,000 psi was placed on automatic control. Acoustic emissions generated by the ceramic cylinder test assembly also were monitored during the first 20 pressure cycles by a transducer bonded to the exterior of the pressure vessel.

TEST RESULTS

1. The ceramic cylinder imploded during the pressurization in the 826th pressure cycle to 10,000 psi. The failure was catastrophic.

2. The average hoop and axial strains at midbay under 10,000-psi pressure generated a 148,250 psi hoop and 74,140 psi. Axial stresses on the interior surface were:

Pressure Cycle	Hoop strain	Axial strain
1st	−3164	−973
2nd	−3025	−961
3rd	−3011	−937

3. The acoustic emissions decreased from 1,600 events during the first, to 20 events during the 20th cycle, displaying a typical Kaiser effect.

FINDINGS

The cyclic fatigue life at 10,000 psi of the 12-inch-OD cylinder fabricated from Lanxide 90-X-089 and equipped with NOSC type Mod 1 titanium end caps equals, or exceeds, that of 94-percent alumina-ceramic cylinders with identical dimensions at 74,000-psi axial bearing loading. At 9,000-psi design pressure, the cyclic fatigue life will, in all probability, exceed 1,000 cycles.

The strains measured on the interior surface of the 12-inch-OD cylinder are identical to the strains previously measured on the interior of 6-inch-OD cylinders after adjustments have been made for a slight difference in scaling ratio.

CONCLUSIONS

1. The material properties of the Lanxide 90-X-089 ceramic composite in the 12-inch-OD cylinder are identical to the material properties of the same composite in 6-inch-OD cylinders.

2. The fabrication process for producing large cylinders from Lanxide 90-X-089 ceramic composite appears to have satisfied all the criteria associated with the scaling up of laboratory type processes.
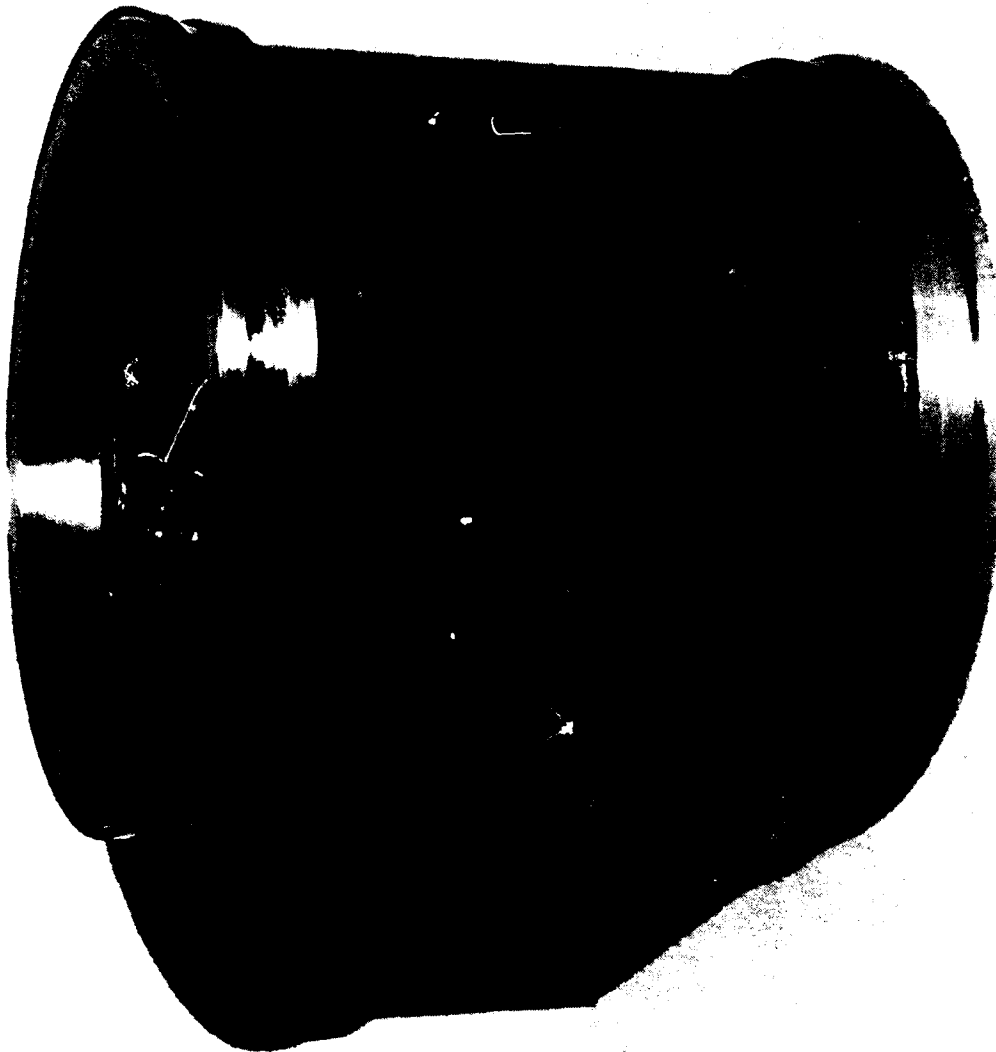
Figure A-1. A 12-inch-OD by 12-inch-long by 0.42-inch-thick ceramic cylinder with Mod 1 titantiun end caps fabricated by Lanxide from SiC/Al$_2$O$_3$/Al composite by the DIMOX^{TM} process.

Figure A-2. Insertion of wooden plug inside the cylinder for shock mitigation.

Figure A-3. Placement of steel bulkheads on the ends of the ceramic cylinders.
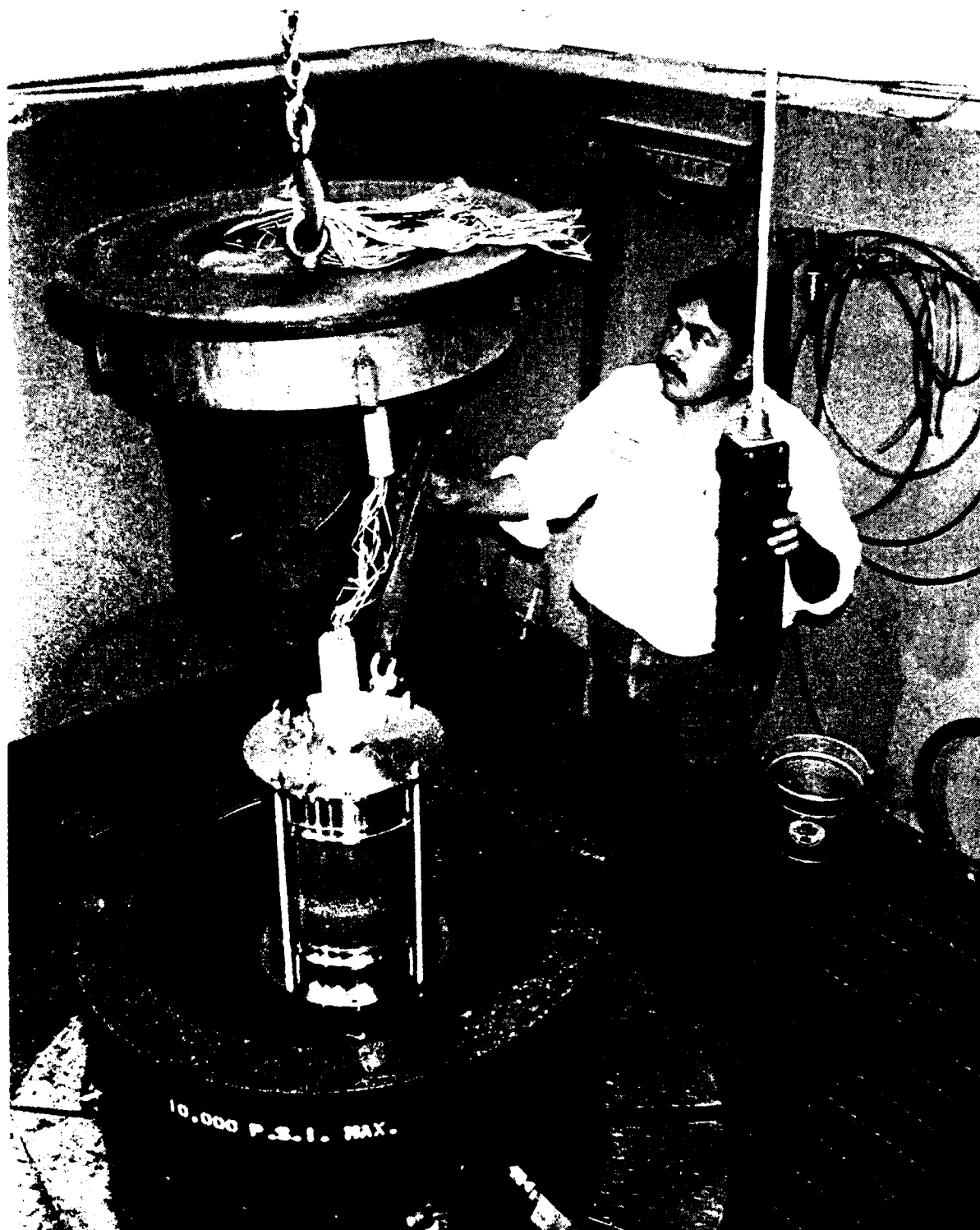
Figure A-4. Lowering of the test assembly into the pressure vessel at SRI.

APPENDIX B: SALT FOG TEST RESULTS

ARTECH CORP.
14554 Lee Road • Chantilly, Virginia 22021-1632
(703) 378-7263 • Washington, D.C. Metro (703) 968-TEST • Fax (703) 378-7274

May 18, 1993

Mr. Thomas A. Johnson
Lanxide
P. O. Box 6077
Newark, DE 19714-6077

Subject: Salt Fog Testing of Torpedo Coupon. Confirmation of Telephone
Report.

Reference: P. O. no. R043571
ARTECH J9301.151

Dear Mr. Johnson:

A sample coupon, 3 inches by 8 inches with a curved surface, green
in color on the outer face and edges and grey on the inner face, was
submitted to ARTECH with a request to perform a salt fog/spray test (per
ASTM B-117) for forty-eight hours. Conditions in the cabinet were
maintained at 95°F, with a 5% sodium chloride solution supplying a
condensing fog. The sample was exposed for 48 hours, as requested.

The sample was removed from the chamber at the end of the exposure
period and rinsed with clean water. The painted surfaces show no sign
of rust or corrosion. The unpainted inner surface shows a small amount
of white deposit which is easily removed from the surface. The tested
coupon is being returned with this letter.

If ARTECH can be of any additional assistance, on this or other
matters, please contact us at any time.

Sincerely,
ARTECH CORP.

Keith W. Flohr
Manager, Analytical Services

APPENDIX C: ENGINEERING DRAW-
INGS OF TEST BAR SPECIMEN

SEE DETAIL (A)

15 / (SEE NOTE 1)

8 / (SEE NOTE 1)

45 mm min

.15 ±.05 MM TYPICAL,
(4 PLACES)

DETAIL A

45° ±5°

A | .015 MM

-A-

B | .015 MM

⊥ | A | .015 MM

-B-

b

d

ALL DIMENSIONS ARE IN MILLIMETERS
(METRIC)

SPECIMEN   b   d
FLEX   6.00 ±.03   3.00 ±.03

NOTES:

1. FOUR LENGTHWISE SURFACES AND FOUR LENGTHWISE CHAMFERED SURFACES GROUND TO 8 RMS MICROINCH FINISH, MEASURED IN LONG DIRECTION AS SHOWN. FINISH TO BE 15 RMS MICROINCH OR BETTER IN THE PERPENDICULAR (CROSS) DIRECTION.

2. THE REQUIRED GRINDING MODE IS TO HAVE A DIAMOND WHEEL. GRIND PARALLEL TO THE LONG AXIS OF THE BAR,CHAMFER INCLUDED. BLANCHARD GRINDING IS NOT PERMITED. THE STOCK REMOVAL RATE SHALL NOT EXCEED .03 MM PER PASS DOWN TO LAST .06 MM FINAL FINISHING SHALL BE PERFORMED WITH A DIAMOND WHEEL THAT IS FINER THAN 200 GRIT NO LESS THAN .06 MM SHALL BE REMOVED DURING THE FINAL FINISHING PHASE AND AT A RATE OF NO MORE THAN .002 MM PER PASS. REMOVE APPROXIMATELY EQUAL STOCK FROM OPPOSITE FACE. DEEP SKIP MARKS, AND DEEP SINGLE STRIATIONS WHICH USUALLY OCCUR DUE TO LACK OF WHEEL DRESSING ARE NOT ACCEPTABLE

3. NO CHIPPING ON THE CHAMFER IS ALLOWED. 50X MAGNIFICATION WILL BE USED TO VERIFY THIS.

4. TO MAINTAIN THE GOOD FINISH WITHOUT SCRATCHES, BARS SHALL BE INDIVIDUALLY WRAPPED WHEN DELIVERED.

5. SPECIMEN END FACES NEED NOT BE PRECISION MACHINED.

6. SURFACE FINISH RMS VALUES OF NOTE 1 CAN BE WAIVED IF MATERIAL IS POROUS.

LANXIDE CORPORATION   TRALE INDUSTRIAL PARK NEWARK, DELAWARE, 19711

TITLE: FLEX BAR SPECIMEN

MT'L: TO BE SPECIFIED   SCALE: 4:1

DWG. ID. A-P-0024

DATE: 1-9-90   SH. 1   OF 1   SHTS.

NOTCH SECTION
(DETAIL)

DEPTH OF CUT
(.357)(d)/2

60°

SEE DETAIL FOR
NOTCH SECTION

ALL DIMENSIONS ARE IN MILLIMETERS
(METRIC)

b
$4.00 \pm .05$ $8.00 \pm .05$

NOTCH WIDTH = 0.762 mm
(CENTERED TO WITHIN 1 mm)

(SEE NOTE 1)

(SEE NOTE 1)

46-54 mm

24-26 mm

1 THE REQUIRED GRINDING MODE IS TO HAVE A DIAMOND WHEEL. GRIND PARALLEL TO THE LONG AXIS OF THE BAR. BLANCHARD GRINDING IS NOT PERMITTED.

THE STOCK REMOVAL RATE SHALL NOT EXCEED .03 MM PER PASS DOWN TO LAST .06 MM FINAL FINISHING SHALL BE PERFORMED WITH A DIAMOND WHEEL THAT IS FINER THAN 200 GRIT NO LESS THAN .06 MM SHALL BE REMOVED DURING THE FINAL FINISHING PHASE AND AT A RATE OF NO MORE THAN .002 MM PER PASS. REMOVE APPROXIMATELY EQUAL STOCK FROM OPPOSITE FACE. DEEP SKIP MARKS, AND DEEP SINGLE STRIATIONS WHICH USULLY OCCUR DUE TO LACK OF WHEEL DRESSING ARE NOT ACCEPTABLE

2 TO MAINTAIN THE GOOD FINISH WITHOUT SCRATCHES, BARS SHALL BE INDIVIDUALLY WRAPPED WHEN DELIVERED.

3 SPECIMEN END FACES NEED NOT BE PRECISION MACHINED.

REVISION RECORD

DR.   APR.   DATE

REV.

LANXIDE CORPORATION	TRALEE INDUSTRIAL PARK NEWARK, DELAWARE, 19711			TOLERANCE (UNLESS NOTED)		DRAWN-	DWG. NO. A P-0027	REV.
TITLE: Chevron Notch Fracture Toughness Bar				.XX ± .03		CHK'D-		
				.XXX ± .010				
WT: TO BE SPECIFIED	SCALE: ---			ANGLES ± 0 1/2°		APPR'D-	DATE: 1-9-90	SH. 1 OF 1

APPENDIX D: TEST SUMMARY: MATERIAL PROPERTIES AND PRESSURE TESTING

TABLES

Table D-1. Test result summary, Cylinder No. LAN 001, 3375-AU.

		SI Units		English Units	
		Top	Bottom	Top	Bottom
Density	gm/cc (lb/cu.in)	3.374	3.364	0.1218	0.124
Flexural Strength	MPa (ksi)	386 ± 6	385 ± 29	56 ± 0.9	55.8 ± 4.2
Comp. Strength	MPa (ksi)	2052 ± 84	2105 ± 43	297.6 ± 12.2	305.3 ± 6.2
Young's Modulus	GPa (Msi)	277 ± 0.8	296 ± 21	40.2 ± 0.1	42.9 ± 3.0
Fracture Toughness	MPa*m$^{1/2}$ (ksi*in$^{1/2}$)	8.95 ± 0.9	8.98 ± 0.6	8.14 ± 0.8	8.17 ± 0.55

Content:

% Metal		% Filler		% Matrix		% Porosity	
Top	Bottom	Top	Bottom	Top	Bottom	Top	Bottom
18.55	19.84	52.73	52.58	28.37	27.37	0.34	0.21

Pressure Test: Tested with titanium hemispheres. One proof test to 12,000 psi withstood 2,000 cycles to
12,000 psi. No leaks or damage noted.

Table D-2. Test result summary, Cylinder No. LAN 002, 3375-BV.

		SI Units		English Units	
		Top	Bottom	Top	Bottom
Density	gm/cc (lb/cu.in)	3.381	3.379	0.122	0.122
Flexural Strength	MPa (ksi)	430 ± 18	418 ± 21	62.4 ± 2.6	60.6 ± 3.0
Comp. Strength	MPa (ksi)	1957 ± 87	1855 ± 92	283.8 ± 12.6	269.0 ± 13.3
Young's Modulus	GPa (Msi)	293 ± 022	268 ± 5	42.5 ± 3.2	38.9 ± 0.7
Fracture Toughness	MPa*m$^{1/2}$ (ksi*in$^{1/2}$)	9.02 ± 0.9	9.00 ± 0.9	8.21 ± 0.82	8.19 ± 0.82

Content:

% Metal		% Filler		% Matrix		% Porosity	
Top	Bottom	Top	Bottom	Top	Bottom	Top	Bottom
18.46	18.98	48.86	49.66	32.10	31.10	0.58	0.27

Pressure Test: Tested with flat steel plates. One proof test to 12,500 psi failed after 1,967 cycles to 12,500 psi.

Table D-3. Raw data: Cylinder No. LAN 001, 3375-AU.

Sample No.	Flexural Strength (MPa)		Toughness (MPa*m$^{1/2}$)		Compressive Strength (MPa)		Modulus (GPa)	
	Top	Bottom	Top	Bottom	Top	Bottom	Top	Bottom
1	387.740	386.731	8.020	9.620	2116.6	2132.9	283.1	276.6
2	389.364	435.522	10.079	9.714	2170.6	2065.9	284.8	277.2
3	380.282	374.370	9.564	8.692	1976.4	2084.0	320.7	275.6
4	387.040	389.751	7.847	8.193	1954.0	2068.0		
5	397.347	388.078	8.911	8.426	2073.6	2101.5		
6	382.583	337.471	9.783	9.186	2020.6	2175.9		
7	379.787	382.408	8.424	9.054				
8								
9								
10								
Mean	386.307	384.904	8.947	8.984	2052.0	2104.7	296.2	276.5
Min	379.787	337.471	7.847	8.193	2065.9	2065.9	283.1	275.6
Max	397.347	435.522	10.079	9.714	2175.9	2175.9	320.7	277.2
Standard Deviation	6.144	28.770	0.885	0.578	83.7	42.8	21.2	0.8

Table D-4. Raw data: Cylinder No. LAN 002, 3375-BV.

Sample No.	Flexural Strength (MPa)		Toughness (MPa*m$^{1/2}$)		Compressive Strength (MPa)		Modulus (GPa)	
	Top	Bottom	Top	Bottom	Top	Bottom	Top	Bottom
1	428.178	433.843	10.329	9.475	1936.6	1834.8	268.6	270.0
2	459.764	404.350	9.712	9.187	2118.0	1890.4	306.8	270.6
3	409.432	439.299	8.849	9.634	1964.6	1845.0	304.7	262.4
4	417.821	369.495	7.934	7.091	1958.3	1979.4		
5	434.598	417.124	8.390	8.031	1898.7	1726.3		
6	445.398	425.793	7.846	10.207	1866.4			
7	422.997	420.459	9.945	9.383				
8		422.140	9.161	9.241				
9		430.969		8.766				
10								
Mean	430.027	418.164	9.021	9.002	1957.0	1855.2	293.4	267.7
Min	409.432	369.495	7.846	7.091	1866.4	1726.3	268.6	262.4
Max	459.764	439.299	10.329	10.207	2118.0	1979.4	306.8	270.6
Standard Deviation	17.612	20.905	0.930	0.933	87.2	91.9	21.5	4.5

Table D-5. Test result summary, Cylinder No. LAN 003, 3375-BT.

		SI Units		English Units	
		Top	Bottom	Top	Bottom
Density	gm/cc (lb/cu.in)	3.369	3.360	0.1216	0.1212
Flexural Strength	MPa (ksi)	370 ± 24	403 ± 20	53.6 ± 3.5	58.5 ± 2.9
Comp. Strength	MPa (ksi)	2079 ± 67	2090 ± 23	301.5 ± 9.7	303.1 ± 3.3
Young's Modulus	GPa (Msi)	302 ± 22	308 ± 28	43.8 ± 3.2	44.7 ± 4.1
Fracture Toughness	MPa*m$^{1/2}$ (ksi*in$^{1/2}$)	8.00 ± 0.3	7.92 ± 1.4	7.28 ± 0.3	7.21 ± 1.3

Content:

% Metal		% Filler		% Matrix		% Porosity	
Top	Bottom	Top	Bottom	Top	Bottom	Top	Bottom
20.24	20.72	52.05	53.82	27.57	25.34	0.14	0.12

Pressure Test: Tested with flat steel plates. One proof test to 16,000 psi withstood 464 cycles to 16,000 psi. No leaks or damage noted.

Table D-6. Test result summary, Cylinder No. LAN 004, 3375-BU.

		SI Units		English Units	
		Top	Bottom	Top	Bottom
Density	gm/cc (lb/cu.in)	3.371	3.326	0.1217	0.1201
Flexural Strength	MPa (ksi)	394 ± 23	374 ± 31	57.14 ± 3.3	54.24 ± 4.5
Comp. Strength	MPa (ksi)	2116 ± 47	2216 ± 32	306.9 ± 6.8	321.4 ± 4.6
Young's Modulus	GPa (Msi)	286 ± 1	297 ± 3	41.5 ± 0.1	43.1 ± 0.4
Fracture Toughness	MPa*m$^{1/2}$ (ksi*in$^{1/2}$)	9.02 ± 0.8	8.06 ± 0.6	8.21 ± 0.7	7.33 ± 0.5

Content:

% Metal		% Filler		% Matrix		% Porosity	
Top	Bottom	Top	Bottom	Top	Bottom	Top	Bottom
18.53	17.53	53.82	52.77	27.57	29.57	0.08	0.13

Pressure Test: Tested with flat steel plates. One proof test to 13,000 psi failed after 801 cycles to 13,000 psi.

Table D-7. Raw data: Cylinder No. LAN 003, 3375-BT.

Sample No.	Flexural Strength (MPa)		Toughness (MPa*m$^{1/2}$)		Compressive Strength (MPa)		Modulus (GPa)	
	Top	Bottom	Top	Bottom	Top	Bottom	Top	Bottom
1	348.646	405.897	8.114	6.519	1958.3	2107.7	326.0	275.9
2	376.200	394.685	7.866	8.222	2085.3	2080.2	296.1	327.3
3	325.778	407.434	8.310	10.221	2112.1	2069.4	282.8	319.7
4	387.815	428.974	8.287	7.169	2073.3	2087.9		
5	411.814	391.044	7.632	9.222	2081.4	2066.0		
6	355.612	372.279	7.802	7.689	2160.9	2125.8		
7	384.912	417.791		6.399				
8	359.100	369.747						
9	375.425	417.791						
10	373.822	419.661						
Mean	369.912	402.531	8.003	7.920	2078.6	2089.5	301.7	307.7
Min	325.778	369.747	7.632	6.399	1958.3	2066.0	282.8	375.9
Max	411.814	428.979	8.310	10.221	2160.9	2125.8	326.0	327.3
Standard Deviation	21.823	20.214	0.278	1.413	67.0	23.2	22.1	27.7

Table D-8. Raw data: Cylinder No. LAN 004, 3375-BU.

Sample No.	Flexural Strength (MPa)		Toughness (MPa*m$^{1/2}$)		Compressive Strength (MPa)		Modulus (GPa)	
	Top	Bottom	Top	Bottom	Top	Bottom	Top	Bottom
1	390.763	385.325	10.222	7.630	2108.2	2244.8	284.9	299.8
2	408.959	384.677	8.043	7.336	2092.9	2215.9	286.0	295.9
3	388.217	413.211	9.265	8.937	2171.5	2199.8	285.6	294.2
4	394.971	371.865	9.175	8.128	2091.7	2175.9		
5	405.816	404.856	8.090	8.355	2173.7	2262.7		
6	340.170	347.078	9.649	8.498	2058.4	2199.2		
7	398.150	338.773	8.680	7.551				
8	429.485	414.414						
9	404.686	332.061						
10	382.402	352.158						
Mean	394.362	374.442	9.018	8.062	2116.1	2216.4	285.5	296.6
Min	340.170	332.061	8.043	7.336	2058.4	2175.9	284.9	294.2
Max	329.485	414.414	10.222	10.222	2173.7	2262.7	286.0	299.8
Standard Deviation	23.165	30.857	0.802	0.580	46.7	32.1	0.6	2.9

Table D-9. Test result summary, Cylinder No. LAN 005, 3375-BS.

		SI Units		English Units	
		Top	Bottom	Top	Bottom
Density	gm/cc (lb/cu.in)	3.367	3.367	0.1215	0.1215
Flexural Strength	MPa (ksi)	397 ± 17	365 ± 29	57.6 ± 2.5	52.9 ± 4.2
Comp. Strength	MPa (ksi)	2154 ± 46	2075 ± 17	312.4 ± 6.7	300.9 ± 2.5
Young's Modulus	GPa (Msi)	292 ± 20	287 ± 27	42.4 ± 2.9	41.6 ± 3.9
Fracture Toughness	MPa*m$^{1/2}$ (ksi*in$^{1/2}$)	9.13 ± 1.1	9.75 ± 1.0	8.31 ± 1.0	8.87 ± 0.9

Content:

% Metal		% Filler		% Matrix		% Porosity	
Top	Bottom	Top	Bottom	Top	Bottom	Top	Bottom
18.73	19.96	54.26	52.33	26.88	27.58	0.12	0.13

Pressure Test: Tested with flat steel plates. One proof test to 12,500 psi withstood 2,902 cycles to 12,500 psi. No leaks or damage noted.

Table D-10. Test result summary, Cylinder No. LAN 006, 3375-BX.

		SI Units		English Units	
		Top	Bottom	Top	Bottom
Density	gm/cc (lb/cu.in)	3.372	3.368	0.1217	0.1216
Flexural Strength	MPa (ksi)	385 ± 21	388 ± 23	55.8 ± 3.0	56.3 ± 3.3
Comp. Strength	MPa (ksi)	2200 ± 141	2120 ± 44	319.1 ± 20.5	307.5 ± 6.4
Young's Modulus	GPa (Msi)	303 ± 16	285 ± 24	43.9 ± 2.3	41.3 ± 3.5
Fracture Toughness	MPa*m$^{1/2}$ (ksi*in$^{1/2}$)	8.67 ± 0.7	9.46 ± 1.2	7.89 ± 0.64	8.61 ± 1.09

Content:

% Metal		% Filler		% Matrix		% Porosity	
Top	Bottom	Top	Bottom	Top	Bottom	Top	Bottom
19.14	18.04	51.22	54.81	29.47	27.05	0.17	0.11

Pressure Test: Tested with flat steel plates. One proof test to 14,000 psi failed after 331 cycles to 14,000 psi.

Table D-11. Raw data: Cylinder No. LAN 005, 3375-BS.

Sample No.	Flexural Strength (MPa)		Toughness (MPa*m$^{1/2}$)		Compressive Strength (MPa)		Modulus (GPa)	
	Top	Bottom	Top	Bottom	Top	Bottom	Top	Bottom
1	396.580	371.209	9.227	10.684	2197.1	2085.6	315.2	271.8
2	376.068	375.869	9.363	9.643	2203.9	2077.7	279.5	272.5
3	402.462	370.289	7.928	8.092	2150.7	2091.2	281.9	319.6
4	403.836	369.669	8.140	10.268	2107.0	2047.0		
5	377.866	372.245	10.557	9.790	2112.0	2074.0		
6	387.796	403.215	7.850	10.982				
7	383.565	336.284	10.199	8.758				
8	428.618	372.265	9.806					
9	418.396	295.993						
10	390.712	382.905						
Mean	396.590	364.994	9.134	9.745	2154.0	2075.0	292.2	287.9
Min	376.068	295.993	7.850	8.092	2107.0	2047.0	279.5	271.8
Max	428.618	403.215	10.557	10.982	2203.9	2091.2	315.2	319.6
Standard Deviation	17.132	29.210	1.053	1.033	45.6	17.1	20.0	27.4

Table D-12. Raw data: Cylinder No. LAN 006, 3375-BX.

Sample No.	Flexural Strength (MPa)		Toughness (MPa*m$^{1/2}$)		Compressive Strength (MPa)		Modulus (GPa)	
	Top	Bottom	Top	Bottom	Top	Bottom	Top	Bottom
1	379.790	368.064	7.573	8.086	2112.4	1923.7	269.7	299.0
2	401.079	373.591	8.864	10.305	2165.5	2291.2	313.2	321.1
3	385.009	379.720	9.163	10.197	2144.7	2153.6	272.4	289.8
4	400.867	398.794	9.283	9.113	2059.0	2276.0		
5	389.174	355.956	9.516	10.047	2081.0	2307.0		
6	381.341	409.141	8.197	10.824	2159.0	2233.0		
7	359.503	368.082	8.177	9.702				
8	416.172	393.483	8.591	7.393				
9	349.224	424.023						
10		413.202						
Mean	384.684	388.406	8.670	9.458	2120.0	2200.0	285.1	303.3
Min	349.224	355.956	7.573	7.393	2059.0	1923.7	269.7	289.8
Max	416.172	424.023	9.516	10.824	2165.5	2307.0	313.2	321.1
Standard Deviation	20.824	22.661	0.660	1.183	43.7	141.0	24.4	16.1

Table D-13. Test result summary, Cylinder No. LAN 007, 3375-BO (as cast).

		SI Units		English Units	
		Top	Bottom	Top	Bottom
Density	gm/cc (lb/cu.in)	3.390	3.363	0.1224	0.1214
Flexural Strength	MPa (ksi)	368 ± 24	372 ± 22	53.4 ± 3.5	54.0 ± 3.2
Comp. Strength	MPa (ksi)	1969 ± 93	1992 ± 41	285.6 ± 13.5	288.9 ± 5.6
Young's Modulus	GPa (Msi)	275 ± 22	291 ± 25	39.9 ± 3.2	42.2 ± 3.6
Fracture Toughness	MPa*m$^{1/2}$ (ksi*in$^{1/2}$)	6.81 ± 0.3	6.94 ± 0.7	6.19 ± 0.3	6.32 ± 0.6

Content:

% Metal		% Filler		% Matrix		% Porosity	
Top	Bottom	Top	Bottom	Top	Bottom	Top	Bottom
19.28	18.94	51.97	51.33	28.28	29.37	0.48	0.36

Pressure Test: Tested with flat steel plates. One proof test to 12,500 psi failed after 531 cycles to 12,500 psi.

Table D-14. Test result summary, Cylinder No. LAN 008, 3375-CB.

		SI Units		English Units	
		Top	Bottom	Top	Bottom
Density	gm/cc (lb/cu.in)	3.374	3.344	0.1218	0.1207
Flexural Strength	MPa (ksi)	409 ± 7	336 ± 67	59.3 ± 1.0	48.7 ± 9.7
Comp. Strength	MPa (ksi)	2116 ± 89	1975 ± 167	306.9 ± 13	286 ± 24
Young's Modulus	GPa (Msi)	284 ± 9	286 ± 12	41.2 ± 1.3	41.5 ± 1.7
Fracture Toughness	MPa*m$^{1/2}$ (ksi*in$^{1/2}$)	7.41 ± 0.4	5.64 ± 1.1	6.50 ± 0.4	5.13 ± 1.0

Content:

% Metal		% Filler		% Matrix		% Porosity	
Top	Bottom	Top	Bottom	Top	Bottom	Top	Bottom
19.26	17.15	50.27	51.34	30.22	31.08	0.24	0.44

Pressure Test: Tested with flat steel plates. One proof test to 10,000 psi. Imploded at 19,000 psi.

Table D-15. Raw data: Cylinder No. LAN 007, 3375-BO.

Sample No.	Flexural Strength (MPa)		Toughness (MPa*m$^{1/2}$)		Compressive Strength (MPa)		Modulus (GPa)	
	Top	Bottom	Top	Bottom	Top	Bottom	Top	Bottom
1	366.086	368.379	6.853	6.470	1895.4	2035.2	261.0	261.9
2	356.069	355.100	6.438	7.133	1850.4	1976.4	300.2	309.1
3	342.175	362.208	6.485	6.104	2075.5	1945.2	262.2	300.7
4	357.411	359.206	7.102	8.057	1998.9	1960.5		
5	379.857	353.810	6.788	7.823	2022.6	1986.0		
6	376.047	395.202	6.722	6.091		2048.9		
7	349.731	341.945	6.608	7.029				
8	348.046	414.036	7.471	6.793				
9	423.861	387.733						
10	377.042	382.894						
Mean	367.633	372.061	6.809	6.938	1968.6	1992.0	274.5	290.6
Min	342.175	341.945	6.438	6.091	1850.4	1945.2	261.0	261.9
Max	423.861	414.036	7.471	8.057	2075.5	2048.9	300.2	309.1
Standard Deviation	23.719	22.271	0.342	0.730	93.0	41.4	22.3	25.2

Table D-16. Raw data: Cylinder No. LAN 008, 3375-CB.

Sample No.	Flexural Strength (MPa)		Toughness (MPa*m$^{1/2}$)		Compressive Strength (MPa)		Modulus (GPa)	
	Top	Bottom	Top	Bottom	Top	Bottom	Top	Bottom
1	408.599	424.119	7.760	5.538	2262.1	2045.2	280.0	276.9
2	394.687	286.227	7.353	5.078	2013.2	1784.5	277.8	280.9
3	415.107	405.557	7.673	8.348	2140.7	2166.2	294.2	299.6
4	417.756	357.150	7.534	4.684	2046.1	2114.9		
5	413.572	404.380	7.796	6.728	2148.7	1771.0		
6	414.033	355.266	6.638	5.615	2086.3	1966.7		
7	408.708	334.239	7.106	5.444				
8	405.107	252.613		4.423				
9	401.689	224.048		5.031				
10		316.288		5.459				
Mean	408.807	335.989	7.408	5.635	2116.2	1974.8	284.0	285.8
Min	394.687	224.048	6.638	4.423	2013.2	1771.0	277.8	276.9
Max	417.756	424.119	7.796	8.348	2262.1	2166.2	294.2	299.6
Standard Deviation	7.362	67.043	0.418	1.139	88.7	166.8	8.9	12.1

Table D-17. Test result summary, Cylinder No. LAN 009, 3375-BR.

		SI Units		English Units	
		Top	Bottom	Top	Bottom
Density	gm/cc (lb/cu.in)	3.359	3.358	0.1213	0.1212
Flexural Strength	MPa (ksi)	394 ± 25	398 ± 15	57.1 ± 3.6	57.7 ± 2.2
Comp. Strength	MPa (ksi)	2195 ± 58	2119 ± 45	318.4 ± 8.4	307.3 ± 6.5
Young's Modulus	GPa (Msi)	294 ± 5	284 ± 1	42.6 ± 0.7	41.2 ± 0.1
Fracture Toughness	MPa*m$^{1/2}$ (ksi*in$^{1/2}$)	8.98 ± 0.9	9.00 ± 0.9	8.17 ± 0.8	8.19 ± 0.9

Content:

% Metal		% Filler		% Matrix		% Porosity	
Top	Bottom	Top	Bottom	Top	Bottom	Top	Bottom
16.39	18.88	56.74	54.48	26.63	26.47	0.24	0.17

Pressure Test: Tested with flat steel ends. One proof test to 15,000 psi withstood 3,003 cycles to 15,000 psl. External chip noted.

Table D-18. Test result summary, Cylinder No. LAN 010, 3375-BQ.

		SI Units		English Units	
		Top	Bottom	Top	Bottom
Density	gm/cc (lb/cu.in)	3.376	3.357	0.1218	0.1212
Flexural Strength	MPa (ksi)	410 ± 18	379 ± 17	59.5 ± 2.6	55.0 ± 2.5
Comp. Strength	MPa (ksi)	2141 ± 62	2015 ± 46	310.5 ± 9.0	292.3 ± 6.7
Young's Modulus	GPa (Msi)	287 ± 3	273 ± 0.3	41.6 ± 0.4	39.6 ± 0.0
Fracture Toughness	MPa*m$^{1/2}$ (ksi*in$^{1/2}$)	8.39 ± 0.9	8.56 ± 0.9	7.64 ± 0.9	7.79 ± 0.9

Content:

% Metal		% Filler		% Matrix		% Porosity	
Top	Bottom	Top	Bottom	Top	Bottom	Top	Bottom
16.81	16.99	55.84	52.28	26.97	29.86	0.39	0.87

Pressure Test: Tested with flat steel ends. One proof test to 13,000 psi withstood 3,001 cycles to 13,000 psi. No leaks or damage noted.

Table D-19. Raw data: Cylinder No. LAN 009, 3375-BR.

Sample No.	Flexural Strength (MPa)		Toughness (MPa*m$^{1/2}$)		Compressive Strength (MPa)		Modulus (GPa)	
	Top	Bottom	Top	Bottom	Top	Bottom	Top	Bottom
1	389.636	388.687	7.842	9.455	2240.5	2162.2	293.8	284.5
2	393.550	382.626	8.574	9.373	2162.5	2142.6	289.2	284.0
3	386.094	415.975	8.220	8.959	2286.8	2156.7	298.4	283.0
4	419.369	394.023	8.964	8.464	2129.0	2046.4		
5	343.229	381.027	10.046	9.171	2164.6	2086.8		
6	420.319	416.469	9.416	9.608	2187.4	2119.6		
7	384.480	391.436	8.495	10.222				
8	413.613	413.597	8.779	8.487				
9			10.521	7.240				
10								
Mean	393.786	397.980	8.984	8.998	2195.1	2119.1	293.8	283.8
Min	343.229	381.027	7.842	7.240	2129.0	2046.4	289.2	283.0
Max	420.319	416.469	10.521	10.222	2286.8	2162.2	298.4	284.5
Standard Deviation	25.272	15.012	0.867	0.858	58.1	45.1	4.6	0.8

Table D-20. Raw data: Cylinder No. LAN 010, 3375-BQ.

Sample No.	Flexural Strength (MPa)		Toughness (MPa*m$^{1/2}$)		Compressive Strength (MPa)		Modulus (GPa)	
	Top	Bottom	Top	Bottom	Top	Bottom	Top	Bottom
1	414.800	348.032	7.222	7.785	2176.9	1986.1	289.6	273.3
2	385.420	383.809	9.290	9.660	2165.5	2061.4	283.6	272.7
3	433.516	371.255	8.865	9.470	2193.4	2000.5	287.2	273.0
4	427.064	400.044	7.836	8.303	2129.0	2003.8		
5	400.027	373.191	7.669	8.532	2022.1	2077.5		
6	409.030	388.350	9.442	7.172	2157.3	1958.8		
7	422.541	372.986	8.085	8.066				
8	385.774	396.628	7.707	9.468				
9			9.400					
10								
Mean	409.771	379.287	8.391	8.557	2140.7	2014.7	286.8	273.0
Min	385.420	348.032	7.222	7.172	2022.1	1958.8	283.6	272.7
Max	433.516	400.044	9.442	9.660	2193.4	2077.5	289.6	273.3
Standard Deviation	18.188	16.701	0.860	0.902	61.9	45.6	3.0	0.3

Table D-21. Test result summary, Cylinder No. LAN 011, 3375-BW.

		SI Units		English Units	
		Top	Bottom	Top	Bottom
Density	gm/cc (lb/cu.in)	3.370	3.368	0.1217	0.1216
Flexural Strength	MPa (ksi)	381 ± 35	383 ± 17	55.3 ± 5.1	55.5 ± 2.5
Comp. Strength	MPa (ksi)	2154 ± 73	2068 ± 26	312.4 ± 10.6	299.9 ± 3.8
Young's Modulus	GPa (Msi)	280 ± 6	270 ± 1	40.6 ± 0.9	39.2 ± 0.1
Fracture Toughness	MPa*m$^{1/2}$ (ksi*in$^{1/2}$)	8.55 ± 0.5	9.42 ± 0.7	7.78 ± 0.5	8.57 ± 0.6

Content:

% Metal		% Filler		% Matrix		% Porosity	
Top	Bottom	Top	Bottom	Top	Bottom	Top	Bottom
17.55	20.06	50.61	48.66	31.21	31.03	0.62	0.25

Pressure Test: Tested with flat steel ends. One proof test to 10,000 psi. Cylinder imploded at 19,000 psi.

Table D-22. Test result summary, Cylinder No. LAN 012, 3375-AZ (as cast).

		SI Units		English Units	
		Top	Bottom	Top	Bottom
Density	gm/cc (lb/cu.in)	3.358	3.349	0.1212	0.1209
Flexural Strength	MPa (ksi)	398 ± 19	384 ± 40	57.7 ± 2.8	55.7 ± 5.8
Comp. Strength	MPa (ksi)	2076 ± 69	2001 ± 70	301.1 ± 10.0	290.2 ± 10.2
Young's Modulus	GPa (Msi)	301 ± 19	270 ± 6	43.7 ± 2.8	39.2 ± 0.9
Fracture Toughness	MPa*m$^{1/2}$ (ksi*in$^{1/2}$)	7.91 ± 0.6	6.80 ± 1.4	7.19 ± 0.5	6.2 ± 1.3

Content:

% Metal		% Filler		% Matrix		% Porosity	
Top	Bottom	Top	Bottom	Top	Bottom	Top	Bottom
13.85	12.15	46.78	46.67	38.61	40.33	0.76	0.86

Pressure Test: Tested with flat steel ends. One proof test to 12,500 psi withstood 2,004 cycles to 12,500 psi. No leaks or damage noted.

Table D-23. Raw data: Cylinder No. LAN 011, 3375-BW.

Sample No.	Flexural Strength (MPa)		Toughness (MPa*m$^{1/2}$)		Compressive Strength (MPa)		Modulus (GPa)	
	Top	Bottom	Top	Bottom	Top	Bottom	Top	Bottom
1	401.758	400.445	9.211	9.739	2170.8	2098.6	276.2	271.5
2	355.475	385.677	8.759	8.667	2052.9	2037.6	276.6	269.9
3	368.750	376.955	8.539	9.089	2088.4	2065.2	287.5	269.0
4	353.966	389.544	8.259	8.643	2155.1	2036.6		
5	441.002	384.081	8.642	9.629	2244.4	2075.7		
6	332.005	373.079	7.455	9.097	2213.5	2091.0		
7	400.924	402.871	8.486	10.489				
8	393.418	349.765	9.056	10.034				
9								
10								
Mean	380.912	382.802	8.551	9.423	2154.2	2067.5	280.1	270.1
Min	332.005	349.765	7.455	8.643	2052.9	2036.6	276.2	269.0
Max	441.002	402.871	9.211	10.489	2244.4	2098.6	287.5	271.5
Standard Deviation	34.878	16.859	0.539	0.660	72.8	26.2	6.4	1.3

Table D-24. Raw data: Cylinder No. LAN 012, 3375-AZ.

Sample No.	Flexural Strength (MPa)		Toughness (MPa*m$^{1/2}$)		Compressive Strength (MPa)		Modulus (GPa)	
	Top	Bottom	Top	Bottom	Top	Bottom	Top	Bottom
1	430.157	374.929	8.387	4.414	2016.1	1974.5	321.9	269.3
2	392.959	401.932	7.661	6.099	2164.9	1984.1	284.7	276.2
3	401.358	409.332	6.929	6.084	2004.9	2101.7	296.6	264.4
4	382.172	423.791	8.498	8.899	2126.0	2032.0		
5	395.797	380.708	8.315	8.498	2066.0	1914.0		
6	413.847	394.273	7.592	6.884				
7	372.458	372.469	7.952	7.768				
8	382.236	276.693		5.175				
9	422.572	411.349		7.048				
10	409.767	371.001		7.091				
11	376.937	402.995						
Mean	398.206	383.588	7.905	6.796	2076.0	2001.0	301.1	270.0
Min	372.458	276.693	6.929	4.414	2004.9	1914.0	284.7	269.3
Max	430.157	423.791	8.498	8.899	2164.9	2101.7	321.9	276.2
Standard Deviation	19.141	10.319	0.558	1.403	69.2	70.2	19.0	5.9

THE AUTHORS

RAMON R. KURKCHUBASCHE is a Research Engineer for the Ocean Engineering Division and has worked since November 1990 in the field of deep submergence pressure housings fabricated from ceramic materials. His education includes a B.S. in Structural Engineering from the University of California at San Diego, 1989; and an M.S. in Aeronautical/Astronautical Engineering from Stanford University in 1990. His experience includes conceptual design, procurement, assembly, testing, and documentation of ceramic housings. Other experience includes buoyancy concepts utilizing ceramic, nondestructive evaluation of ceramic components. He is a member of the Marine Technology Society, and has published "Elastic Stability Considerations for Deep Submergence Ceramic Pressure Housings," *Intervention '92*, and "Nondestructive Evaluation Techniques for Deep Submergence Housing Components Fabricated from Alumina Ceramic," *MTS '93 Proceedings*.

RICHARD P. JOHNSON is an Engineer for the Ocean Engineering Division. He has held this position since 1987. Before that, he was a Laboratory Technician for the Ocean Engineering Laboratory, University of California at Santa Barbara from 1985–1986, and Design Engineer in the Energy Projects Division of SAIC from 1986–1987. His education includes a B.S. in Mechanical Engineering from the University of California at Santa Barbara in 1986, and an M.S. in Structural Engineering from the University of California, San Diego, in 1991. He is a member of the Marine Technology Society and has published "Stress Analysis Considerations for Deep Submergence Ceramic Pressure Housings," *Intervention '92*, and "Structural Design Criteria for Alumina-Ceramic Deep Submergence Pressure Housings," *MTS '93 Proceedings*.
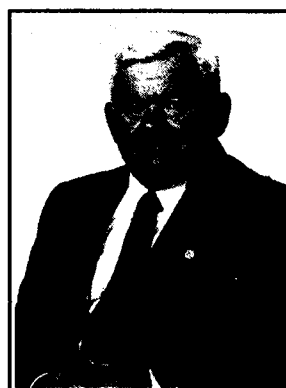
DR. JERRY STACHIW is Staff Scientist for Marine Materials in the Ocean Engineering Division. He received his undergraduate engineering degree from Oklahoma State University in 1955 and graduate degree from Pennsylvania State University in 1961.

Since that time he has devoted his efforts at various U.S. Navy Laboratories to the solution of challenges posed by exploration, exploitation, and surveillance of hydrospace. The primary focus of his work has been the design and fabrication of pressure resistant structural components of diving systems for the whole range of ocean depths. Because of his numerous achievements in the field of ocean engineering, he is considered to be the leading expert in the structural application of plastics and brittle materials to external pressure housings.

Dr. Stachiw is the author of over 100 technical reports, articles, and papers on design and fabrication of pressure resistant viewports of acrylic plastic, glass, germanium, and zinc sulphide, as well as pressure housings made of wood, concrete, glass, acrylic plastic, and ceramics. His book on "Acrylic Plastic Viewports" is the standard reference on that subject.

For the contributions to the Navy's ocean engineering programs, the Navy honored him with the Military Oceanographer Award and the NCCOSC's RDT&E Division honored him with the Lauritsen-Bennett Award. The American Society of Mechanical Engineers recognized his contributions to the engineering profession by election to the grade of Lite-Fellow, as well as the presentation of Centennial Medal, Dedicated Service Award and Pressure

Technology Codes Outstanding Performance Certificate.

Dr. Stachiw is past chairman of ASME Ocean Engineering Division and ASME Committee on Safety Standards for Pressure Vessels for Human Occupancy. He is a member of the Marine Technology Society, New York Academy of Science, Sigma Xi and Phi Kappa Honorary Society.
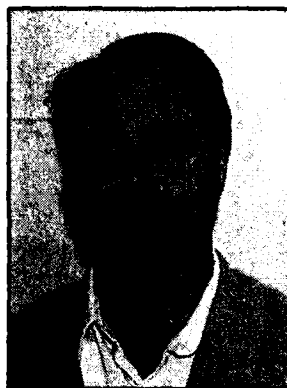
THOMAS A. JOHNSON is a member of the techical staff of Lanxide Corporation in Newark, Delaware. He has worked in the development of advanced ceramic matrix composites at Lanxide since 1986. His education includes a B.S. in Ceramic Engineering in 1970 and an M.S. in Ceramic Engineering in 1972, both from the Georgia Institute of Technology, Atlanta, Georgia.

He worked as a Senior Research Engineer for the Babcock & Wilcox Company at the Lynchberg Research Center, Lynchburg, Virginia (1972 to 1986). His experience includes high temperature thermal insulations, fiber reinforced ceramic matrix composites, and particulate reinforced ceramic matrix composites.

He has performed developmental and applications engineering for varius ceramic matrix composite prototypes for industrial wear, turbine engine, aerospace, automotive, and heat management applications for Lanxide and several Landixe joint venture partners.

1. AGENCY USE ONLY (Leave blank)	2. REPORT DATE	3. REPORT TYPE AND DATES COVERED
	December 1993	Final

4. TITLE AND SUBTITLE

STRUCTURAL PERFORMANCE OF CYLINDRICAL PRESSURE HOUSINGS OF DIFFERENT CERAMIC COMPOSITIONS UNDER EXTERNAL PRESSURE LOADING
Part IV, Silicon Carbide Particulate Reinforced Alumina Ceramic

5. FUNDING NUMBERS

PE: 0603713N
PROJ: S0397
ACC: DN302232

6. AUTHOR(S)

R. R. Kurkchubasche, R. P. Johnson, and J. D. Stachiw (NRaD) and T. A. Johnson (Lanxide Corporation)

7. PERFORMING ORGANIZATION NAME(S) AND ADDRESS(ES)

Naval Command, Control and Ocean Surveillance Center (NCCOSC)
RDT&E Division
San Diego, CA 92152-5001

8. PERFORMING ORGANIZATION REPORT NUMBER

TR 1594

9. SPONSORING/MONITORING AGENCY NAME(S) AND ADDRESS(ES)

Naval Sea Systems Command
Washington, DC 20362

10. SPONSORING/MONITORING AGENCY REPORT NUMBER

11. SUPPLEMENTARY NOTES

12a. DISTRIBUTION/AVAILABILITY STATEMENT

Approved for public release; distribution is unlimited.

12b. DISTRIBUTION CODE

13. ABSTRACT (Maximum 200 words)

Twelve 12-inch-OD by 18-inch-long by 0.412-inch-thick silicon-carbide particulate reinforced alumina-ceramic cylinders were fabricated, assembled, and pressure tested to determine their suitability for use as external pressure-resistant housings for underwater applications. The material, designated 90-X-089, is made by Lanxide Corporation (Newark, DE) by a proprietary directed metal oxidation (DIMOX™) process. The primary advantages of this material are its high compressive strength, high elastic modulus, high fracture toughness, low specific gravity, and ability to be cast in near net shapes, eliminating the need for expensive diamond grinding. Pressure test results are presented along with strain gage data, cyclic fatigue-life data, and acoustic emissions. Conclusions regarding the suitability of the material for application to pressure housings for underwater applications are presented along with a comparison to WESGO's AL-600 96-percent alumina ceramic, which was chosen as a base of comparison for various advanced materials being evaluated under the same program. Recommendations for design implementation, nondestructive evaluation, and further research are made.

14. SUBJECT TERMS

ceramics
external pressure housing
ocean engineering

15. NUMBER OF PAGES

135

16. PRICE CODE

17. SECURITY CLASSIFICATION OF REPORT	18. SECURITY CLASSIFICATION OF THIS PAGE	19. SECURITY CLASSIFICATION OF ABSTRACT	20. LIMITATION OF ABSTRACT
UNCLASSIFIED	UNCLASSIFIED	UNCLASSIFIED	SAME AS REPORT

UNCLASSIFIED

21a. NAME OF RESPONSIBLE INDIVIDUAL	21b. TELEPHONE (include Area Code)	21c. OFFICE SYMBOL
R. R. Kurkchubasche	(619) 553–1949	Code 564

UNCLASSIFIED